EGG-C91-103450

HEAT FLOW MODELING OF THE SNAKE RIVER PLAIN, IDAHO

David D. Blackwell
Shari Kelley
John L. Steele

April, 1992

Department of Geological Sciences
Southern Methodist University
Dallas, Texas 75275

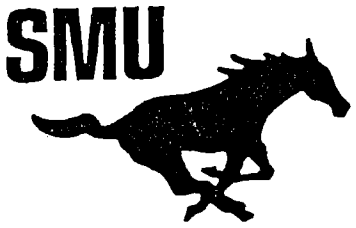

Prepared for the U. S. Department of Energy
Office of New Production Reactors
Under DOE Idaho field Office
Contract DE-AC07-761DO1570

ABSTRACT

Heat flow data have been summarized for the Snake River Plain and vicinity, Idaho. In addition, new data have been collected and analyzed. The thermal data document that the heat flow and thus the crustal temperatures are higher in the Snake River Plain/Yellowstone region than in the surrounding provinces. The thermal effects of the passage of an energetic mantle hot spot beneath the region have been investigated with the aid of numerical modeling. Particular attention was focused on the lateral effects of the hot spot. The most intense thermal effects are associated with the center of the hot spot, which covers an area about 75 to 100 km in diameter and is centered at the present time on the Yellowstone region. There is evidence for thermal effects outside the apex of the hot spot, however. The heat flow data and the model results were compared with some aspects of the regional geology and geophysics. The implications of the thermal field on the rheology of the crust were investigated based on calculation of crustal strength envelopes. The weakest part of the lithosphere is the Basin and Range crust along the edge of the Snake River Plain/Yellowstone province. Because of this fact and because the stress and strain rate regimes inside the Snake River Plain/Yellowstone region are dominated by the thermal and igneous effects, stress and strain rate fields within the Basin and Range province may not have a strong influence on structures in the Snake River Plain.

ACKNOWLEDGEMENTS

Special assistance in locating information on geothermal data was received from John Mitchell, Dennis Dunn, and Paul Castelin of the Idaho Department of Water Resources, R.E. Lewis, R.G. Whitehead and H.W. Young of the U.S. Geological Survey, Chuck Horsborough of the U.S. BLM, and William Pittman of the Idaho Department of Lands. Jack Barraclough of the U.S. Geological Survey (now at EG&G, Idaho) was a source of information on the Snake Plain aquifer in eastern Idaho. Roger Jensen of the U. S. Geological Survey made available the temperature logs for two wells at Butte City. John Knox and Edward Western of Sunedco made possible release of exploration information in southeastern Idaho. Exploration data in the eastern Snake River Plains and Island Park areas collected under the direction of Malcolm Mossman and Robert Crewdson was released by Oxy Geothermal Incorporated. Roger Bowers obtained the release of the northern margin thermal data. David Becker made the calculations of residence time versus temperature in the Snake River aquifer. Steve Mueller made the calculations of the crustal elastic effects of the Snake River Plain loading. Robert E. Spafford, Larry S. Carter, and David Crouch assisted in the various aspects of the laboratory and field studies. This study was funded by EG&G Idaho via contract EGG-C91-103450. In addition to the support for this study collection of data in central Idaho was supported by NSF-RANN Grant No. AER-76-00108 and NSF Grant No. GA-11351. Collection of data in the eastern Snake River Plains included in Table 2 was supported in part by NSF Grant No. EAR-8213156.

CONTENTS

HEAT FLOW MODELING OF THE SNAKE RIVER PLAIN, IDAHO

INTRODUCTION

Purpose and Scope

A particularly important tool in the evaluation of the geothermal resources is the technique of heat flow. A heat flow study measures the heat which originates within the earth and flows out at the surface of the earth. A quantity which is measured as part of a heat flow study is the geothermal gradient or the rate of temperature increase with depth increase. Thus information relevant to the temperature in the crust is a natural outcome of the heat flow studies. In recent years it has been recognized that the temperature in the crust has a major effect on the strength of the crust and the nature of seismicity, thus the seismicity in the vicinity of the Snake River Plain will be affected by the heat flow and resultant temperatures.

As part of this study thermal data from various sources were collected and incorporated in the extensive database of heat flow and geothermal information for Idaho maintained at SMU. Between 1974 and about 1983 the geothermal resources of the State of Idaho were the subject of extensive heat flow studies to evaluate the energy potential they represent. Most of the data collected to 1980 have been published, but data collected since that time have not. In addition extensive commercial geothermal and hydrocarbon exploration took place in Idaho in the early 1980's as a result of the energy crisis. A large amount of this data was filed with various government offices and confidentiality time limits have passed and/or the data have been released by companies. Thus a large component of the new data discussed in this report is from these types of sources. Of special interest for this study are thermal data from several deep wells south and east of the Snake River Plain. In addition a program of logging of wells of opportunity was carried out. A number of wells in areas not previously studied were logged. Finally a deep well was drilled on the INEL site and preliminary thermal measurements were made in that well.

Idaho has a diverse geology and many volcanic and tectonic processes have been active within the environs of the State over the last few million years, particularly in the southern part of the State. The objectives of this study are to review existing and to process new thermal data for the eastern Snake River Plain and vicinity, and to evaluate the validity of the propagating hot spot concept as a basis for the modeling of the crustal thermal structure. Further the goals of this investigation are to evaluate the temperature conditions in the Snake River Plain compared to the surrounding Basin and Range province and to determine the possible significance of the thermal effects on the stress regime and earthquake potential of the eastern Snake River Plain. The results of this study can also be used as constraints for regional tectonic interpretations and, because of the ability of moving water to transport heat, the study

also furnishes information on flow of water in regional aquifer systems. Thermal data measured during this project and geothermal exploration data not previously published from 68 wells are presented. In addition bottom hole temperature measurements from a number of hydrocarbon exploration wells are summarized. Samples (core or cuttings) were collected from many of the holes for thermal conductivity measurements (the property of the rock which measures its ability to conduct heat) and those data are presented here also.

Some of the wells were drilled for the specific purpose of geothermal evaluation. Most of these exploration holes were drilled to depths on the order of 100 to 150 m. The holes which were drilled for geothermal studies were logged for gradients and core or cutting samples were generally obtained for thermal conductivity measurement. In addition, several deep geothermal, hydrologic, and hydrocarbon exploration tests have been drilled in Idaho during the last few years. Thermal results from some of these holes will be used because of the information they contribute to the deep thermal conditions.

Previous Investigations

The Snake River Plain (Figure 1) has been a focus of several heat flow studies (Brott and others, 1976, 1978, 1981; Blackwell, 1988, 1989). The other published heat flow studies dealing with Idaho have been local in nature (Sass and others, 1971; Urban and Diment, 1975; Nathenson and others, 1980). An extensive study of the western Snake River Plain was presented by Smith (1980, 1981). In addition several reports of geothermal potential emphasizing well and spring temperatures have been published (Ross, 1971, Mitchell and others, 1980). Reports dealing with specific areas will be discussed in appropriate sections of this report. The electrical resistivity of the crust has been investigated by Stanley (1982).

GEOLOGY OF IDAHO

The State of Idaho can be divided into a number of different physiographic provinces. The relevant areas for this report are the southern provinces (solid lines) and subprovinces (dashed lines) shown in Figure 1. The provinces of interest north of the Snake River Plain are the Blue Mountains, the Southern Idaho Batholith and its Challis subdivision, and the Central Idaho Basin and Range province. The Snake River Plain is divided into four different areas consisting of the Western Snake River Plain, the Eastern Snake River Plain, the Camas Prairie/Mount Bennett Hills, and the Island Park region. South of the Snake River Plain two physiographic divisions, the Owyhee Uplands and the Southeast Idaho Basin and Range, are considered as separate areas for the purposes of this report.

The geologic features of these various provinces are well known. Within Idaho the mid-Miocene Columbia Plateau basalts lie on an older basement of Mesozoic sedimentary and igneous rocks

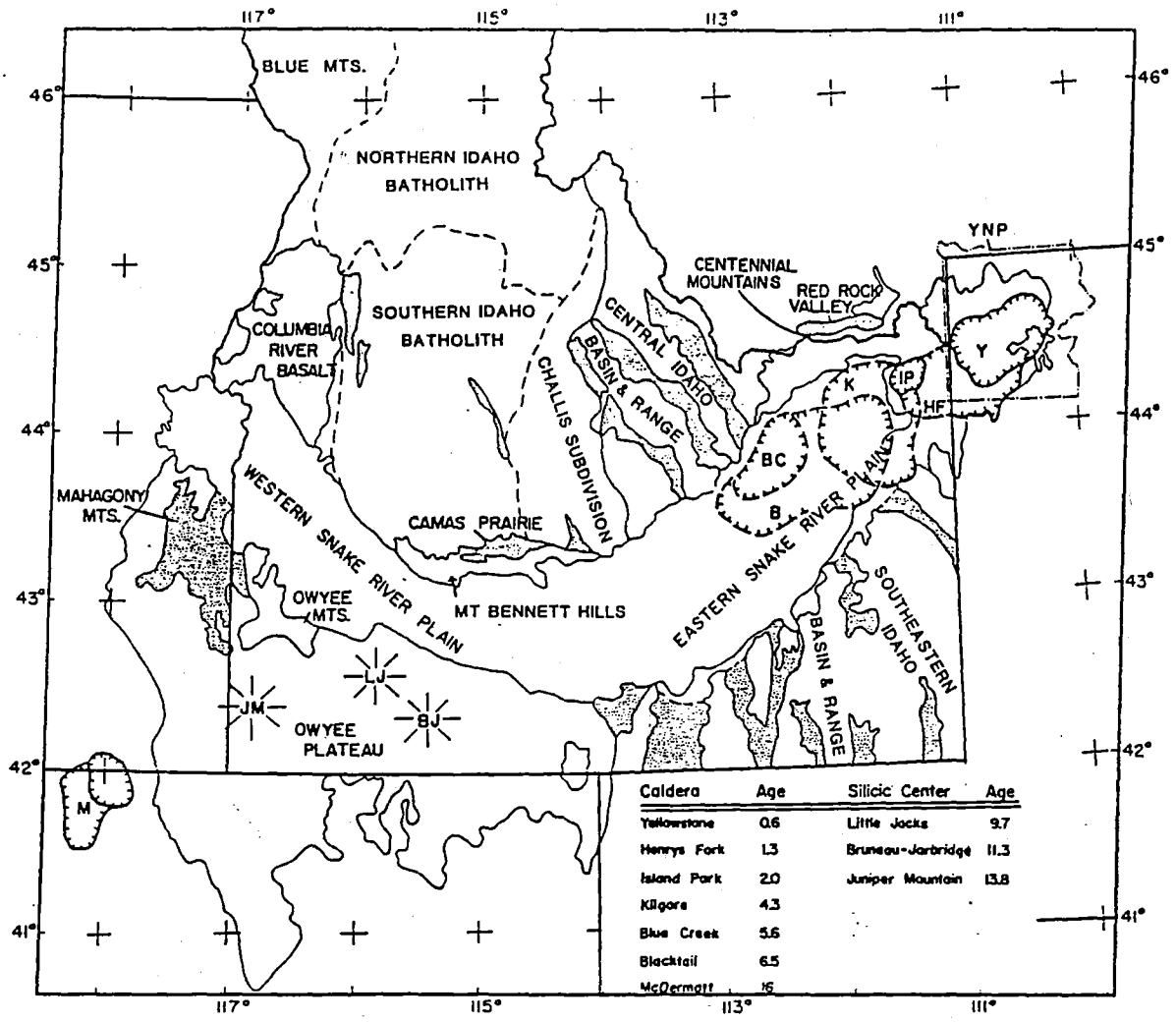

Figure 1. Physiographic province map of southern Idaho. Boundaries of major provinces are shown as solid lines, subprovinces are shown as dashed lines. The dot pattern indicates primarily alluvial-filled Basin and Range type valleys intersecting the Snake River Plain and those associated with it (Red Rock Valley, Camas Prairie and Mahagony Mountains). Location of ages of major silicic volcanic centers associated with the proposed hot spot as summarized by Malde (1991) are shown.

in the Blue Mountains and the Wallowa Mountains. The Southern Idaho batholith and the Challis sections of the Northern Rocky Mountains are composed almost exclusively of granitic and volcanic rocks. The plutonic rocks are predominantly Mesozoic in age, although an extensive early Cenozoic (Eocene) plutonic episode has also been recognized (Armstrong and others, 1975; Criss and others, 1983, 1984). The Challis region contains the eastern part of the Idaho batholith and has extensive exposures of volcanic rocks associated with this Eocene magmatic activity. These volcanic rocks sit on a complex basement of Mesozoic granitic rocks and Paleozoic to Precambrian sedimentary and metamorphic rocks. The area is crosscut by numerous linear valleys with diverse orientations. The orientation of these valleys is related to differential erosion along faults and/or zones of fracturing. This area is characterized by extensive hot spring activity that is focused along some of these major linear zones. Because of this distribution the heat flow data from the southern Idaho batholith are listed separately in Table 1.

A major portion of the Northern Rocky Mountain province in Idaho is identified as the central Idaho Basin and Range subprovince. This area is composed of Basin and Range topography and structure with high relief ranges separated by alluvial valleys. The general trend of the topography is northwest/southeast. The youthfulness of the ranges in this area is clearly indicated by the numerous young fault scraps (see summary by Crone and Haller, 1991, and paper by Turko and Knuepfer, 1991, for example) and the occurrence of the magnitude 7.3 Borah Peak earthquake beneath the Lost River valley near Mackay on October 28, 1983 (Dosier and Smith, 1985; Scott and others, 1985). The bedrock of the ranges consists of folded and thrust faulted Paleozoic and Precambrian sedimentary rocks. The structure and hydrology of this area is extremely complex.

The Snake River Plain province comprises the area of southern Idaho modified by a moving hot spot during the late Cenozoic. As a major igneous/tectonic event propagated eastward at a rate of approximately 3.5 cm/year (Christiansen and Lipman, 1972; Armstrong and others, 1975; Rogers and others, 1990), a predictable sequence of geologic events related to the response of the continental lithosphere to the passage of a very energetic thermal event (Brott and others, 1978) followed. Large scale silicic ash flows and associated caldera systems similar to those that are now characteristic of the Yellowstone Plateau formed initially. Subsequent to the passage of the hot spot, the area began to subside due to thermal contraction and basaltic volcanism became dominant. The result was an extensive plain covered by as much as 1 kilometer of basalt. This stage is represented by the eastern Snake River Plain. The site of the youngest stage of silicic volcanism now mostly covered by basalt is the area directly west of Island Park. The calderas formed during this episode of silicic volcanism between 2 and 5 MY ago have been described by Morgan and others (1984). Following continued subsidence, deposition of lacustrine and fluvatile sediments occurred in the trough resulting in the formation of a deep sedimentary basin associated with minor basaltic volcanic activity (Newton and Corcoran, 1963). This area is now represented by the Western Snake River Plain. Capture of the

TABLE 1. Average geothermal gradient and heat flow values for the various provinces. Updated from Brott and others (1981) as noted.

Province	Geothermal Gradient (°C/km)	Heat Flow (mWm^{-2})	Number
Northern Idaho			
Granite (14)	22±1	65±3	23
Basalt (9)	40±10		
Southern Idaho Batholith (Excluding SRP Margin and Geothermal Systems)	27±3	77±4	12
Wieser Area	56±5	79±7	19
Western Snake River Plain	69±3	99±4	80
Owyhee Plateau	51±4	98±7	23
Eastern Snake River Plain			
Northern Margin			
Brott and others	55±9	93±13	23
Present study-all data	61±11	109±16	17
Present study-highs out	50±6	90±9	15
Southern Margin			
Brott and others	71±7	113±11	80
present study-new data		88±23	8
Above Snake River Aquifer	18±2	27±4	125

Snake River in the last 2 Ma by the Columbia River drainage has resulted in lowering of the base level so that the trough is no longer collecting sediments (Malde, 1991). Within this simple framework there are many complexities, however. For example there are two "anomalous" east-west trending range and valley areas associated with the Snake River Plain. These are the Camas Prairie-Mt. Bennett Hills area in central Idaho, and the Centennial Mountains-Redrock Valley area of southwestern Montana.

These seemingly disparate physiographic areas are related to one another by their unusual crustal structure (see Blackwell, 1989). A typical crustal section, based on gravity and refraction experiments (Hill, 1963; Hill and Pakiser, 1965; Braile and others, 1982; Mabey, 1976, 1978) consists of an unusually thick lower crust and an unusually thin upper crust. The unique feature of the crust which underlies the Eastern Snake River Plain, Western Snake River Plain, the Owhyee Plateau, and which may be evolving under the Yellowstone region, is that it is unusually thick and mafic, even though the Snake River Plain has been interpreted as an extensional feature (rift valley). The crust is thicker because during passage of the continent over the hot spot a large intrusive body (probably of grabbroic composition) has been emplaced in the mid to lower crust. This mafic intrusive body has differentiated and also partially melted the lower and middle crust and as a result extensive magma chambers and calderas have formed in the upper crust (Brott and others, 1978, 1981; Leeman, 1982a). As part of this process, there may have been a small amount of extension as well as significant density changes associated with erosion, and with loss of the light granitic component of the crust due to voluminous ash flow expulsion (Brott and others, 1981). So as the crust (and underlying mantle) cools following the passage of the hot spot, thermal contraction may be responsible for as much as two to two-and-a-half km of subsidence, although simple analysis is complicated in the west by the formation of the sedimentary basin. The actual observed topographic surface west of Yellowstone is approximately exponential in form and drops over 1.5 km.

South of the Snake River Plain there are two major physiographic provinces, the Owyhee Uplands on the west and the southeastern Idaho Basin and Range province on the east. The Owyhee Uplands consists of an extensive volcanic plateau of late Cenozoic ash flows and basalts sitting on top of an essentially unknown basement. Relief is relatively subdued and tectonic activity in the last few million years has been relatively minor. Malde (1991) points out that this province represents a southwestward continuation of the Snake River Plain silicic volcanism associated with the hot spot track (the sites and ages of major silicic volcanism are shown on Figure 1).

The southeastern Idaho Basin and Range province is an area of complicated geology and active tectonics. The effects of late Cenozoic Basin and Range normal faulting are superimposed on the Northern Rocky Mountain thrust-fault terrain of late Mesozoic to early Cenozoic age. Sedimentary rocks of Mesozoic to Precambrian age are involved in the thrusting. The geology and hydrology of this area are extremely complex, and are of great interest at the moment. Several significant hydrocarbon discoveries have been made in the Utah portion of this province in recent years and several deep

exploration tests have been drilled in Idaho so that some information on the deep thermal character of the area is available (Ralston and Mayo, 1983). The province is crossed by the Intermountain Seismic Belt (Smith and Sbar, 1974; Arabaz and others, 1980; Smith and Arabaz, 1991) along its eastern margin. Very young volcanism has occurred in this province. The rocks are both basaltic and rhyolitic in composition and cover extensive areas near Grey's Lake and Blackfoot Reservoir.

TECHNIQUES OF HEAT FLOW MEASUREMENT

Introduction

In a thermal study of an area there are three quantities of interest. Two of these are measured and the third is calculated from measurements of the first two. The three quantities are: temperature gradient, thermal conductivity, and heat flow. In order to obtain the heat flow measurement the geothermal gradient, the rate of temperature increase with depth, and thermal conductivity of the rocks must be known. The gradient is obtained from measurements of temperature as a function of depth in drill holes. Thermal conductivity measurements must be made in the laboratory on core or cutting samples from a well or from representative outcrop samples. The laboratory technique used in this study is the divided bar measurement for core and cuttings samples (Birch, 1950; Sass and others, 1971). The units used for thermal conductivity are Watts per meter per degree Kelvin ($Wm^{-1} K^{1}$).

Disturbances to the geothermal gradients may arise from topographical features, circulation of water, temporal changes in the mean ground surface temperature, and temperature anomalies at the surface resulting from contrasts in vegetation (Blackwell and others, 1980). The geothermal gradient may also vary because of complexities in geology reflected as lateral thermal conductivity variations. In much of the Snake River Plain and the Owyhee Plateau (Figure 1) , the topographical, cultural, and vegetation disturbances are moderate and do not have significant effects on the temperature gradients. In the mountainous regions of central and northern Idaho, however, such effects cause significant gradient perturbations. Terrain corrections have been made to the holes in areas where the effects are significant. In the heat flow data tables a column titled "corrected heat flow" includes values that have been adjusted for terrain effects (if needed). Most of the heat flow determinations were made in relatively flat lying rocks or in regions of homogeneous rocks such as the granite of the Idaho batholith, therefore disturbances in gradient due to geological complications are usually small.

The units used in the present report are based on the SI system. Conversions to the cgs system of units are 41.84 mWm^{-2} equal 1 HFU, etc. In SI units the worldwide average heat flow is about 60 mWm^{-2}. Typical low values of heat flow are 20 to 40 mWm^{-2} and typical high values of heat flow are 80 to 120 mWm^{-2}. Values greater than about 120 mWm^{-2} are not usually found except in geothermal areas. The sources of all of the data collected as part of this study are listed in Appendix A.

Water Circulation Disturbances

Disturbances in geothermal gradient due to the circulation of water cannot be easily eliminated. This situation is particularly difficult because many of the holes used for heat flow determination in Idaho were originally drilled as water wells. Thus there is a possibility of water being naturally in motion in these areas. In fact the shallow thermal measurements in the eastern part of the Snake River Plain give more information on water circulation than they do on the regional temperature gradient and heat flow coming conductively from the interior of the earth.

Regional water disturbances are caused by naturally occurring water movement in and between major aquifers due to differences in piezometric levels along and between the aquifers. For example, low temperature water may enter an aquifer from the surface, causing the geothermal gradient to be decreased above the aquifer because the lower temperature water absorbs heat and transports it downward or laterally in the aquifer. In other areas down gradient the water flow may be up, i.e. the deeper aquifers may have positive potential heads. In wells where upflow occurs the geothermal gradient below the aquifer will be higher than the regional value of the geothermal gradient, while in the aquifer the gradient will be lower than the regional value (see Domenico and Palciauskus, 1973, for some simple models). Regional water circulation effects will cause similar disturbances in all wells in the same region. In other areas high temperature water from depth may enter a shallower aquifer along a fault or fracture zone and cause the geothermal gradient to be anomalously high above the shallower aquifer. These phenomena are clearly shown in some areas of the Eastern Snake River Plain discussed below.

Data Table Description

The data are presented in two tables discussed below. Wells are identified by both township-range-section and by latitude and longitude in the tables. The township range and section numbering system used by the Idaho Department of Water Resources and the U.S. Geological Survey in Idaho is used in this report. The section number is followed by up to three letters which indicate the quarter section, the 40 acre tract, and 10 acre tract, respectively. One or more numerals representing the serial number of the well within the tract may be occasionally included. Quarter sections are lettered A, B, C, D, in counterclockwise order from the northeast quarter of each section. Within the quarter sections 40-acre and 10-acre tracts are lettered in the same manner. Well 7S/19E - 23CAC is in the SW 1/4 of the NE 1/4 of the SW 1/4 of Section 23, Township 7 South, Range 19 East.

In addition, the name of each hole as shown, as is the tectonic province. The depth interval over which the geothermal gradient and heat flow were calculated is indicated. In holes that did not have a uniform gradient with depth, gradient and heat flow over several intervals are given. In cases where the

change in gradient coincides with variations in conductivity, a higher level of confidence is assigned to the calculated heat flow value. Where variations do not correspond to changes in conductivity, non-conductive influences on the heat flow data or errors in gradient or thermal conductivity values are indicated. Average thermal conductivity values and the number of thermal conductivity measurements used to calculate the average values for some holes are also shown in the tables. Thermal conductivity values in parenthesis are assumed values based on knowledge of the rock type and/or measurements on the same rock type in nearby wells or from surface samples. Since many of the measurements of thermal conductivity were made on cuttings, a major potential error source for the thermal conductivity values is a lack of knowledge of the in situ porosity of the rocks (Sass and others, 1971). Columns for corrected and uncorrected gradient, and corrected heat flow are presented. The values in the corrected gradient column indicate the gradient after corrections have been made for topographic effects. Calculated standard error values are provided for the uncorrected gradient.

In cases where both the corrected heat flow and uncorrected heat flow values are the same, the topographic effects were calculated or estimated to be less than $\pm 5\%$. The topographic corrections were made by the technique discussed by Blackwell and others (1980). Almost all of the measurements outside the Snake River Plain required terrain corrections. The error of these corrections is approximately $\pm 10\%$ of the correction. The total error in most cases will be less than $\pm 5\%$ of the corrected heat flow. No statistical error is given for corrected heat flow values because it is difficult to establish reasonable error limits that take into account the many environmental factors that might affect heat flow. Overall error estimation is given qualitatively in the column to the right of the corrected heat flow. Sites which are estimated to have heat flow values with an error of $\pm 5\%$ or less are of A quality, sites with estimated error of $\pm 10\%$ or less are of B quality, and sites with estimated errors of $\pm 25\%$ or less are of C quality. Data indicated by a G are within a geothermal system and do not reflect regional heat flow values. If no information was available on the lithology of the hole so that no heat flow can be calculated, the heat flow column is blank. A brief lithologic summary for each hole is included and the age of the rock units is given when known. In a few cases the data values for the sites shown in Table 2 will be different from published values due to collection of additional data and/or changes in interpretation based on new information. Thus these values supersede the results of the five published reports. Data published since the compilation of Brott and others (1981) are also included in this table.

TABLE 2. Thermal data from Urban and others (1986), (points with asterisks), and Blackwell (1988-unpublished).

TWN/RNG SECTION	N LAT DEG MIN	W LONG DEG MIN	HOLE (DATE)	COLLAR ELEV (m)	DEPTH RANGE (m)	AVG TCU <SE> (W/m/K)	UN GRAD <SE> (°C/km)	CO GRAD <SE> (°C/km)	CO H.F. <SE> (mW/m^2)	Q HF	LITHOLOGY SUMMARY
13N/39E 9ACC	44-28.38	111-51.85	OXY-5B 0/ 0/77	2009	30.0 40.0 60.0 82.0	(1.88)	32.8 3.6 9.1 5.6	32.8 9.1	63 17	G G	RHYOLITE
13N/40E 10CDB	44-27.80	111-43.90	OXY-6B 0/ 0/77	1981	15.0 95.0 95.0 135.0	(1.88) (1.38)	65.5 5.5 38.2	65.5 38.2	121 54	G G	RHY 1-82
13N/42E 22CAD	44-26.10	111-29.35	OXY-20 0/ 0/77	1951	10.0 100.0 100.0 150.0	(1.63) (1.63)	14.6 25.5	14.6 25.5	25 42	D D	BASALT 0-140 RHY 140-152
13N/42E 24DAD	44-26.09	111-26.25	WW-IPB2 6/24/77	1923	10.0 38.0	(1.88)	189.3 36.4	189.3	310	G	BASALT
13N/42E 25ABC	44-25.64	111-26.95	WW-IPB1 6/17/77	1926	15.0 38.0	(1.88)	121.9 9.1	121.9	201	G	SILICIC VOL
12N/44E 10BBC	44-23.00	111-15.00	OXY-18 0/ 0/77	1939	10.0 175.0 175.0 280.0	(1.88) (1.88)	 12.7	 12.7	 25	X D	RHYOLITE
12N/38E 19DAC	44-21.03	112- 0.92	OXY-4 0/ 0/77	1882	10.0 125.0 125.0 143.0	(1.88) (1.88)	21.8 67.3	21.8 67.3	42 126	D D	RHYOLITE
12N/36E 24BAD	44-20.95	112- 9.20	OXY-2 0/ 0/77	1820	60.0 150.0	(1.88)	41.9 3.6	41.9	79	C	RHY 2-90 BASALT TO TD
12N/36E 34ABC	44-19.75	112-12.13	OXY-1 0/ 0/77	1768	40.0 89.0	(1.88)	29.1	29.1	54	C	RHYOLITE
12N/42E 36CCB	44-19.20	111-27.25	OXY-19 0/ 0/77	1867	100.0 180.0 180.0 350.0	(1.63) (1.88)	52.8 65.5 1.8	52.8 65.5	88 109	B B	BASALT 5-274 CLAY 274-303
11N/41E 14BAB	44-17.30	111-35.35	OXY-15 0/ 0/77	2070	40.0 96.0	(1.63)	9.1	9.1	17	X	NO RETURNS

TABLE 2. (continued) Thermal data from Urban and others (1986), (points with asterisks), and Blackwell (1988-unpublished).

TWN/RNG SECTION	N LAT DEG MIN	W LONG DEG MIN	HOLE (DATE)	COLLAR ELEV (m)	DEPTH RANGE (m)	AVG TCU <SE> (W/m/K)	UN GRAD <SE> (°C/km)	CO GRAD <SE> (°C/km)	CO H.F. <SE> (mW/m^2)	Q HF	LITHOLOGY SUMMARY
11N/41E 15DBD	44-17.10	111-36.53	OXY-16 0/ 0/77	2060	20.0 205.0 205.0 305.0	(1.88)	-5.6 7.3 1.8	-5.6 7.3	 13	X X	BASALT 5-73 RHY 73-303
11N/41E 15BDB	44-16.95	111-35.48	OXY-14 0/ 0/77	2062	20.0 200.0 200.0 290.0	(1.88)	14.6 7.3 -5.5	14.6 -5.5	29 	X X	BASALT 8-61 RHY 61-290
9N/43E 11BDA	44- 7.45	111-20.78	OXY-17 0/ 0/77	1695	20.0 60.0 60.0 135.0	(1.88) (1.88)	12.7 1.8 (155.0) 64.0	12.7 (155.0) 64.0	17 (356) 146	X G	RHYOLITE
9N/43E 11BDA	44- 6.10	111-36.53	OXY-8 0/ 0/77	1515	30.0 133.0	(1.88)	10.9 1.8	10.9	13	X	BASALT 0-50 NO RET TO TD
9N/43E 19BDC	44- 5.55	111-25.73	STURM-1 8/29/79	1602	0.0 1210.0	2.26	(48.0)	(48.0)	(109)	C	SILICIC VOLCANICS
8N/35E 22ADA	44- 0.68	112-19.00	OXY-9 0/ 0/77	1487	30.0 157.0	(1.63)	3.6 7.2	3.6	4	X	BASALT 0-60 NO RET TO TD
6N/42E 20CAC	43-49.85	111-31.88	OXY-10 0/ 0/77	1926	10.0 145.0	(1.88)	3.6	36.0	8	X	RHYOLITE TUFF
6N/40E 31BBA2	43-48.65	111-47.15	GT-MCG1 9/ 3/81	1511	0.0 1495.0	(1.88)	(11.3)	(11.3)	(21)	X	BASALT 0-296 RHY TO 957
6N/40E 31B	43-48.58	111-47.58	RBHTW-1 1/ 5/80	1483	100.0 250.0					X	SILICIC VOLCANICS
6N/42E 35CCD	43-47.85	111-28.40	OXY-11 0/ 0/77	1780	50.0 153.0	(1.88)	9.1	9.1	17	X	BASALT 0-79 RHY 79-152
5N/40E 5CD	43-47.10	111-46.60	RBHTW-2 6/11/80	1563	10.0 393.0					G	SILICIC VOLCANICS
5N/41E 17CCC	43-45.38	111-39.85	OXY-12 0/ 0/77	1658	10.0 153.0	(1.88)	34.6	34.6	67	C	SEDIMENTS VOLCANICS
5N/41E 25ACD	43-44.05	111-34.45	OXY-13 0/ 0/77	1911	10.0 100.0	(1.88)	-7.3	-7.3		X	RHYOLITE

TABLE 2. (continued) Thermal data from Urban and others (1986), (points with asterisks), and Blackwell (1988-unpublished).

TWN/RNG SECTION	N LAT DEG MIN	W LONG DEG MIN	HOLE (DATE)	COLLAR ELEV (m)	DEPTH RANGE (m)	AVG TCU <SE> (W/m/K)	UN GRAD <SE> (°C/km)	CO GRAD <SE> (°C/km)	CO H.F. <SE> (mW/m^2)	Q HF	LITHOLOGY SUMMARY
3N/27E 9AB	43-36.50	113-14.63	WW-BUTT	1620	119.5 141.4	(1.46)	999.0	999.0	1920	G	BASALT
2N/29E 15ACA	43-30.17	112-58.95	INEL106 8/ 6/83	1524	20.0 225.0					X	BASALT
2N/29E 24DDDA	43-28.80	112-56.13	INEL104 8/ 6/83	1517	20.0 214.0					X	BASALT
2N/29E 33DCC	43-26.97	113- 0.12	INEL105 8/ 6/83	1549	20.0 225.0					X	BASALT
2N/29E 35CCC	43-26.95	112-57.95	INEL108 8/ 6/83	1534	20.0 225.0					X	BASALT
2N/30E 16CCA	43-29.67	112-53.42	INEL107 8/ 5/83	1499	20.0 210.0					X	BASALT
2N/30E 31CCB	43-27.17	112-56.10	INEL103 8/ 6/83	1527	20.0 215.0					X	BASALT
2N/30E 35DDB	43-27.12	112-50.33	INEL110 8/ 5/83	1521	20.0 225.0					X	BASALT
4S/16E 33DA	43- 1.90	114-33.35	PALACI01 6/ 9/80	1015	0.0 610.0	(1.46)	(73.2)	(73.2)	(107)	C	BASALT AND RHY TUFF
5S/14E 12AAA	43- 0.70	114-44.00	RWINK1 5/15/80	1098	0.0 610.0	(1.46)	(68.4)	(68.4)	(100)	C	BASALT
7S/15E 12CBA1	42-49.95	114-39.03	USGS-WTW 0/ 0/84	1097	70.0 342.0					X	BASALT
9S/18E 1DD	42-39.90	114-17.30	ANDCMPWW 3/27/86	1194	65.0 650.0	(1.46)	62.5	62.5	92	C	BASALT 0-237 RHY&CLAY TD
	42-14.25	113-22.10	RDH G-W* 12/18/76	1350	200.0 1498.0	(2.09)	54.0	54.0	113	C	
	42-10.10	113-25.75	USGS-ID5* 8/ 6/76	1650	76.0 128.0 140.0 216.0	1.97 2.38	63.0 45.0	61.0 43.0	120 103	A A	

TABLE 2. (continued) Thermal data from Urban and others (1986), (points with asterisks), and Blackwell (1988-unpublished).

TWN/RNG SECTION	N LAT DEG MIN	W LONG DEG MIN	HOLE (DATE)	COLLAR ELEV (m)	DEPTH RANGE (m)	AVG TCU <SE> (W/m/K)	UN GRAD <SE> (°C/km)	CO GRAD <SE> (°C/km)	CO H.F. <SE> (mW/m^2)	Q HF	LITHOLOGY SUMMARY
15S/39E 6CA	42- 8.75	111-56.71	SUN-1001 6/15/78	1446	0.0 110.0	(1.46)	857.0	857.0	1255	G	PHYLLITE AND SCHIST
15S/26E 12ACC	42- 8.00	113-21.85	USGS-ID1* 0/ 0/76	1478	50.0 260.0	1.09	120.0	120.0	131	A	CENOZOIC SEDIMENTS
15S/26E	42- 6.50	113-23.50	SCHMITT*	1500	0.0 126.0	> 1.05	63.5	63.5	> 106	G	CENOZOIC SEDIMENTS
15S/26E 22DDD	42- 5.85	113-23.61	USGS-ID3* 8/11/76	1487	20.0 330.0	1.67	200.0	200.0	335	G	CENOZOIC SEDIMENTS
15S/26E 25ABC	42- 5.55	113-21.75	USGS-ID2* 1/15/76	1475	20.0 190.0	1.30	210.0	210.0	335	G	CENOZOIC SEDIMENTS
	42- 4.95	113-36.60	USGSALM2* 8/ 8/76	1700	50.0 200.0	(2.09)	52.0	52.0	109	C	
	42- 0.75	113-12.30	STREVELL* 10/17/75	1675	75.0 220.0	(2.09)	56.0	56.0	117	C	

THERMAL DATA NORTH OF SNAKE RIVER PLAIN

Northern Idaho and Blue Mountains

A summary of the geothermal gradients and heat flow for the northern and western part of the state of Idaho is listed in Table 1 and shown in Figure 2. North of the Snake River Plain and west of the Central Idaho Basin and Range the heat flow/temperature gradient measurements indicate that heat transfer is primarily by conduction and interpretation of the results is straightforward. Histograms of geothermal gradients and heat flow are shown in Figure 2. Average gradients range from approximately 40°C/km in Columbia River basalt to 22°C/km in granite and in the Belt Series rocks. These variations reflect differences in the average thermal conductivity of the rock because the variation in heat flow values is quite small, as shown by the histogram in Figure 2. The average heat flow for this area of Idaho is 65 ± 3 mWm^{-2} based on 23 determinations. Taking onto account the low heat production due to radioactivity of the crust in this area (Swanberg and Blackwell, 1973), this value is typical of the heat flow in the Northern Rocky Mountains in the United States and Canada (Blackwell, 1978; Davis and Lewis, 1984), including areas in Washington and Montana. Furthermore, adding the heat flow component from radioactivity of typical granites (about 20 mWm^{-2}), this average heat flow value is identical to heat flow values in the Basin and Range province (Roy and others, 1972; Blackwell, 1978). Thus this heat flow pattern is characteristic of the conductive heat flow for much of the interior part of the North American Cordillera from British Columbia to central Mexico where active volcanism has not taken place in the last 10 to 15 m.y. (Blackwell, 1978, Blackwell and others, 1991).

Southern Idaho Batholith and Challis Section

The thermal regime in the southern part of the Idaho batholith is somewhat different than that in northern part of the Idaho batholith because there are major effects on the heat flow associated with deeply circulating groundwater. Hot springs are common in the southern part of the Idaho batholith and locally these hot springs occur along major topographic lows with a spacing of only a few kilometers. Estimates of the heat loss from the hot springs within this area using the geochemical temperatures and observed flow rates suggest a total heat loss from the hot springs that is more than 4×10^7 W (Ross, 1971; Mitchell and others, 1980; and Lewis and Young, 1980a, 1982). This value corresponds to 10 to 20% of the regional heat flow in this area of Idaho, so that major effects on the conductive transport pattern can be expected.

The regional heat flow in the granitic rocks of the batholith is well characterized. The gradients and heat flow values are generally of high quality and were obtained from either cored mining exploration

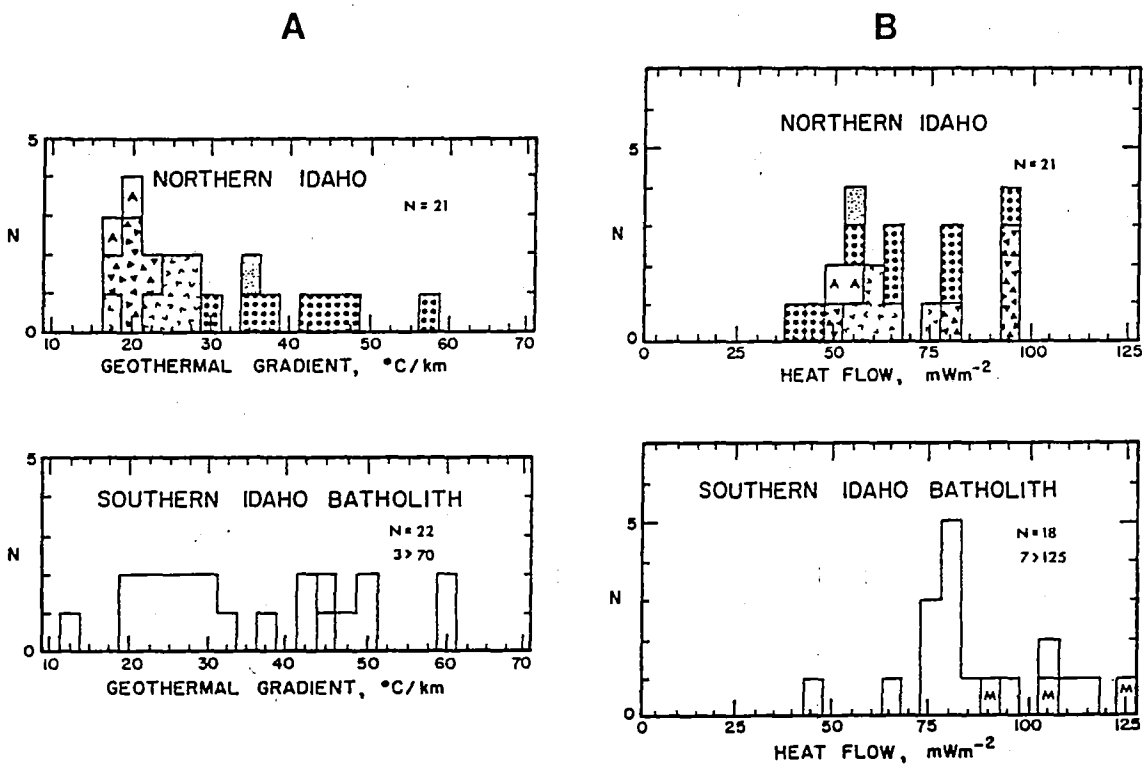

Figure 2. Figure 2a. Histograms of geothermal gradient for northern Idaho and the southern Idaho batholith. The dominant lithology at each site is shown by a pattern (granite, caret; basalt, large dots; Precambrian sediments, triangles; unconsolidated sediment, dots; andesite, A). Figure 2b. Histograms of heat flow for northern Idaho and the southern Idaho batholith. The dominant lithology of each site is shown by the same pattern as in Figure 2a. M indicates holes near the margin of the Snake River Plain. Other sites with heat flow values in excess of 80 mWm^{-2} are associated with hot spring systems.

holes or from holes drilled specifically to investigate the regional heat flow (Blackwell, 1989). Histograms of gradient and heat flow are shown in Figure 2. The average "background" values are about 26°C/km and about 75 mWm^{-2}. These values are consistent with the heat flow observed in the back-arc region of the western United States (Blackwell, 1978; Blackwell and others, 1991). The values are slightly higher (about 10 mWm^{-2}) than the heat flow in Northern Idaho and along the Snake River because of the heat generation of the granitic rocks in the batholith. The holes considered to represent "background" are at least 10 km from the nearest hot spring or major topographic lineament and are not near the margin of the Snake River Plain. High heat flow values (greater than $85mWm^{-2}$) coincide with hot spring locations/lineations or the margin of the Snake River Plain.

The Challis section as shown on Figure 1 is a subsection of the Southern Idaho batholith. Geothermal data are very sparse in this area, consisting primarily of a series of holes in the Eocene Challis volcanics and Paleozoic sediments near the town of Challis and in the Bayhorse mining district. Two holes near the Salmon River are in the east edge of the Idaho batholith. All the data sites are shown on Figures 7 and 13 below. Average heat flow values of this small data set appear to be 10-20% higher than in the Idaho batholith and gradients are significantly higher because the volcanic rocks have lower thermal conductivity than the granites. Significant high heat flow anomalies occur in the Bayhorse mining district (12N/8E) and along the Salmon River (hole 11N/14E-21ccd). The anomalous value along the Salmon River is not surprising because this part of the Salmon River flows along a major hot spring lineament. The high geothermal gradients and heat flow in the Bayhorse mining district are not near any known geothermal manifestation and suggest the presence of a blind geothermal system in this area. The data are geographically too sparse to draw detailed conclusions about the characteristic heat flow in this region at this time.

As part of this study heat flow data were obtained from two localities in this province (not including sites at the edge of the Snake River Plain to be discussed below): at Challis in two holes 750 and 600 m deep; and in the Mackay area in shallow exploration holes. The temperature-depth curve for the deepest Challis hole as well as a deep hole in the Idaho batholith (DDH-3) are shown in Figure 12 (below) for comparison to the data from the Snake River Plains to be discussed.

Central Idaho Basin and Range

Geologically and tectonically the Central Idaho Basin and Range province differs from the remainder of the provinces north of the Snake River Plain. Because of the undeveloped nature of the area, very little is known about the hydrology and the geothermal character away from the margin of the Eastern Snake River Plain. A few low quality sites show low gradients in shallow holes drilled for mineral or water exploration. Several relatively high quality geothermal gradients and heat flow values have been obtained in the vicinity of the Gilmore Mining district (13N/26E and 27E). Heat flow values in the

bedrock of the Lemhi Range are 55-59 mWm^{-2}, significantly below average values elsewhere in the greater Northern Rocky Mountain province. On the other hand the gradient in a deep hole in the adjacent Lemhi River valley is 84°C/km and the estimated heat flow is greater than 105 mWm^{-2}. As is the case with the Southeastern Idaho Basin and Range province, deep drill holes are need to evaluate the intrinsic thermal characteristics of this province.

The only deep thermal data are bottom hole temperature measurements (BHT) measurements from several hydrocarbon exploration wells drilled near the Idaho/Montana border in the general vicinity of the Lima anticline (Perry and others, 1983) and two wells drilled in Birch Creek and Lemhi Valleys. The average gradients are shown in Table 3 (below) for the wells in Idaho using corrected BHT's. There has not been sufficient time nor funds to complete analysis of the lithology and heat flow for these wells. Unlike some of the wells described in the Southeastern Idaho Basin and Range described in a later section, none of these wells appear to have gradients in excess of 40°C/km. The deepest well, the EXXON Meyers Federal Unit #1 reaches an uncorrected BHT of 197°C at 5.7 km.

THERMAL CONDITIONS IN SOUTHWESTERN IDAHO

Western Snake River Plain

The geothermal character of the Western Snake River Plain was first studied in detail by Brott and others (1976, 1978). Subsequent studies were carried out by Smith (1980, 1981). The Weiser and the Bruneau-Grand View-Oreana areas have been the object of several studies (Young and others, 1978, 1982; Lewis and Young, 1980b). New data and reinterpretations of some of the data contained in the papers by Brott and others (1976, 1978) and by Smith (1980, 1981) are included in the data tabulated by Blackwell (1988 and 1989). The broad outlines of the distribution are quite clear. The results are demonstrated by a heat flow map of the western Snake River Plain shown in Figure 3. The contours in Figure 3 near the Oregon border are based on data from the western Snake River Plain in Oregon (Blackwell and others, 1978). This map has been discussed in detail by Blackwell (1989). Areas of contrasting heat flow and geothermal gradient are shown on Figure 3 and identified by name for ease of reference in this discussion. Typical heat flow values in the high heat flow regions are 120-150 mWm^{-2}, while in the low heat flow region of the central Western Snake Plain the values are less than 80 mWm^{-2}.

There are over twenty holes in the depth range 300 to 500 m in this area. The data within the Western Snake River Plain in general fall into two categories. These categories correspond to areas of relatively high gradient and heat flow (on the order of 100°C/km and 120 to 150 mWm^{-2}), and areas of moderate gradients (about 40°C/km) and average heat flow values (60-80 mWm^{-2}). Histograms of gradient and heat flow are shown in Figure 4. Most of the gradients range between 45 and 85°C/km.

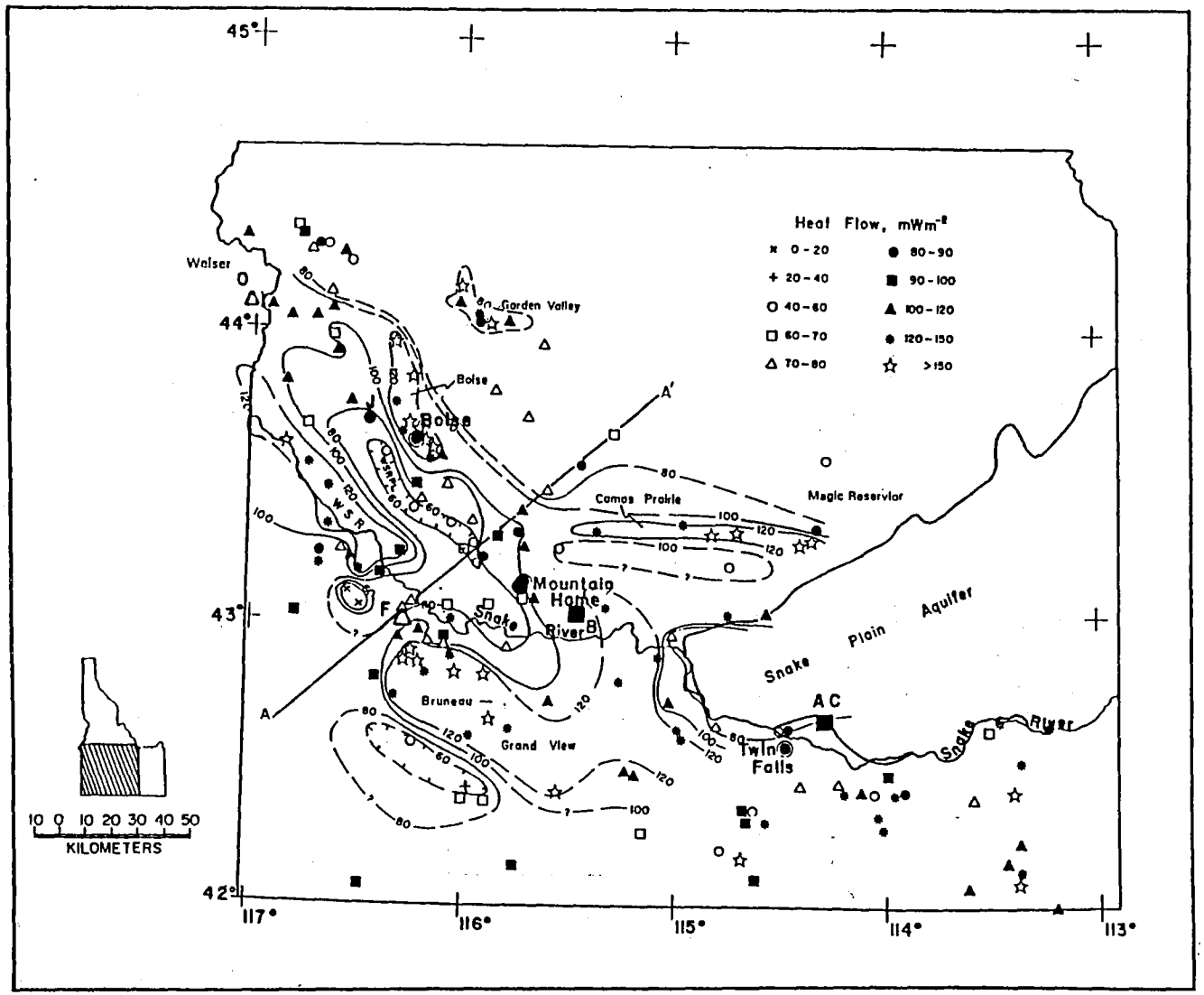

Figure 3. Detailed heat flow map of southwestern Idaho. Contours of heat flow at 20 mWm^{-2} intervals are shown. Locations of deep wells discussed by Blackwell (1989) are shown (WSRPL is low heat flow band and WSR is western Snake River high heat flow anomaly). The line of the cross section (AA') in Figure 5 is shown. The deep wells discussed in the text are identified by a letter, i.e. O is Ore-Ida #1 well, B is Bostic well, AC is Anderson Camp well, J is James well and F is Federal 60-13 #1 well.

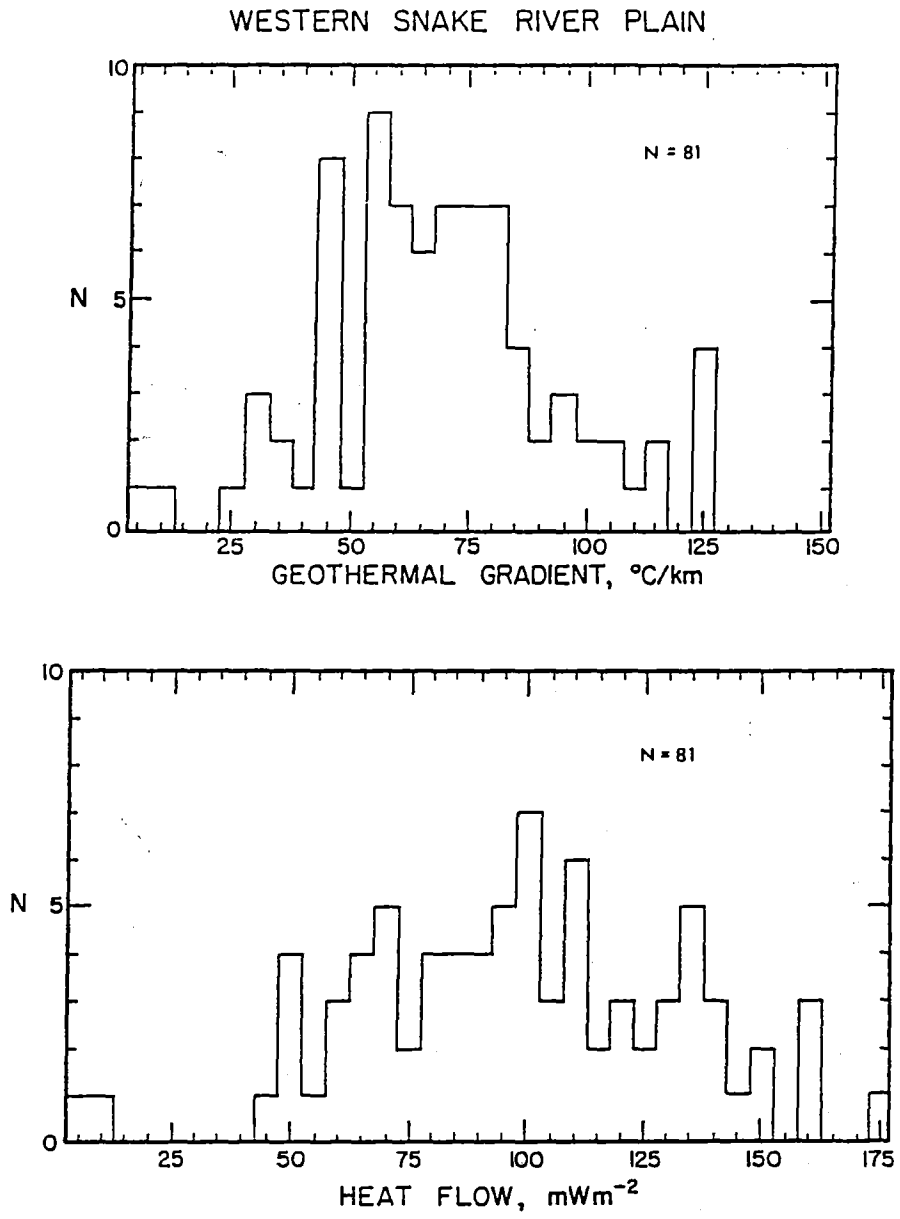

Figure 4. Histograms of geothermal gradient and heat flow for the Western Snake River Plain area. The holes are all in basalt or sedimentary rocks.

Heat flow values range from 50-150 mWm^{-2} with an average of 100 ± 10 mWm^{-2}. The lithology in most of the holes is lacustrine sediment with a few of the holes drilled in basalt. Areas of high heat flow are distributed in two bands along the northern and southern margins. Lower gradients and heat flow are found along the axis of the Snake River Plain between Caldwell and Mountain Home.

A heat-flow cross-section is shown in Figure 5. The line of the section is shown on Figure 3. The observed pattern was discussed in detail by Brott and others (1978) on the basis of a substantially smaller data set. With additional data the origin of some parts of the pattern has now become clearer. Deep drilling in the Boise area and in the Bruneau-Grand View region has demonstrated that the high heat flow values there are related to intermediate temperature (40-80°C) geothermal systems and relatively local geothermal anomalies. Typical temperature-depth curves in the Boise front geothermal system and in the Bruneau-Grand View geothermal system show isothermal or low gradient sections starting between 80 and 280 m with temperatures of 40 to 80 °C. The occurrence of warm water in wells along the Snake River has been described by Lewis and Young (1980b). Geochemistry suggests that maximum temperatures in the geothermal systems are 70-100°C. Thus the high gradients and heat flow that are measured in holes 50-200 m deep do not project to great depth. Maximum temperatures in the depth range 200-500 m in the wells range up to 80°C. This pattern of heat flow and gradient is due to systematic regional flow of groundwater toward the edges of the Snake River Plain from the higher elevation margins. Very low heat flow that may represent part of the recharge system occurs south of the Bruneau-Grand View area (see Figure 3). At the edge of the Snake River Plain hydraulic boundaries cause upflow, which gives rise to the geothermal systems at the various locations. The effects on the heat flow are generally modest, however, because the average heat flow values observed are only on the order of 50-100% above the regional background values. The approximate heat flow pattern is shown by the dashed lines on Figure 5. Outside the areas of most active fluid flow, temperature-depth curves are linear to depths of at least 400-500m, and in the case of the Bostic 1-A well (4S/3E-25cbb, Arney and others, 1982, Arney, 1982) to a depth of 2500m (see Blackwell, 1989).

High gradients and heat flow values are also found in holes drilled in granitic rocks on both margins of the Snake River Plain (Urban and Diment, 1975; Brott and others, 1978; Blackwell, 1988, 1989). The high heat flow in these rocks, presumably not associated with the regional groundwater flow systems, is related to the large scale nature of crustal disruption associated with the Snake River Plain margins (Brott and others, 1978). These holes are shown by a special symbol on Figure 3.

The heat flow values that may represent regional conductive values are connected on Figure 5 by a solid line. The regional heat flow is about 100 mWm^{-2} south of the Snake River Plain and about 75 mWm^{-2} north of the Snake River Plain. In the center of the Snake River Plain the heat flow is about 60-75 mWm^{-2}; the heat flow on the margins is 25-50% higher than in the center because of the thermal conductivity refraction effect discussed by Brott and others (1978).

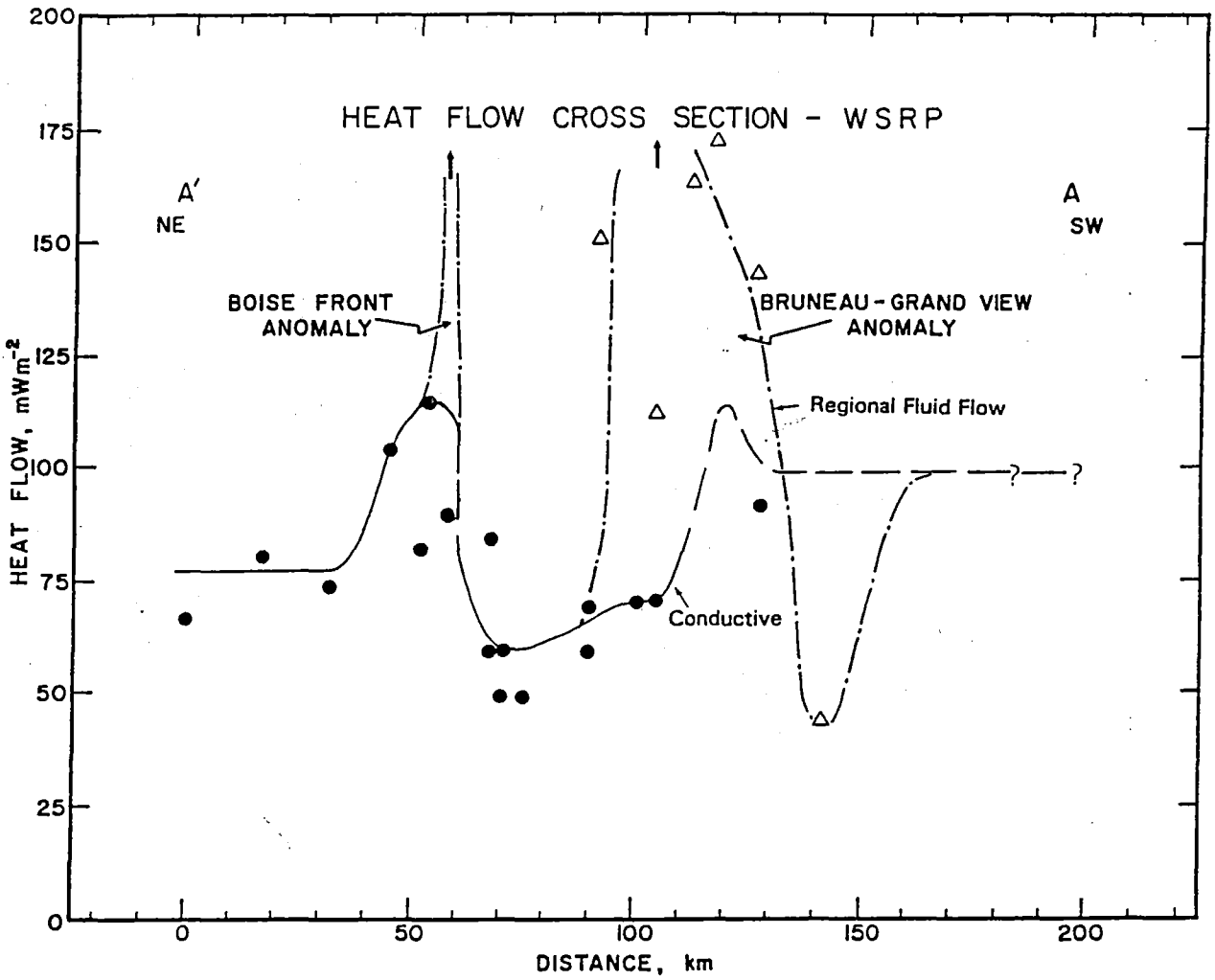

Figure 5. Heat flow cross section of the Western Snake River Plain. The line of the cross section is shown on Figure 3. Points on the cross section are shown by dots. Generalized heat flow east and west of the line of the section is shown diagramatically and the geothermal areas identified. Dots represent heat flow values least influenced by shallow convective fluid flow, and the triangles represent heat flow values affected by convection.

Owyhee Uplands

The Owyhee Uplands province is south of the Snake River Plain. It is a low relief volcanic plateau built on a largely unknown basement. The boundary between the Snake River Plain and the Owyhee Upland is not abrupt at the surface but is marked in the subsurface by buried faults. These structures may be the hydrologic barriers that locate the geothermal systems of the Western Snake River, Bruneau-Grand View, and Twin Falls areas. The south to north lateral flow model of the geothermal systems proposed by Young and Lewis (1982) suggests that lower than regional heat flow values should be characteristic of shallow depths over at least part of the province (see Figure 3).

Histograms of geothermal gradient and heat flow are shown in Figure 6. Gradients range from over 75°C/km to 16°C/km. The low values may be due to regional down flow because the two lowest values are directly south of the Bruneau-Grand View area. The average geothermal gradient in the province is 51 ± 4°C/km and the average heat flow is 98 ± 7 mWm^{-2}. These values are not well determined because the data spacing away from the margin of the Snake River Plain is large. The gradient average for the Owyhee Plateau is less than in the Western Snake River Plain, but the difference in heat flow is not significant. The rocks in the Owyhee Plateau holes are mostly silicic volcanic rocks that have higher thermal conductivity values than the sedimentary rocks in the Western Snake River Plain; consequently the lower gradients coupled with the higher thermal conductivity result in a similar heat flow.

Camas Prairie/Mt. Bennett Hills

The Camas Prairie/Mt. Bennett Hills area is discussed separately as it is not clearly part of the Idaho batholith or Snake River terrains. The general geothermal features have been discussed by Mitchell (1976a). Walton (1962) calculated an average gradient of 92°C/km based on the increase in flowing temperature with well depth in the artesian wells in the valley, a value that is verified by the gradients measured in wells in the Camas Prairie. The holes are in low thermal conductivity clays, but estimated heat flow values (100-123 mWm^{-2}) are significantly above those in the adjacent Idaho batholith. The gradients should decrease with depth in the valley and decrease by a factor of approximately 100% when the basement is encountered.

There are extensive exposures of Quaternary basalts in the area. These Quaternary basalts have been cut by normal faults in several locations, demonstrating both active volcanism and tectonism in this area within the last few million years. Mitchell (1976a) reports geochemical data from 79 m deep well (1S/17E-23aab1) at the northern end of Magic Reservoir with a flowing temperature of 74°C. Based on the assumption that the hot water has mixed with shallow groundwater he argues for a possible subsurface temperature as high as 200°C.

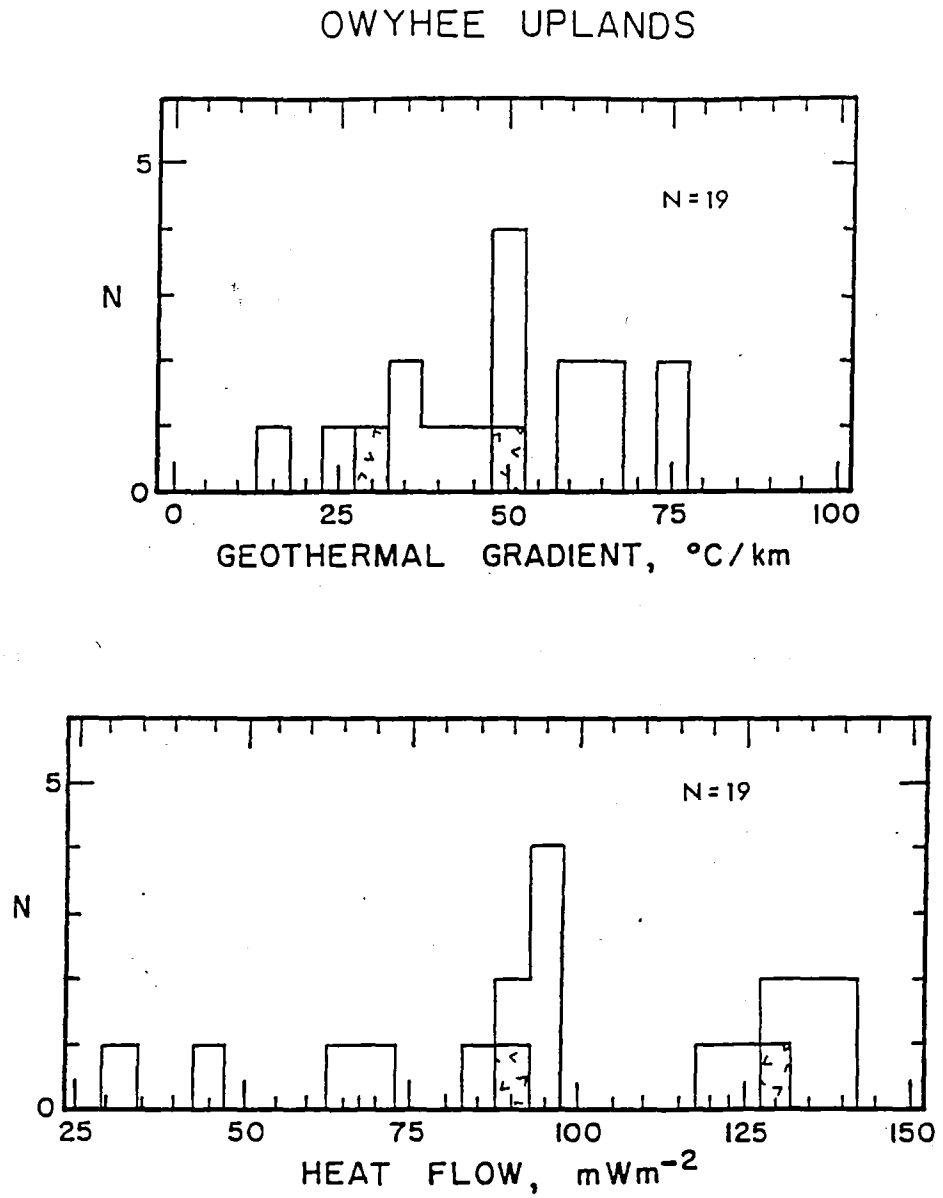

Figure 6. Histograms of geothermal gradient and heat flow for the Owyhee Plateau. Holes in granite are shown by the caret pattern.

Heat flow data from two holes that were drilled for geothermal studies in granite of the Idaho batholith about 5 km west and southwest of the hot well near Magic Reservoir and one water well 5 km south of the hot well were presented by Brott and others (1981). In addition new data from 10 geothermal exploration test wells are presented here for the first time (see Table 2). Outside the geothermal system, the background heat flow values average about 100 mWm^{-2} for sites in granite and volcanic rocks. Based on a contouring of the anomalous heat flow values a conservative estimate of the anomalous conductive heat loss from the Magic Reservoir system is 10 MW. Gradients of over 125°C/km occur along the west side of Magic Reservoir for a distance of 7 km. Thus the area may have a major geothermal system present at depth.

Unfortunately, all of the holes are relatively shallow and little is known about the deep thermal conditions. Struhsacker and others (1982; see also Leeman 1982b) dated the nearby ash flows and a silicic flow. The K-Ar ages they obtained ranged from 4.9 to 6.0 m.y. compared to 3.1 m.y. for the Wedge Butte rhyolite dome 10 km southeast of the hot well (Armstrong and others, 1975) and about 10-11 m.y. for the Mt. Bennett Hills rhyolites (the typical age of volcanism associated with the Snake River Plain hot spot). The ages of 6 m.y. or less are much younger than the age of the hot spot event that generated the Mt. Bennett Hill rhyolites and suggests long continued or recurrent silicic volcanism in this area. Leeman (1982b) has suggested that the rhyolites near Magic Reservoir and Wedge Butte mark the ring of a large caldera system. However, Struhsacker and others (1982) argue that these ages, although relatively young, are too old to support the hypothesis that residual heat from the silicic magma chamber associated with the ash flows is the source of the heat for the geothermal anomaly. Thus the heat source is either deep groundwater circulation in the typical Snake River Plain margin thermal setting, remnant heat associated with the young basaltic volcanism, unusually deep circulation along fractured areas associated with the young faulting, a more recent phase of silicic intrusion with no surface effects, or some combination of these possible causes. The background heat flow is similar to that shown in Figure 5 along the northern margins of the Western Snake River Plain.

THERMAL CONDITIONS IN THE EASTERN SNAKE RIVER PLAIN

New Thermal Data

Geothermal data from 45 holes in eastern Idaho are listed in Table 2. Data categories shown in Table 2 and in Table 3 are discussed above. Terrain corrections were applied to the few holes for which such corrections were necessary. The data included in the Table 2 , which are discussed by Blackwell (1988, 1989), were collected between 1980 and 1990 and were not available to Brott and others (1981). Several sets of data from geothermal exploration projects have become available and are included in Table 2. These sets of data include holes drilled for geothermal gradient studies in the

Eastern Snake River Plain and within the Island Park caldera to depths of up to 300 m. Data from two deeper gradient test wells in southeastern Idaho, 450 m and 2.5 km deep, are also included. In all cases there are sufficient data on thermal conductivity to calculate heat flow values for the sites if the quality of the gradient is appropriate.

Data from 36 holes with detailed temperature data and 31 hydrocarbon tests with BHT data are listed in Table 3. These data are from sites visited in 1991 for this study and collected from government and SMU files not available to Blackwell (1988, 1989). These data include 1991 temperature logs for 14 wells up to 1.5 km deep, wells from geothermal gradient exploration data sets along the margin near Craters of the Moon and in the vicinity of Magic Reservoir, and temperature data for three deep geothermal test wells from the files of the Idaho Department of Water Resources. Also included are locations and estimated gradients to depths in excess of 5 km based on BHT's for 30 hydrocarbon exploration test wells located in eastern Idaho.

The data from most of the wells in the Snake Plain aquifer do not represent heat flow measurements in the conventional sense (see discussion by Brott and others, 1981, and below). The data are summarized in Figures 7 and 13 (below) where the 'corrected' heat flow values from Tables 2 and 3 and the 'above' heat flow values (see below) from Brott and others (1981) are plotted (for locations where two or more wells are too close to be resolved, a representative value is shown).

Snake River Plain Aquifer

The data shown within the solid line in Figure 7 are from wells that bottom in or pass through the Snake River Plain aquifer. The predominant lithology of these holes is basalt, although volumetrically minor interbeds of sedimentary rocks are present. The interval gradient and heat flow data from wells located within the boundary of the Snake River Plain aquifer as shown in Figure 7 can be divided into as many as three heat flow regimes identified as 'above,' 'in,' and 'below' the aquifer system, as discussed by Brott and others (1981). Abbreviations for these categories are shown in place of the heat flow quality in Tables 2 and 3. The 'above' regime appears to be generally conductive; the heat flow is controlled by the difference between the mean annual surface temperature and the local aquifer temperature and may be negative over large areas. Within the top tens of meters of the aquifer the heat flow regime is convective and the temperatures are approximately isothermal due to the mixing of circulating fluid. Below the aquifer system the heat flow regime is little known because only a few holes are deep enough to sample subaquifer conditions. The bottom of the aquifer is generally associated with an increase in the alteration of the basalts due low grade metamorphism in association with age or burial depth.

TABLE 3a. Thermal data for holes logged in 1991.

TWN/RNG SECTION	N LAT DEG MIN	W LONG DEG MIN	HOLE (DATE)	COLLAR ELEV (m)	DEPTH RANGE (m)	AVG TCU <SE> (W/m/K)	NO TCU	UN GRAD <SE> (°C/km)	CO GRAD <SE> (°C/km)	CO H.F. <SE> (mW/m^2)	Q HF	LITHOLOGY SUMMARY
13N/18E 4ABD	44-29.39	114-20.52	SHAMA872 8/20/91	2246	200.0 592.0	(4.11)		20.3	18.3	75	A	LOWER PALEO SLATE & DOLO
13N/18E 3BCCA	44-29.33	114-19.20	SHAMA861 8/20/91	2088	300.0 840.0	(4.11)		24.3	21.9	90	A	LOWER PALEO SLATE & DOLO
9N/33E 3D	44- 8.08	112-33.65	SULLIVAN 8/ 8/91	1565	46.0 60.0	(2.30)		123.3 3.8	123.3	285	G	RHYOLITE
7N/42E 8AA	43-57.23	111-31.28	UN-ST-08 8/ 5/80	1637	0.0 1023.0	(1.46)		67.0	67.0	98	C	RHYOLITE
7N/42E 7DCB	43-56.63	111-32.70	UN-ST-07 12/15/81	1609	0.0 890.0	(1.46)		83.0	83.0	122	C	RHYOLITE
7N/22E 13BCB	43-56.37	113-48.04	BVRC-2 9/22/91								C	
6N/31E 13CDD	43-50.56	112-42.28	TAN-CH2 7/29/91	1460	30.0 286.0	(1.46)		13.3	13.3	19	X	BASALT
4N/26E 5BCD	43-42.08	113-23.43	ANDERSON 7/24/91	1666	20.0 86.0						X	BASALT
4N/27E 21ABB	43-40.00	113-14.68	JACOBOT1 7/31/91	1689	20.0 74.0			16.2 0.1	16.2		X	ALLUVIUM
4N/27E 29	43-38.50	113-15.95	JACOBWW1 7/31/91	1652	20.0 126.0			25.8	25.8		X	ALLUVIUM
3N/41E 5BCCA	43-37.28	111-39.80	BYINGTON 8/ 6/91	1530	16.0 82.5	(1.46)		156.1 0.2	156.1	230	G	BASALT
3N/27E 9DBAA	43-36.14	113-14.48	RICHRDSN 10/21/80	1617	0.0 275.0	(1.46)		167.0	167.0	244	G	BASALT AND GRAVEL
					51.8 228.6	(1.46)		179.8 13.6	179.8	264	G	
3N/24E 11CDD	43-35.84	113-33.96	CHAMPAGN 7/23/91	1993	20.0 180.0			156.0 6.7			G	
					100.0 180.0	2.34 0.21	7	105.5 1.3	105.5	247	G	
3N/30E 16DDD	43-34.55	112-52.52	INEL-WO- 9/26/91		570.0 1517.0			46.0	46.0		C	

TABLE 3a. (continued) Thermal data for holes logged in 1991.

TWN/RNG SECTION	N LAT DEG MIN	W LONG DEG MIN	HOLE (DATE)	COLLAR ELEV (m)	DEPTH RANGE (m)	AVG TCU <SE> (W/m/K)	NO TCU	UN GRAD <SE> (°C/km)	CO GRAD <SE> (°C/km)	CO H.F. <SE> (mW/m^2)	Q HF	LITHOLOGY SUMMARY
1N/22E 22CAA	43-24.13	113-49.43	CAR-4212 11/16/81		30.5 57.8			37.8 0.2	837.8		D	BASALT AND SAND
					30.5 104.6	1.67	2	19.9	19.0	32	D	
1N/24E 19DAC	43-24.08	113-38.31	CAR-4211 11/27/81		30.5 100.0	3.85	3	12.5	12.5	48	D	QUARTZITE & SHALE
1N/23E 25DB	43-23.33	113-39.60	CAR-4209 11/28/81		61.0 91.4	2.34	5	23.7 0.8	22.7	53	D	QTZT TO 33M SLATE TO TD
1N/23E 32AAA	43-22.93	113-44.00	CAR-4203 11/24/81		50.0 146.5	3.14	4	29.7	28.3	89	C	SHALE AND SILTSTONE
1N/23E 31	43-22.03	113-45.84	CAR-4201 11/24/81		51.8 103.2	3.72	2	33.8 0.5	32.2	120	C	QUARTZITE
1S/17E 24ACA	43-19.49	114-22.98	UMR-13 8/23/78	1478	45.7 152.4	1.67	5	91.5	91.5	155	G	BASALT, PUMICE & GRV
1S/17E 23BDC	43-19.38	114-24.50	UMR-12 8/ 9/78		70.1 121.9	2.18	3	218.4	218.4	460	G	BASALT AND CLAY/GRAVEL
1S/17E 26DBC	43-18.25	114-24.34	UMR-10 9/ 6/78	1481	15.2 42.7	(1.46)		(200.0)	(200.0)	176	G	CLAY/SAND & BASALT
					42.7 67.1	(1.46)		(200.0)	(200.0)	460	G	
1S/18E 30CDA	43-18.24	114-21.90	UMR-11 7/29/78	1606	45.7 152.4	2.63 0.21	6	50.8	53.5	141	G	GRANODIORITE & CLAY
2S/17E 3BAB	43-17.18	114-25.68	UMR-9 8/ 9/78	1490	9.1 39.6	1.46	1	60.1	60.1	88	X	BASALT, CLAY & ANDESITE
2S/18E 8ACC	43-15.98	114-21.18	UMR-8 6/13/78	1494	18.3 79.2	1.92	4	92.3	92.3	176	C	BASALT AND CLAY/GRAVEL
2S/17E 13CDC	43-14.65	114-23.28	UMR-7 7/21/78	1467	51.8 121.9	1.59	5	80.4	80.4	4	B	TUFF, BASALT WELDED ASH
2S/18E 20DDC	43-13.79	114-22.30	UMR-16 9/21/78	1455	15.2 137.1	2.05 0.17	6	53.1	53.1	109	B	SILICIC VOLC
2S/18E 29CBD	43-13.13	114-21.10	UMR-6 7/10/78	1425	85.3 97.5	(1.59)		50.4	50.4	79	X	BASALT AND CLAY/GRAVEL

TABLE 3a. (continued) Thermal data for holes logged in 1991.

TWN/RNG SECTION	N LAT DEG MIN	W LONG DEG MIN	HOLE (DATE)	COLLAR ELEV (m)	DEPTH RANGE (m)	AVG TCU <SE> (W/m/K)	NO TCU	UN GRAD <SE> (°C/km)	CO GRAD <SE> (°C/km)	CO H.F. <SE> (mW/m^2)	Q HF	LITHOLOGY SUMMARY
2S/17E 27CCA	43-13.03	114-25.81	UMR-17 8/21/78	1600	91.4 152.4	1.59 0.17	5	65.3	65.3	104	B	TUFF & BASALT
3S/17E 2DBB	43-11.49	114-24.15	UMR-5 7/11/78	1518	109.0 149.5	(1.46)		85.0	85.0	126	B	TUFF
3S/17E 14BC	43- 9.90	114-24.66	UMR-18 9/18/78	1497	91.4 152.4	1.59 0.17	3	63.5	63.5	101	B	SILICIC VOLCANICS
3S/18E 19BAC	43- 9.23	114-22.15	UMR-4 6/30/78	1398	73.1 88.4	(1.46)		76.1	76.1	113	X	BASALT AND CLAY/GRAVEL
4S/35E 22BCA	43- 3.68	112-21.18	FTHALL-2 8/ 2/91	1422	30.0 152.0			99.3 0.2	99.3		G	
					0.0 178.0	1.67 0.17	3	90.0	90.0	151	G	
5S/36E 8BBB	43- 0.41	112-16.50	FTHALL-1 8/ 2/91	1472	100.0 161.2	(1.67)		52.8 0.5	52.8	88	C	
7S/41E 25	42-47.20	111-36.70	SUNHUB25 10/ 4/82	1890	600.0 2300.0	(1.83)		30.0	30.0	55	C	CENO & MESO SEDIMENTARY
1S/17E			UMR-20 9/22/78	1530	30.5 61.0	1.51	3	76.4	76.4	113	D	BASALT

TABLE 3b Thermal data from hydrocarbon exploration wells

TWN/RNG SECTION	N LAT DEG MIN	W LONG DEG MIN	HOLE (DATE)	COLLAR ELEV (m)	DEPTH RANGE (m)	AVG TCU <SE> (W/m/K)	GRAD <SE> (°C/km)	H.F. <SE> (mW/m^2)	LITHOLOGY SUMMARY
15N/27E 19CBD	44-36.60	113-17.36	MILFORD	1898	0.0 3009.9		26.0 1.0		PALEO & MESO SED. ROCKS
14N/35E 14AC	44-32.43	112-18.37	MEYERFED	2116	0.0 5648.3		36.0 3.0		PALEO & MESO SED. ROCKS
13N/34E 24A	44-26.69	112-23.88	TARGHEE	2356	0.0 4649.4		33.0 1.0		PALEO & MESO SED. ROCKS
12N/28E 16CDB	44-22.08	113- 7.71	IDSTATE1	2095	0.0 2043.1		27.0 1.0		PALEO & MESO SED. ROCKS
5N/45E 9AC	43-46.55	111- 8.89	HANSENA1	1853	0.0 2541.1		36.0		PALEO & MESO SED. ROCKS
5N/44E 26BAB	43-44.14	111-13.99	COOK26_1	1856	0.0 2003.2		44.0 3.0		PALEO & MESO SED. ROCKS
5N/44E 28CD	43-43.50	111-16.03	HRSESHOE		0.0 3867.9		38.0 8.0		PALEO & MESO SED. ROCKS
5N/44E 33ABA	43-43.32	111-16.00	BEVANS1	2003	0.0 2755.7		32.0 1.0		PALEO & MESO SED. ROCKS
5N/44E 34BCB	43-43.11	111-15.54	MINER34	2017	0.0 1132.3		27.0		PALEO & MESO SED. ROCKS
3N/45E 16DCB	43-34.87	111- 8.92	VBAGLEY	1862	0.0 3268.1		26.0 4.0		PALEO & MESO SED. ROCKS
2N/44E 4DC	43-31.46	111-16.51	MSPNRCNY		0.0 4259.3	3.64	22.0 2.0	80	PALEO & MESO SED. ROCKS
2N/44E 20BC	43-29.36	111-18.44	GRNDVLLY	1920	0.0 4931.1	3.28	25.0 2.0	82	PALEO & MESO SED. ROCKS
2S/41E 2ACA	43-16.65	111-37.05	KING-2-1 0/ 0/78	2012	0.0 3810.0		(60.0)		PALEO & MESO SED. ROCKS
2S/44E 2	43-16.36	111-15.81	TJWEBER1	2429	0.0 2963.3		50.0 3.0		PALEO & MESO SED. ROCKS
2S/44E 23DB	43-13.80	111-15.75	BEMTN 1 0/ 0/50	2473	0.0 1545.0		(61.0)		PALEO & MESO SED. ROCKS
3S/45E 35CC	43- 6.85	111- 8.35	BLACKMTN	2493	0.0 4158.1		28.0 1.0		PALEO & MESO SED. ROCKS

TABLE 3b (continued) Thermal data from hydrocarbon exploration wells

TWN/RNG SECTION	N LAT DEG MIN	W LONG DEG MIN	HOLE (DATE)	COLLAR ELEV (m)	DEPTH RANGE (m)	AVG TCU <SE> (W/m/K)	GRAD <SE> (°C/km)	H.F. <SE> (mW/m^2)	LITHOLOGY SUMMARY
4S/45E 6	43- 6.33	111-13.35	BALDMTN2	2369	0.0 3830.7	(2.42)	33.0 2.0	80 5	PALEO & MESO SED. ROCKS
3S/45E 36CC	43- 6.30	111- 7.05	BMFED-1 0/ 0/77	2693	0.0 4158.0		(22.0)		PALEO & MESO SED. ROCKS
4S/45E 5AA	43- 6.26	111-12.03	BALDMTN1	2499	0.0 2747.8		31.0 1.0		PALEO & MESO SED. ROCKS
4S/42E 9AAC	43- 5.40	111-31.80	GENVA1-9 9/18/80	2080	0.0 2877.0	(2.07)	61.5 0.2	127 20	PALEO & MESO SED. ROCKS
5S/44E 2?	43- 0.75	111-15.90	STOOR-A1 11/27/80	2059	0.0 4483.0		39.0 7.0		PALEO & MESO SED. ROCKS
5S/45E 6DC	43- 0.39	111-13.64	TINCUPMT	2431	0.0 5059.7	(2.40)	36.0 2.0	85 5	PALEO & MESO SED. ROCKS
6S/44E 16AB	42-54.18	111-17.90	IDST_A1	2038	0.0 4952.1		36.0 2.0		PALEO & MESO SED. ROCKS
10S/46E 8BDA	42-34.20	111- 6.08	FED-1-8 0/ 0/78	2337	0.0 5105.0		35.0 3.0		PALEO & MESO SED. ROCKS
10S/43E 13DCD	42-32.85	111-18.46	BCF-1-13 0/ 0/79	2070	0.0 3551.0		(43.0)		PALEO & MESO SED. ROCKS
10S/46E 20DD	42-32.10	111- 5.55	FEV-1 0/ 0/76	2294	0.0 1194.0		27.0		PALEO & MESO SED. ROCKS
10S/46E 28BDD	42-31.65	111- 5.10	AM-T1-W1 0/ 0/63	2285	0.0 1219.0		34.0 7.0		PALEO & MESO SED. ROCKS
13S/44E 22CCD	42-16.35	111-18.00	JEN21-11 0/ 0/78	1806	0.0 3500.0		24.0		PALEO & MESO SED. ROCKS
16S/46E 6BBA	42- 3.90	111- 7.50	NRCF6-21 0/ 0/80	2055	0.0 3537.0		26.0		PALEO & MESO SED. ROCKS
16S/46E 10BC	42- 2.85	111- 4.05	GRF-10-1 0/ 0/78	2323	0.0 3615.0		25.0		PALEO & MESO SED. ROCKS
16S/45E 21BBC	42- 1.20	111-12.15	NEF22-11 0/ 0/80	2103	0.0 2618.0		(20.0)		PALEO & MESO SED. ROCKS

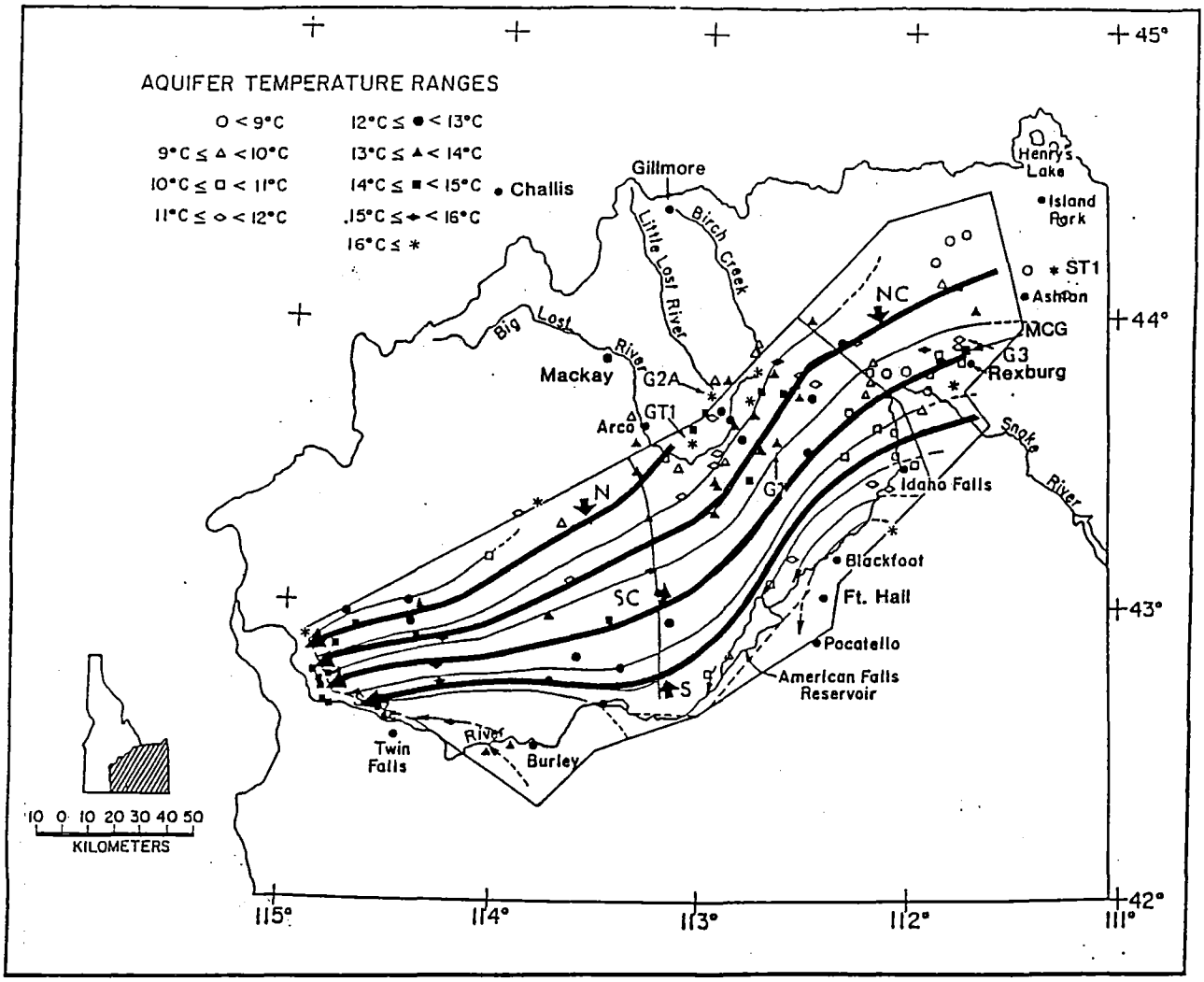

Figure 7. Temperatures and site location map of the Snake River aquifer. The Snake Plain aquifer outline is generalized. The solid and dashed lines around the edges show the locations of recharge and discharge respectively (after Mundorff and others, 1964). The NNW-SSE trending solid lines show the location of the Mud Lake (western) and Arco (eastern) hydrological barriers (after Hasket and Hampton, 1979). The aquifer temperatures are listed in Brott and others (1981). The locations of six deep (i.e., >400 m) holes are shown. Each WSW-ENE line is a flow line representing 18.5 $m^3 s^{-1}$ of water flow. Flow paths for temperatures plotted in Figure 11 are heavy lines indicated by N, NC, SC, and S labels. Modified after Brott and others (1981).

In a significant fraction of the holes the 'above' category temperatures are disturbed by the 'vesicular' basalt effect (Brott and others, 1976), which is characterized by an exaggerated annual effect that may penetrate to 100 to 150 m in depth in areas where the water table is deep, as opposed to the theoretical depth of penetration of 10 to 20 m for conductive heat flow conditions. This effect is probably related to areas of extremely porous basalt in the near surface. No 'above' values of gradient or heat flow are reported for holes that display this disturbance.

The Snake River Plain aquifer is approximately 95 km wide and 300 km long (Mundorff and others 1964). The heavy solid lines along the margins of the Snake River Plain on Figure 7 show the recharge areas, and the dashed lines show the discharge areas of the aquifer. The E-W lines in the aquifer are flow lines. Each flow line on the figure represents 18.5 $m^3\ s^{-1}$ flow of ground water, about 10% of the total aquifer flow. The two solid lines that cross the aquifer show the locations of the Mud Lake (eastern) and Arco (western) hydrologic barriers. The water table drops approximately 30 to 60 m across each of these barriers. Hasket and Hampton (1979) suggested that these barriers may be sediment zones on the 'downstream' side of old centers of volcanic activity that now are covered by younger basalt flows. Wells in the aquifer are shown on Figure 7 with the observed aquifer temperature given by the coded symbols. Generally, the aquifer temperature ranges from 8 to 9°C in the recharge zones to 14 to 15°C in the discharge zone. The temperatures in the central part of the aquifer vary from 10 to 20°C, with a general trend toward high aquifer temperatures to the west.

The hydrological features of the Snake River Plain aquifer have been extensively described by Mundorff and others (1964), Norvitch and others (1969), Hasket and Hampton (1979), Lindholm (1985), Whitehead (1986), Garabedian (1989) and many others. The total discharge of the aquifer is approximately 185 $m^3\ s^{-1}$ and occurs primarily on the western edge of the aquifer at Thousand Springs. Reported horizontal flow rates range from about one to several meters per day, but the average horizontal flow rate is less than 1.6 km yr^{-1}. In the western part of the Snake River Plain aquifer the younger flows (basalt of the Snake River Group) that contain the aquifer system overlie a thick sequence of older basalt flows, consolidated sedimentary rocks, and silicic volcanic rocks of Cenozoic age (Malde and Powers, 1962). In general the permeability of these older rocks is less than that of the Snake River Group, and they are not considered to be part of the aquifer system. Moreland (1976) reported that a large number of the springs in the canyon walls at Thousand Springs occur at the contact between the Tertiary and Quaternary basalts. Whitehead and Lindholm (1985) found that the permeability in a test well near Wendell (7S/15E-12cbal) decreased drastically at the contact between the older and younger basalts, i.e. the Banbury/Snake River basalt contact.

Snake River Plain Aquifer Thermal Model

Brott and others (1981) presented a transient two-dimensional Snake River Plain aquifer thermal

model (reproduced in Figure 8). The illustrated results were obtained by a finite difference solution of the two-dimensional heat flow equation with a one-dimensional velocity term. Because of its importance to understanding the thermal character of the Eastern Snake River Plain, the model of Brott and others (1981) is briefly summarized here. The aquifer parameters used in the thermal model were selected to be consistent with the hydrological models of Mantei (1974) and Moreland (1976). The heat flow at the base of the model was obtained from the finite-width, moving-source regional model discussed by Brott and others (1981). The surface geothermal gradient profile without convection is shown above the model (dashed line at top of Figure 8). The individual isotherms without convection (which are not shown) have approximately the same shape as the topographic surface.

The model velocity assumed for the flow in the aquifer was 1 km yr^{-1} (about 3 m d^{-1}). The active convection zone shown in Figure 8 extends from approximately the Island Park area to Thousand Springs. The top of the convection zone is the water table. The thickness of the aquifer was assumed to range from about 200 to over 300 m. The temperature distribution does not change above and within the aquifer after a period of circulation of about 10,000 years. The temperature distribution below the aquifer calculated by Brott and others (1981) shown in Figure 8 corresponds to the numerical solution after convection has occurred for a period of 100,000 years. The actual temperatures below the aquifer will depend on the history of evolution of the aquifer. In the case of the INEL-GT1 and USGS-2A wells the heat flow is constant below the aquifer to a depth of 3 km. This result (see below) implies that either the effective surface thermal boundary condition is given by the base of the aquifer, not the actual surface of the earth so that the heat flow below the aquifer is not affected by the flow, or that the aquifer has existed in its present condition for several hundred thousand years. The temperatures shown in Figure 8 are consistent with observation in either case. At a lateral distance of a few kilometers from the aquifer its effects on temperatures are negligible. In the model the calculated gradient profile above the aquifer becomes positive approximately 100 km 'downstream' from the inflow region, indicating that the fluid has been heated to a temperature greater than the surface temperature.

The simple two-dimensional aquifer model was developed to evaluate the effects of rapid groundwater flow and to see if such effects could explain the observed temperature-depth curves. The model is not to be taken literally because of its simplicity. For example, the western inflow regions (of which there are several) are not taken into account. In addition, many of the pertinent aquifer parameters are uncertain.

Comparison of Snake River Plain Aquifer Model to Observed Data

Brott and others (1981, Figures 5-7) compared temperature-depth curves observed in the Eastern Snake River Plain to the predictions shown in Figure 8. As another illustration of the aquifer effects,

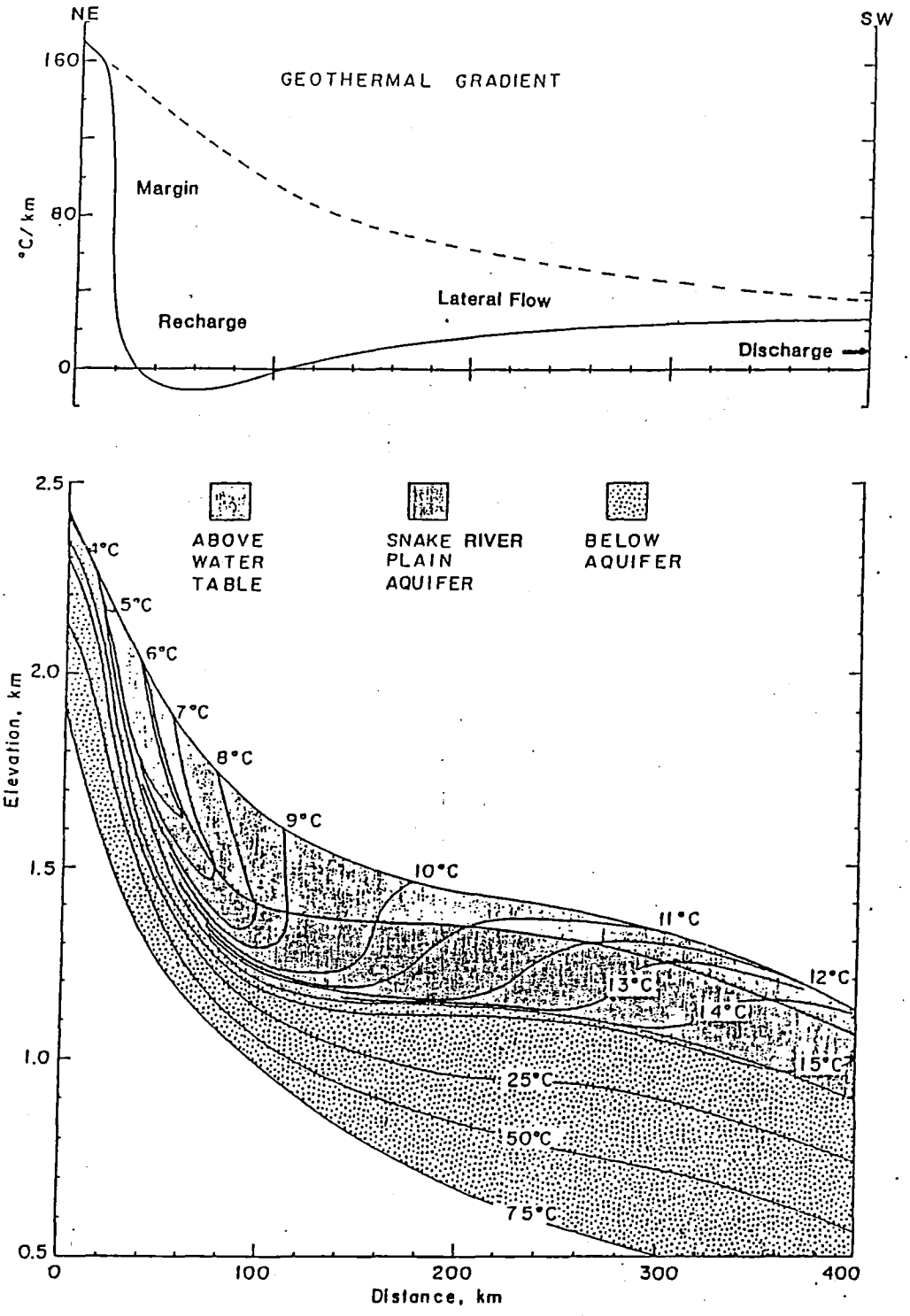

Figure 8. Two-dimensional, transient, three layer Snake Plain aquifer model. The upper layer represents the rocks above the aquifer; the mechanism for the transport of heat in this layer is purely conductive. The center layer represents the aquifer convection zone and the mechanisms for the transport of heat are convection and conduction. The lower layer is below the aquifer, and the mechanism of heat transfer is purely conductive. The surface geothermal gradient profiles before initiation of convection and in the presence of convection are shown above the model (dashed and solid lines, respectively). The cross section is oriented parallel to the plain. Figure from Brott and others (1981).

temperature-depth curves observed in wells on the Idaho National Engineering Laboratory (INEL) are shown in Figure 9 arranged in map format. Outside of the aquifer, regional to supraregional heat flow and gradient values are typical. The highest gradients shown on Figure 9 are observed in wells along the west side of the INEL near the margin of the Eastern Snake River Plain (numbers 19, 22, and 23). In addition Ross (1971) reported data from well 3N/27E-9ab1 at Butte City about 3 km east of Arco where a temperature of 42°C was measured at a depth of 150 m. Temperature data from the nearby Idaho Roses well (3N/27E-9baa) indicate a consistent increase of temperature to at least 240 m and a temperature of 50 °C based on mercury thermometer readings in the bailer as the well was drilled (see Figure 10). The behavior of the gradient at greater depth is unknown. Zero or negative temperature gradients probably occur at some depth, as is typical of other places along the margins.

The temperature-depth curves of wells in the recharge areas of the aquifer show negative or very low temperature gradients and heat flow, and very low aquifer temperatures. Examples are wells ANP-7, PW, 8, and 86. These characteristics occur because the recharge water, which originates mainly from snow melt at higher elevations in the areas north of the Snake River Plain, is at a lower temperature than the mean annual surface temperature of the recharge areas at the sides of the Snake River Plain. The aquifer thermal model (see Figure 8) is two-dimensional, whereas in reality, water enters the aquifer at many locations along the aquifer boundary (see Figure 7).

As the groundwater becomes heated in the aquifer, the temperature of the water becomes equal to, or greater than, the mean annual surface temperature. In this lateral flow region of the aquifer the gradients become positive. At greater distances from the recharge zones or in regions of low flow rate or higher heat flow from below the aquifer, gradients increase with flow distance. Temperature-depth curves at various locations in the aquifer show that gradients become positive at a distance of 10-100 km from the recharge areas of the aquifer. Holes on the INEL test site demonstrate this change as higher gradients above the aquifer occur away from the vicinity of the Big Lost River, Little Lost River, and Birch Creek sink (recharge) areas. As shown in Figure 9 most of the wells away from the recharge areas have positive gradients and show a trend of increasing aquifer temperatures as a function of time or distance from the input point. Almost all of the wells in the southeast half of the INEL site have positive, but low (10 to 15 °C/km), gradients, and aquifer temperatures increase from 8 to 9°C in the recharge areas to values of 14 to 15°C at the discharge point at Thousand Springs. The model shown in Figure 8 has a monotonic trend of increasing geothermal gradient and surface heat flow from negative values in the recharge areas to values of about 25 °C/km and 60 mWm^{-2}, respectively, in the discharge area of the aquifer. These observed trends and their magnitude on INEL are consistent with the predictions based on the two-dimensional model. Also shown in Figure 9 is the close geographic association of wells which do, and do not, show the "vesicular" basalt effect (HW1 and HW2; 15 and 12; 23 and 17).

temperature-depth curves observed in wells on the Idaho National Engineering Laboratory (INEL) are shown in Figure 9 arranged in map format. Outside of the aquifer, regional to supraregional heat flow and gradient values are typical. The highest gradients shown on Figure 9 are observed in wells along the west side of the INEL near the margin of the Eastern Snake River Plain (numbers 19, 22, and 23). In addition Ross (1971) reported data from well 3N/27E-9ab1 at Butte City about 3 km east of Arco where a temperature of 42°C was measured at a depth of 150 m. Temperature data from the nearby Idaho Roses well (3N/27E-9baa) indicate a consistent increase of temperature to at least 240 m and a temperature of 50 °C based on mercury thermometer readings in the bailer as the well was drilled (see Figure 10). The behavior of the gradient at greater depth is unknown. Zero or negative temperature gradients probably occur at some depth, as is typical of other places along the margins.

The temperature-depth curves of wells in the recharge areas of the aquifer show negative or very low temperature gradients and heat flow, and very low aquifer temperatures. Examples are wells ANP-7, PW, 8, and 86. These characteristics occur because the recharge water, which originates mainly from snow melt at higher elevations in the areas north of the Snake River Plain, is at a lower temperature than the mean annual surface temperature of the recharge areas at the sides of the Snake River Plain. The aquifer thermal model (see Figure 8) is two-dimensional, whereas in reality, water enters the aquifer at many locations along the aquifer boundary (see Figure 7).

As the groundwater becomes heated in the aquifer, the temperature of the water becomes equal to, or greater than, the mean annual surface temperature. In this lateral flow region of the aquifer the gradients become positive. At greater distances from the recharge zones or in regions of low flow rate or higher heat flow from below the aquifer, gradients increase with flow distance. Temperature-depth curves at various locations in the aquifer show that gradients become positive at a distance of 10-100 km from the recharge areas of the aquifer. Holes on the INEL test site demonstrate this change as higher gradients above the aquifer occur away from the vicinity of the Big Lost River, Little Lost River, and Birch Creek sink (recharge) areas. As shown in Figure 9 most of the wells away from the recharge areas have positive gradients and show a trend of increasing aquifer temperatures as a function of time or distance from the input point. Almost all of the wells in the southeast half of the INEL site have positive, but low (10 to 15 °C/km), gradients, and aquifer temperatures increase from 8 to 9°C in the recharge areas to values of 14 to 15°C at the discharge point at Thousand Springs. The model shown in Figure 8 has a monotonic trend of increasing geothermal gradient and surface heat flow from negative values in the recharge areas to values of about 25 °C/km and 60 mWm^{-2}, respectively, in the discharge area of the aquifer. These observed trends and their magnitude on INEL are consistent with the predictions based on the two-dimensional model. Also shown in Figure 9 is the close geographic association of wells which do, and do not, show the "vesicular" basalt effect (HW1 and HW2; 15 and 12; 23 and 17).

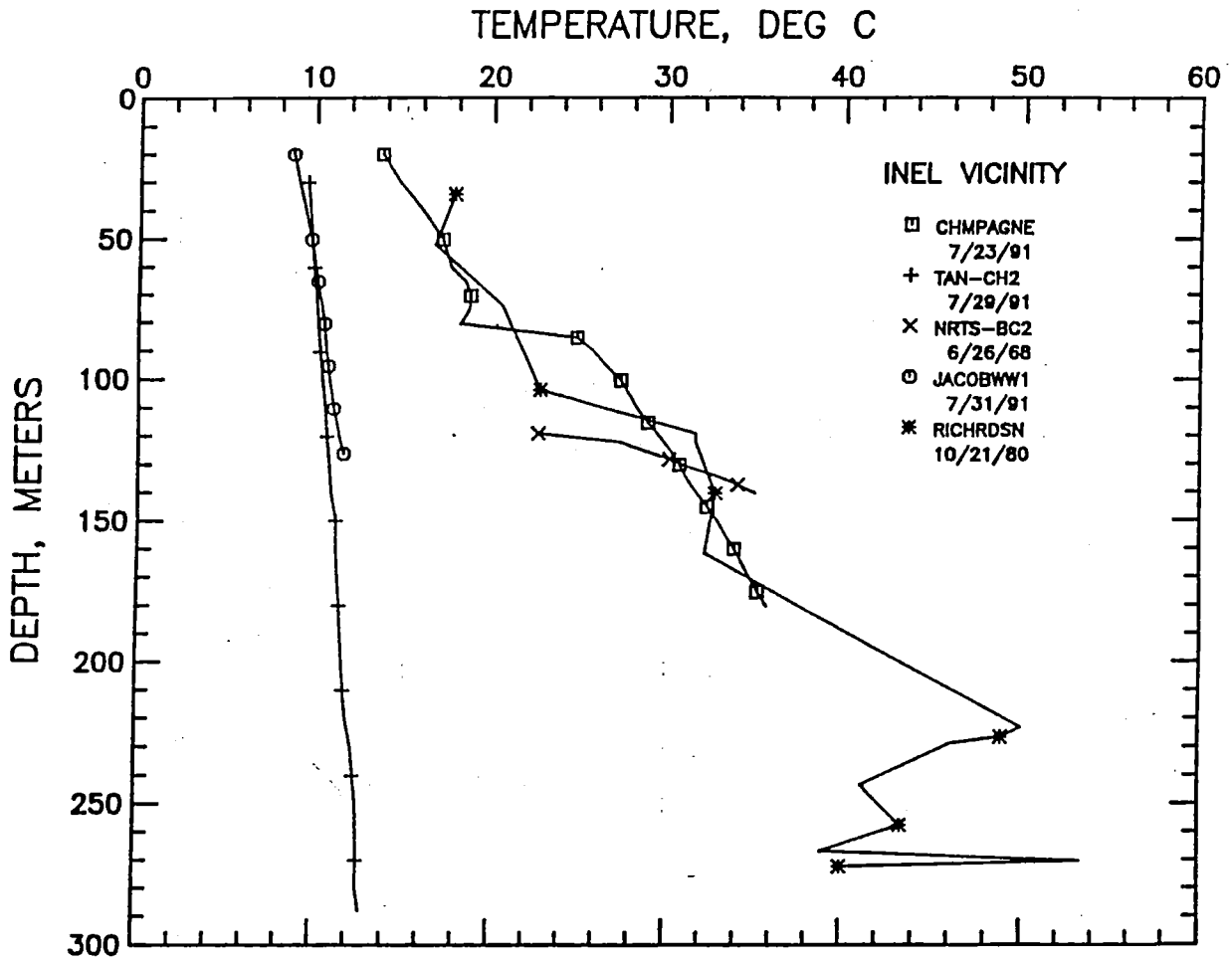

Figure 10. Temperature-depth curves of several wells on and in the vicinity of INEL obtained in 1991. Every 5th point is plotted.

As another way of evaluating the thermal effects of the aquifer, the observed aquifer temperatures as a function of distance of flow and residence time of the water in the aquifer were analyzed. Temperatures in wells along four flow paths (marked N, NC, SC, S in Figure 7) are plotted as a function of distance from the recharge point (Figure 11a) and average residence time in the aquifer (Figure 11b). The residence times in Figure 11 were calculated by assuming a permeability of 0.8 km d^{-1}, a flow rate of 18.5 m^3s^{-1}, and the geometry of the water table given by Mundorff and others (1964). The results in both cases show an increase in aquifer temperatures downstream, although there is significant scatter. Most of the scatter is near the recharge area or margins of the aquifer. This scatter may be due to the inclusion of areas influenced by thermal discharge from the moderate temperature geothermal systems typical of the margins. If so this water appears to be rapidly diluted since the downstream temperatures are more consistent and lower on the average. Regardless of the input temperatures the aquifer temperature approaches 14-15 °C at the discharge point. No major anomalies have been found in the central part of the aquifer.

The highest temperatures in the aquifer are along the north-central (NC) path and in fact occur on the INEL site. The temperature-depth curves shown in Figure 9 illustrate that the temperatures are much higher in the aquifer north and west of the course of the Big Lost River after it passes Arco. The 'above the aquifer 'heat flow values are 60 to 100 mWm^{-2}, well in excess of typical values at similar longitudinal sites elsewhere in the aquifer. Thus the warm aquifer exploited at Butte City may be extensive along the end of the Lost River Range and thus may be present on the INEL site.

Some constraints on the heat flow distribution were obtained during the summer's logging. Data from the Idaho Roses well were obtained, a well was logged north of Butte City (4N/27E-29cad), and a water well was logged at the Champagne Mine west of Arco (3N/24E-11cdd). These temperature-depth curves are shown in Figure 10. The data from the TAN-2 well on the INEL site are also shown on the plot as is a log from another well in Butte City from the USGS INEL office files (Roger Jensen, personal communication, 1991). The gradient and heat flow values in the Champagne mine water well northeast of Craters of the Moon are almost twice the regional values, and a temperature of 33°C was measured at the bottom of the well. Even though the well is at least 5 km from the edge of the Snake River Plain and in low permeability shale and quartzite, it must be associated with a previously unknown geothermal system along the margin of the Snake River Plain. Regional values of heat flow were encountered in two geothermal exploration wells at the margin west of the Craters of the Moon (Table 3, wells 1N/23E-32aaa and 31cdd). A single BHT point from an 846 m deep well between the Champagne mine and the Craters of the Moon is 32 °C (compare to the temperature of 33°C at only 180 m in the Champagne well); this data point is of limited usefulness by itself, but it is consistent with the regional gradient values determined near the Craters of the Moon. The presence of significant geothermal systems along the north margin of the Snake River Plains seems to be required by the results now available.

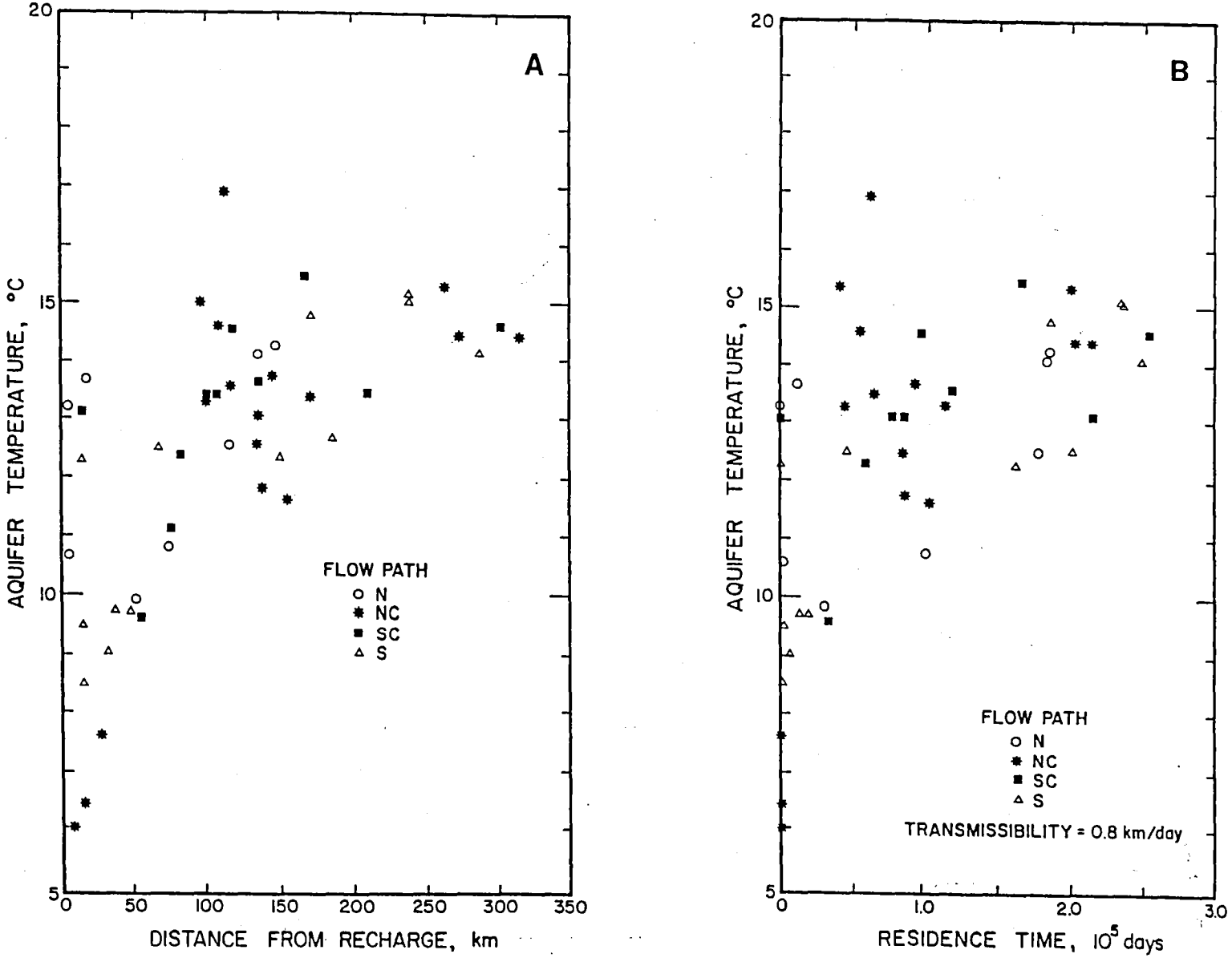

Figure 11. Figure 11a. Aquifer temperature versus distance along the northern, north- central, south-central, and southern part of the Snake Plain aquifer. Figure 11b. Aquifer temperatures versus residence time along the northern, north-central, south-central, and southern part of the Snake Plain aquifer. The locations of the flow paths are given in Figure 7.

Heat Flow Below the Aquifer

Temperature-depth curves of several wells that are deeper than 500 m (see heat flow data section) are shown in Figure 12. Four of the wells shown in Figure 12a are on the INEL site near the northern margin of the aquifer east of Arco (see Figures 7 and 13, and Tables 2 and 3). The positive gradient starting at 400 m in USGS-G2A marks the lower boundary for the aquifer at this locality. INEL-GT1 (Doherty and others, 1979) has a positive gradient beginning near 250 m, apparently indicating a shallower and thinner aquifer compared to the site of USGS-G2A. However, the INEL-GT1 temperature-depth curve (Figure 12a) shows local gradient disturbances at 800 m and 1050 m. These disturbances are due to slow flow along fracture zones. Below the aquifer, wells USGS-G2A and INEL-GT1 have similar heat flow values of 110 and 107 mWm^{-2} (Table 4).

The heat flow in both wells is constant below the aquifer to, in the case of INEL-GT1, depths as great as 3130 m, as discussed in detail by Blackwell (1990). To explain the constant heat flow in INEL-GT1 from 1 to 3 km, the aquifer must have either been in existence in its present thermal conditions for several hundred thousand years, or the crust above the base of the aquifer is transparent, i.e. the true surface boundary condition (at essentially the surface temperature) is the base of the aquifer. Thus the aquifer appears to have a minimal effect on the heat transfer below the aquifer in this area.

During the summer of 1991 a new deep well was drilled on the INEL site, WO-2. The well was completed at a depth of 1524 m on September 24, 1991 and was logged on September 26, 1991 (Figure 12a). The temperatures are definitely not in equilibrium, but the overall trends are clear. There is a major zone of downflow, probably just in the well bore, between about 250 and 550 m. The major reentrants in the log below that depth are associated with zones of major fluid loss during the drilling process. The gradient looks like it will be dominated by conduction below 500 m with the temperatures being lower than GT1 at a depth of 750 m and higher by 3 to 5 °C at total depth. No thermal conductivity measurements have been made on the core at this point, but the values will probably be somewhat lower than those in INEL-GT1. The heat flow is probably within 10% of that in INEL-GT1 and USGS-G2A.

The USGS-G1 well, located between East and West Twin Buttes, is most distant from the edge of the Snake River Plain. It has the lowest temperatures and heat flow of the deep wells. It is also the shallowest and, based on the low heat flow, probably does not penetrate below the thermal effect of the aquifer.

Also shown for comparison on Figure 12a are temperature-depth plots from two deep wells in the area north of the Snake River Plain. Well DDH-3 is in central Idaho near Idaho City in Idaho batholith granite, and the SHAMA 86-1 well is in Lower Paleozoic metasediments near the town of Challis. The heat flow value for DDH-3 is 79 mWm^{-2}. The gradient for DDH-3 is 26 °C/km, which is markedly

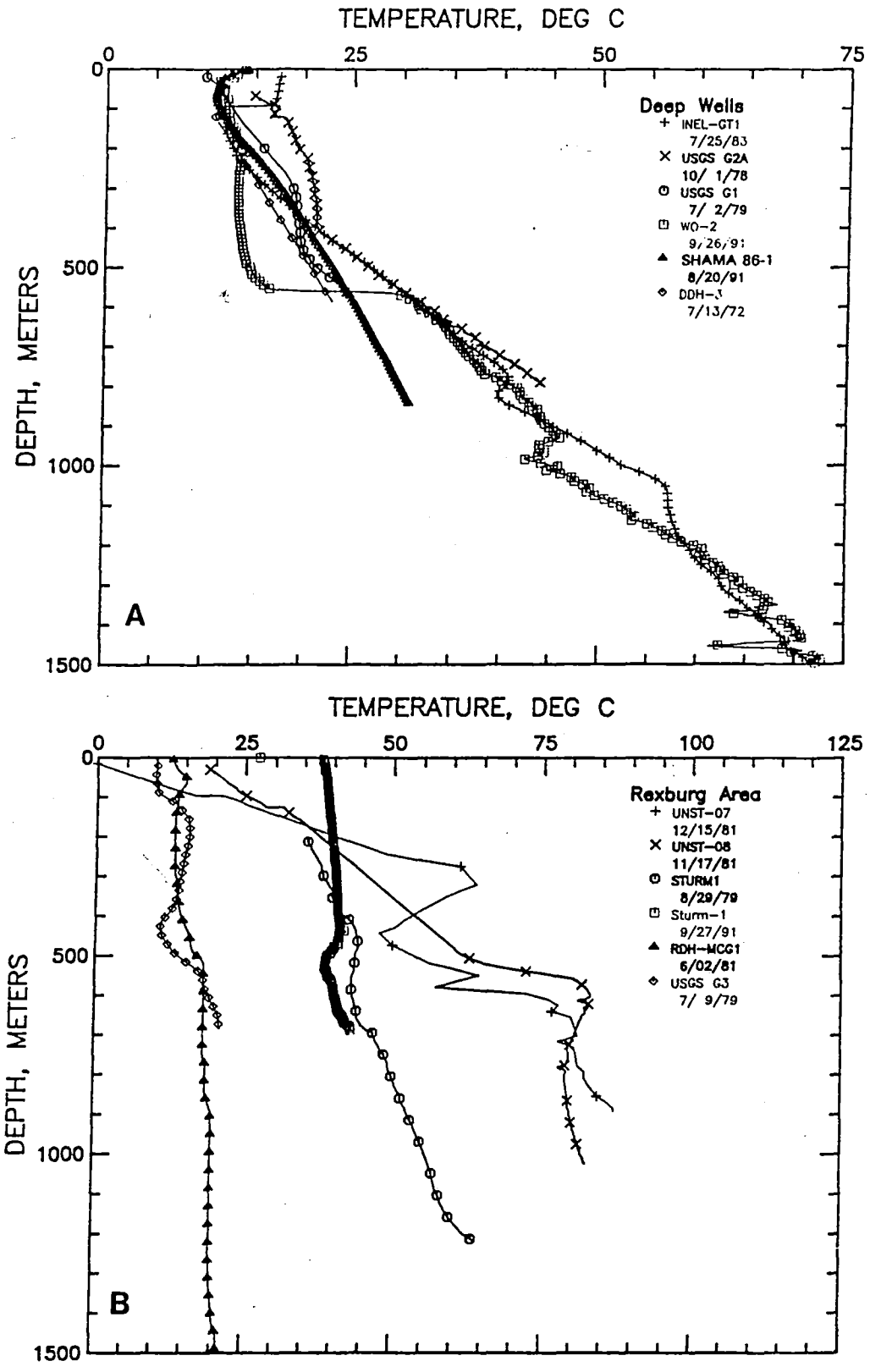

Figure 12. Figure 12a. Temperature-depth curves in intermediate and deep wells. Every 5th point is shown by the appropriate symbol. Figure 12b. Temperature-depth curves for deep wells along the southeast margin between Rexberg and Ashton. A non-equilibrium log (Kunze and Marlor, 1982) is shown for the Rogers Potatoes-Madison County Geothermal well (RDH-MCG1, 6N/40E-31bbal).

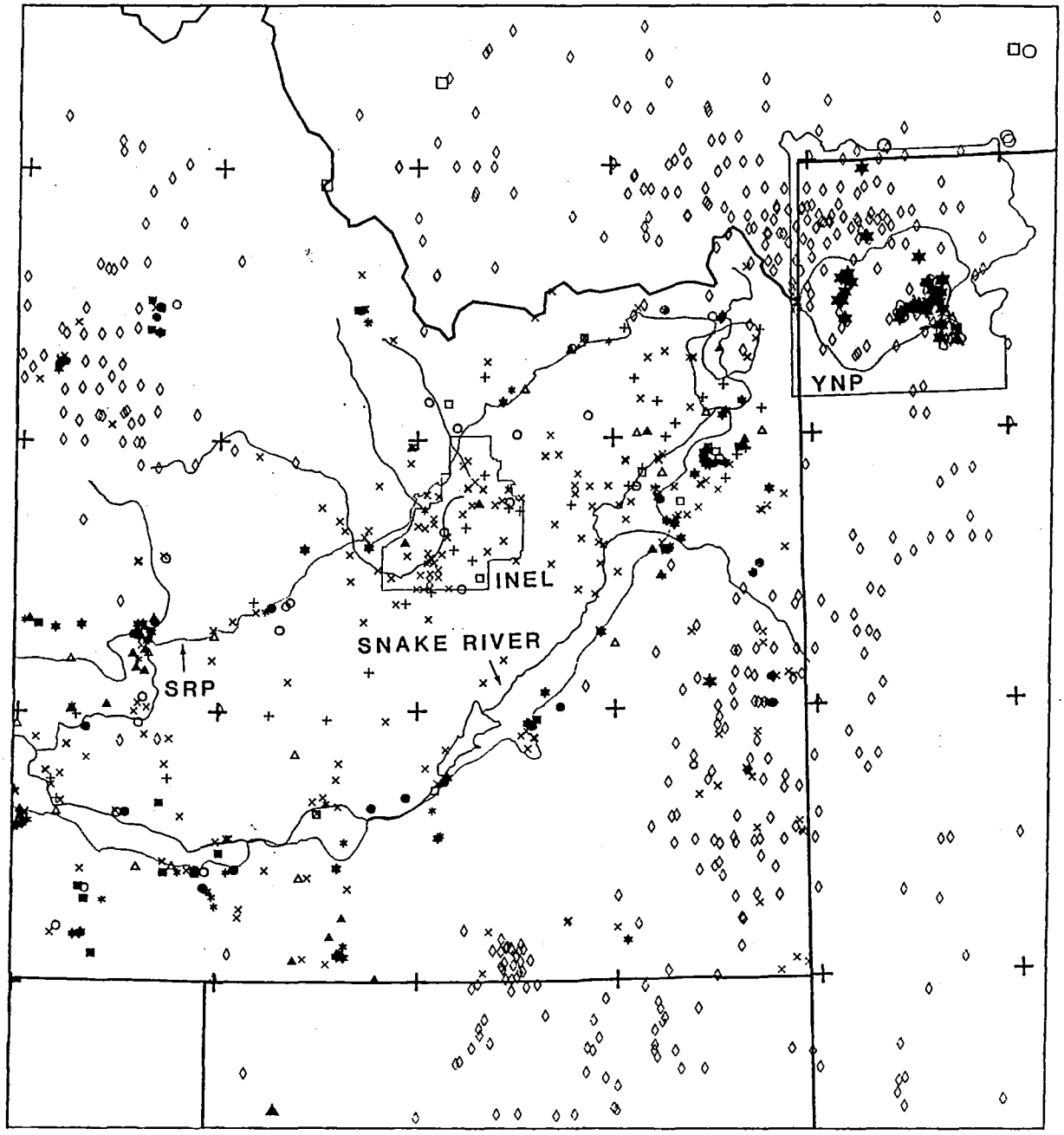

Figure 13. Heat flow map for eastern Idaho. The heat flow is coded by symbols and the categories are coded by color. Data from Brott and others (1981), data from Table 2, data from Table 3a, and data from Table 3b, are shown in purple, green, red and orange respectively. The large orange star is the Gentile Valley well. Earthquake locations from Smith and others (1985) are shown in brown. The outline of the INEL is shown in green. Heat flow symbols x, <20; +, 20-40; o,40-60;□, 60-70; △, 70-80; ●, 80-90; ■, 90-100; ▲, 100-120; *, 120-150;✱, > 150 mWm^{-2}.

TABLE 4. Thermal data from deep wells in Southern Idaho (modified from Blackwell, 1989).

Well Name	Latitude	Longitude	Depth Range (m)	Average Gradient (C/km)	Average Thermal Conductivity ($Wm^{-1} K^{-1}$)	Average Heat Flow (mWm^{-2})	Temp. Log Type
Sturm #1	44°05.55'	111°25.73'	0-1210	(48.0)	2.26	103	Non Eq.
Union State #08	43°57.23'	111°31.28'	0-1023	67.0	(1.46)	98	Eq?
Union State #07	43°56.63'	111°32.70'	0-890	83.0	(1.46)	122	Eq?
Madison Co.	43°48.65'	111°47.15'	0-1495	11.3	(1.5)	17	Non Eq?
INEL-GT1	43°37.41'	113°03.95'	250-3100	43.6	2.76	107	Eq.
INEL-WO-2	43°34.55'	112°52.52'	570-1517	46.0			Non Eq
Anderson Camp	42°39.90'	114°17.30'	65-645	63.0	(1.45)	91	Eq.
Gentile Val. #1-9	42°05.40'	111°31.80'	0-2877	61.5	(2.07)	127	Eq.
Bostic #1-A	43°02.45'	115°27.55'	0-2712	65.9	1.38	96	Eq.
Mt. Home AFB	43°03.26'	115°50.35'	823-1207	67.2	1.23	83	Non Eq.
Federal 60-13 #1	42°59.06'	116°17.20'	0-3390	(39.8)	1.91	76	Non Eq.
Hubbard #25-1	42°47.20'	111°36.70'	600-2300	30.0	(1.83)	55	Eq.
Ore-Ida #1	44°01.93'	116°57.22'	0-3100	54.8	1.50	82	Eq.
			0-2700	62.0	1.42	88	(Art)

Values in parenthesis are estimated.

values are 151 mWm^{-2} and 88 mWm^{-2} for the wells 5 km and 10 km from the edge of the Snake River Plain, respectively. A well drilled as a water supply well was logged near Heise hot springs (the Byington site, 3N/41E-5bcca). The well has a very high gradient (156°C/km) that is probably influenced by thermal fluid associated with the hot springs.

A gradient of 155°C/km was measured between 60 and 135 m depth in hole 9N/43E-11bda (see Figure 14) just south of the caldera rim of the Island Park caldera (see Figure 13). A deep well was subsequently drilled nearby (Sturm #1, 9N/43E-19bdc). A nonequilibrium temperature log shows a distinctly anomalous temperature of about 30-35°C at 200 m, but a more regionally typical temperature of 65°C at 1200 m. As part of this project, Sturm #1 was relogged. The two temperature logs are shown in Figure 12b. The well is artesian at 4 l/s with the water entering the hole at a depth of about 475 m (see Figure 12b); the well is presently being used for heating of a house. The well was drilled to 1200 m, but caved back to 600 m before abandonment to the landowner. The well currently produces 38 °C water from 475 m. The nonequilibrium log is warmer, as is to be expected, but the shape is similar. Blackwell (1989) estimated a heat flow of 103 mWm^{-2} for the well. The log in 1991 confirms the general trend of temperature in the nonequilibrium log and the interpretation of an overall gradient of 48 °C/km for the well (Blackwell, 1989) seems reasonable. The high heat flow at shallow depth in both the shallow and the deep wells is probably related to lateral flow of warm water from the Island Park caldera immediately to the north.

There is no guarantee that the temperature-depth curves of the wells shown are drilled in areas that are typical of conditions below the Snake River Plain aquifer. The four deep wells drilled east of Arco are located in an area where aquifer temperatures and surface heat flow are higher than in the areas to the south and west (Figures 7 and 9). This difference implies that the flow rates are restricted and the aquifer is thinner and/or less permeable, and/or the volume of water flow is less than in areas to the east and south. The wells near Rexburg are also located in an area that may not be characteristic of the aquifer. The aquifer temperature (at 150 to 300 m) in USGS-G3 is higher than in surrounding areas of the aquifer, which may indicate leakage of hot water from the Newdale geothermal anomaly (which is about 10 km to the east) into the aquifer system. Temperature and hydrologic data indicate that much of the recharge for the Snake River Plain aquifer occurs along the Snake River between Rexburg and Idaho Falls. Apparently fluid flow also goes quite deep in this area.

Island Park Caldera

The largest silicic volcanic feature in the Snake River Plain is the large Island Park caldera (Hamilton, 1965). Christiansen (1982) redefined this feature, which is part of the larger Yellowstone volcanic system that formed during a major ash flow eruption 1.3 MY ago, as the Henrys Fork caldera (shown in Figure 13, also see Hildreth and others, 1984). According to Smith and Shaw (1978), this

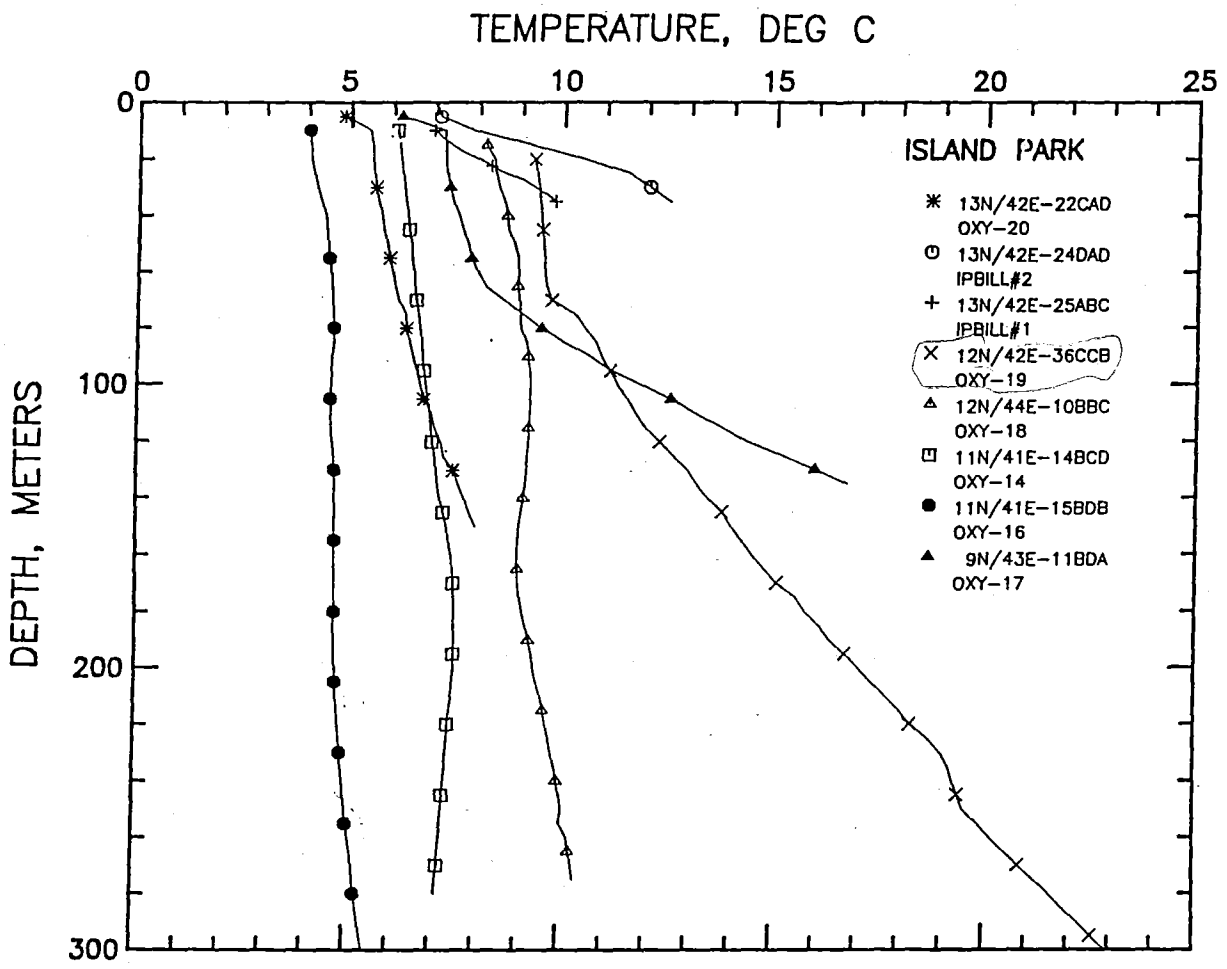

Figure 14. Temperature-depth curves for wells in the Island Park area.

area contains over 50% of the total thermal energy in igneous complexes of the United States outside national parks. However, there are no known thermal manifestations and groundwater temperatures in shallow wells (30-60 m deep) are generally low (Brott and others, 1976). Although the 1:250,000 scale Ashton topographic map indicates hot springs in 11S/41E-14 and 15, no surface evidence of a geothermal system is present at this time. Hoover and Long (1975) suggested that the area had little geothermal potential based on electrical resistivity studies. Recently, however, Hoover and others (1985) recanted their earlier conclusions and speculated that there may in fact be significant geothermal potential there. Whitehead (1978) noted that groundwater temperatures at the south edge of the caldera are elevated and suggested possible input of geothermal heat into the system. The thermal data described above are consistent with this view (i. e. the Sturm #1 well).

The results of a geothermal exploration drilling project carried out in 1977 and 1978 are included in Table 2 and temperature-depth curves from several of the wells are shown in Figure 14. Two 300 m and one 100 m holes were drilled in the general vicinity of the reported hot springs in Antelope Flats (11S/41E-14 and 15). This area is a topographic breach in the caldera, and the hole locations are one or two kilometers outside of the edge of the caldera. The results from these drill holes (Figure 14) indicate a very deep water table (150-200 m) and suggest that the area is in the recharge zone of the Snake River Plain aquifer. The two deep holes were essentially isothermal to total depth, both having gradients less than 10°C/km below 150 m (one positive and one negative).

Another heat flow test hole was drilled to a depth of 278 m in 12N/44E-10bbc (HFT-18) near the east side of the caldera (close to the toe of the Plateau rhyolite flows coming from the Yellowstone caldera). This hole has the typical temperature-depth curve expected in a lateral or down-flow section of a major aquifer system. The gradient is zero to 180 m and 13°C/km to 300 m. A 300 m hole was also drilled near the center of the caldera in 12N/42E-36ccb. In this hole (HFT-19), the gradient increases systematically from 27°C/km to 66°C/km with depth. The heat flow in the 180 to 350 m depth interval is 109 mWm^{-2}. Thus the results from this hole suggest that there may be areas of high heat flow in the caldera.

Thermal Conditions in Deep Wells

The results that have been discussed clearly show that in some areas the thermal data are affected by groundwater flow to depths of approximately 500 m. Thus temperature and heat flow data from deep holes are valuable in investigating the deep conditions for comparison with the shallow conditions. Blackwell (1989) discussed thermal data from several wells over 500 m deep in the Snake River Plain, and additional wells in and around the Snake River Plain are available as a result of this study.

These deep holes are listed in Table 4. Included in the table are the name of the hole, the location, and some information on the depth, gradient, and heat flow. Adequate equilibrium temperature-depth

information are available for the Ore-Ida #1, Bostick #1-A, INEL-GT#1, UNST #7, UNST #8, Gentile Valley #1, Hubbard #25-1, and Anderson Camp wells. Logs measured shortly following completion of drilling are available for the INEL WO-2, Sturm #1, the Madison County #1, the Federal 60-13 #1, and the Mountain Home Air Force Base wells. All the wells in the Snake River Plain penetrate the typical geologic sequence for their location, and so the lithologies in the holes are volcanic rocks of rhyolitic and basaltic composition and lacustrian sedimentary rocks. The Federal 60-13 #1 well bottoms in Idaho batholith granite. The westernmost wells cut a predominantly sedimentary and basalt section with few rhyolitic volcanic rocks.

Temperature-depth curves for the wells not discussed in previous sections are shown and discussed by Blackwell (1989). Blackwell (1989) concluded that temperatures at a depth of about 3 km are 25-50 °C warmer in the Western Snake River Plain than in the Eastern Snake River Plain. For example, in the Eastern Snake River Plain the upper part of the INEL-GT1 well has very low gradients and near isothermal conditions because of the Snake Plain aquifer and the temperature-gradient below a depth of 1000 m averages 40°C/km. The bottom hole temperature is about 150 °C. The heat flow value for this well is higher than in the wells in the west because the average thermal conductivities are higher in the eastern portion of the plain.

The highest temperatures are in the 2.9 km deep Bostic #1-A well discussed in detail by Arney and others (1982; Arney, 1982) which has an average gradient of 66 °C/km. The temperature at 2700 m is 170 °C in the Ore-Ida #1 well at the extreme western end of the Snake River Plain. The maximum temperature in this well is almost 200 °C at a total depth of 3033 m. This hole has an very thick sedimentary package because almost the total depth of the hole is composed of sedimentary rocks. Only the bottom few hundred meters of the well encountered interbedded basalts, sedimentary units and tuffs. The gradient averages approximately 90°C/km between 0 and 1 km and 60°C/km between 1 and 3 km.

The Federal 60-13 #1 well along the southwestern boundary of the Snake River Plain is in an area of very high, shallow heat flow values (the Bruneau/Grandview area). The temperature-depth data are nonequilibrium, but there are multiple logs so a reasonable picture of the thermal regime is possible. Even though the well may penetrate a shallow moderate-temperature geothermal system, the deeper temperatures are not anomalously high for the Snake River Plain. The gradient in the depth range of 1500 to 3390 m averages over 32°C/km, and the estimated heat flow value for the well is 76 mWm^{-2} .

Thus the heat flow in deep wells along the Snake River Plain is on the order of 85 ± 10 mWm^{-2} in the west where the age of silicic volcanism is 12 to 15 Ma, and is 105 ± 10 mWm^{-2} in the east where the age of the silicic volcanism is 2 to 5 Ma. On the other hand, the temperatures do not show such a systematic variation. The differences between the temperatures in these holes are associated as much with the lithologic variations as the heat flow. The presence of the thick, low thermal conductivity, sedimentary package in the western part of the plain is an important contributor to the high temperatures observed there.

Regional Heat Flow

A composite cross section of the heat flow values across the eastern part of the Snake River Plain is shown in Figure 15. The heat flow values are plotted on a scale that shows their perpendicular distance from the axis (0 position) of the Snake River Plain. This figure is similar to the Figure 2 of Brott and others (1981) except much more data (Tables 2 and 3, and Figure 13) have been added. The most important points are the asterisks, as these sites represent the deepest wells, which most likely reflect deep thermal conduction conditions. The averages for the area have been updated using the new data and are shown in Table 1. The figure shows generally high heat flow values (many over 120 mWm^{-2}) on the margins and low values (mostly in the range of -30 to 20 mWm^{-2}) in the Snake River Plain aquifer.

The average values are shown in Table 1 for areas along the north and south margins of the Eastern Snake River Plain. The average values for the northern margins in Table 1 are better constrained than in the study of Brott and others (1981) because the data set is almost twice as large. The low heat flow values on the northern margin near Arco are due to lateral movement of groundwater into the Snake River Plain aquifer, and these values are not included in the averages. Many of the wells along the northern margin were drilled specifically for heat flow. The large variation of values internal to each of the areas suggests that geothermal and groundwater aquifer systems have a major effect on the distribution of surface heat flow along the margins of the Snake River Plain aquifer. In fact, based on the evidence presented here, the existence of geothermal systems along the northern edge of the Snake River Plain appears to be as common as along the southern margin. In addition to Liddy and Carey hot springs, the existence of systems with no surface expression has been documented at Magic Reservoir, Butte City, and in the vicinity of the Champagne Mine.

The heat flow averages for the various areas range from 90 to 113 mWm^{-2} , with typical standard errors of the mean of 10%. Thus for practical purposes the values cannot be differentiated. The actual averages in each area are dependent on the weighting of the values from the geothermal systems, the low temperature aquifer areas, and the deep heat flow values. In spite of these complexities, the average surface heat flow values are 100 ± 15 mWm^{-2} for every grouping of data; these values are similar to the heat flow values actually measured below the aquifer in wells USGS-G2A and INEL-GT1 (110 and 107 mWm^{-2}, respectively).

Based on the present data set, either estimate has wide uncertainties and no northeast-southwest trend in heat flow can be proved. The data set is still sparse in the far eastern area of the Snake River Plain and there are few deep wells available to investigate the thermal character below a few hundred meters for all of the Eastern Snake River Plain. Thus at present the data neither support nor refute the prediction of the hot spot model that the heat flow should increase toward the east along the Snake River Plain.

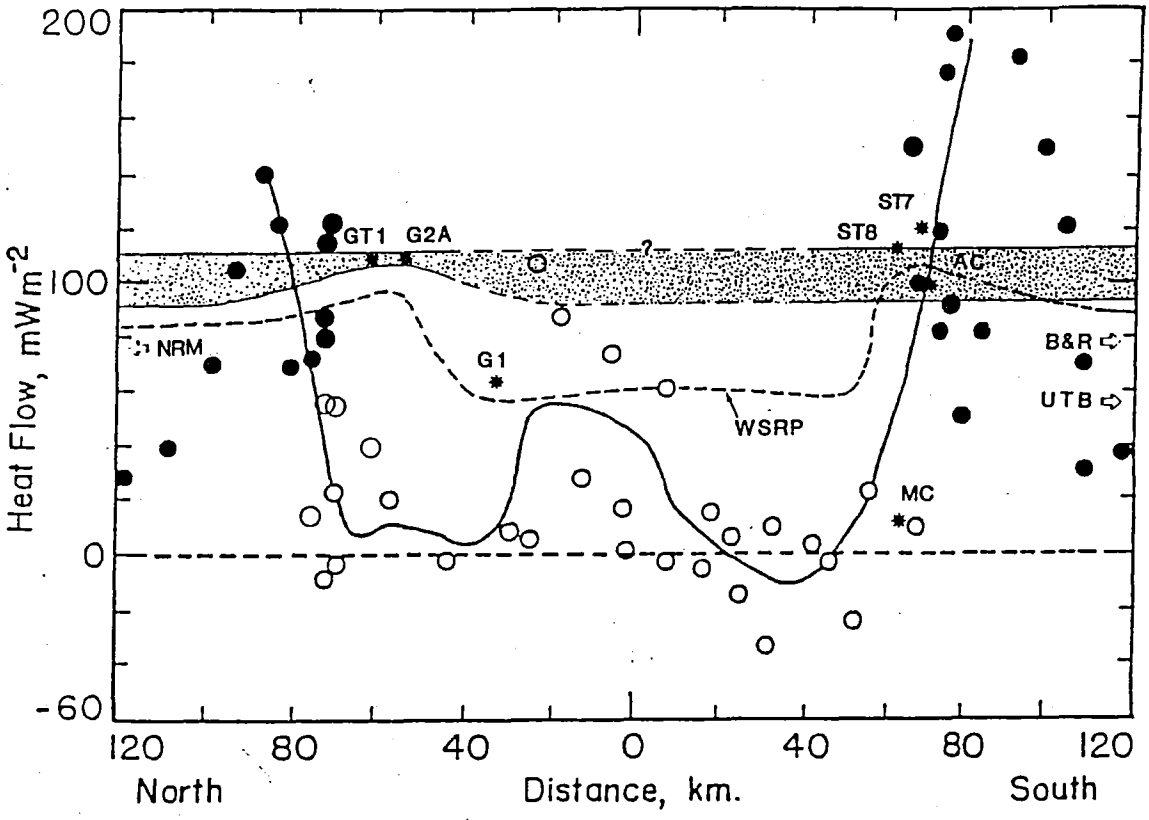

Figure 15. Heat flow profile perpendicular to the axis of the Snake River Plain. The solid curve is the smoothed eastern Snake River Plain profile (fit to the data represented by solid and open circles) and the dashed curve is a theoretical heat flow profile (from the model 1, 12.5 m.y. solution of Brott and others, 1978) which best fits the western Snake River Plain (WSRP) data. The open and solid circles represent data taken inside and outside the Snake Plain aquifer; the stippled pattern represents the estimated regional heat flow. These data are projected into the profile extending east from Magic Reservoir on the north side and Pocatello on the south side. The values are plotted on a scale which shows their perpendicular distance from the axis (modifed after Brott and others, 1981). NMR is Northern Rocky Mountains, B&R is Basin and Range, and UTB is Utah Thrust Belt. The deep wells are also labeled.

Brott and others (1981) made a heat budget analysis of the Snake River Plain aquifer. The surface heat flow within the boundaries of the Snake River Plain aquifer (Figure 7) was areally integrated, and the total loss of heat above the aquifer was calculated to be 42.3 MW. The heat required to change the temperature of the discharged water of the aquifer (18.5 $m^3 s^{-1}$) from 8°C to 14.5°C is 287.3 MW. Thus the total amount of heat required from below the aquifer system would be 329.6 MW or an average heat flow of approximately 190 mWm^{-2}. A similar areal integration was done using the heat flow predicted by the finite-width, time-progressive regional thermal model presented by Brott and others (1981). The predicted heat loss is 221 MW, and the predicted temperature increase is 4.9°C. This predicted temperature increase is consistent with the observed temperature increase (see Figures 7, and 11). The heat flow values based on the Brott and others (1981) model are higher than those calculated for the models presented in a following section. However, the uncertainties are large in all of the estimated parameters. For example, there may be local input of heat from shallow basalt intrusions associated with east-west extension at places along the Eastern Snake River Plain (William Hackett, personal communication, 1991)

Although a qualitatively similar heat flow distribution is observed in the Western Snake River Plain (shown in Figure 5), i.e., low heat flow in the Snake River Plain and high heat flow on the margins, the causes for the pattern there are somewhat more complicated. The low heat flow in the Western Snake River Plain results from large-scale refraction of heat due to crustal thermal conductivity contrasts, as well as minor regional aquifer motion, while the low heat flow in the central part of the Eastern Snake River Plain is caused by regional cold groundwater circulation in a major aquifer system. The thermal refraction effect in the Eastern Snake River Plain is minor because a large, deep sedimentary basin has not developed. The temperatures in the Western Snake River Plain are quite high in spite of the lower heat flow because the thermal conductivity of the sedimentary rocks is so low (Blackwell, 1989).

THERMAL CONDITIONS IN THE SOUTHEASTERN IDAHO BASIN AND RANGE

The geology of the southeastern Idaho Basin and Range province is summarized in an earlier section. The area is part of the Basin and Range province and the thermal characteristics of that province extensively discussed by Lachenbruch and Sass (1978) and Blackwell (1983) should apply to this area. However, because of the extensive faulting, the high topographic relief, and the nature of the rocks, which are predominantly carbonates, the hydrology of the province is complicated and shallow exploration holes and water wells give heat flow results that are uniformly poor. So most of the holes logged are not listed in Tables 2 or 3. Furthermore, unlike the Snake River Plain groundwater system, there has been little study of the large scale flow in hydrologic systems in this part of Idaho with the exception of the study by Ralston and Mayo (1983). There are several hot springs in this province and some results from shallow geothermal gradient exploration studies and from geothermal test wells are

available.

The temperature-depth logs from deep wells are shown in Figure 16. Well SUN-1001 (15S/39E-6ca) is near the southern boundary of Idaho about 2 km from Battle Creek (Wayland) Hot Springs and about 3.5 km from Squaw Hot Springs (the blue star on Figure 13). The temperatures in this well are dominated by shallow lateral flow of hot water (almost 110°C at this location) in the shallow groundwater aquifer recharged by upflow of hot water, some of which comes to the surface at the hot springs. This temperature is the highest observed at shallow depth in any well in Idaho.

Ralston and Mayo (1983) summarized geothermal gradients from temperature logs and bottom hole temperature measurements in oil wells. These BHT data are of poor quality, but in the deep holes do give some idea of possible geothermal gradients. We have collected BHT data from wells drilled since the Ralston and Mayo (1983) study. Locations of all of the wells are shown on Figure 13. Geothermal gradients for these wells (Table 3b) were calculated using corrected BHT values (Kahle and others, 1970). BHT data from some of the newer wells is quite extensive as multiple logging runs were made. As an example, data from eight wells are shown in Figure 16. The well sites are both north and south of the Snake River Plain and the estimated BHT values range from just over 100 °C at 4 km to almost 180 °C at 5 km. These data can be used to establish some controls on the thermal character of the region to depths of 5 km, or almost halfway through the seismogenic zone. These data should permit more detailed corrections, given the multiple points. Heat flow values could be calculated using well log data from most of the wells, but due to project deadlines, thermal conductivity from only six wells has been analyzed. The results for the two wells with temperature logs are discussed in detail below. Four other wells with BHT data only were also studied.

The Hubbard #25-1 well (7S/41E-25, Table 3a)) is near Blackfoot Reservoir. Numerous Quaternary rhyolite and basalt volcanoes are found in the vicinity; however, groundwater geochemistry shows no evidence of high temperature geothermal systems (Mitchell, 1976b). The temperatures were measured 4 months following completion by a commercial well logging company (see Figure 17). Typical temperature logs obtained by logging companies are of poor quality due to instrument limitations and the fact that logging usually occurs within a few days following well completion. There is a 2°C offset at 1200 m in the log, apparently due to different calibrations between tools used for two separate runs, but otherwise the log looks satisfactory. There are no samples available for thermal conductivity measurement, so a heat flow cannot be precisely determined, although an estimate can be made based on the lithology. The average geothermal gradient from 600 to 2300 m, below the Cenozoic section, is 30°C/km and the maximum temperature reached at 2300 m is 68°C. The lithologies encountered are predominantly basalt, shale and limestone with some sandstone. A predicted temperature-depth curve was constructed using the computer program of Gallardo (1989) for the well based on the lithologies described on the mud log and the assumption of constant heat flow over the well. The best fit of predicted to observed temperature-depth curve is for a heat flow of 50 ± 5 mWm^{-2}. This value seems

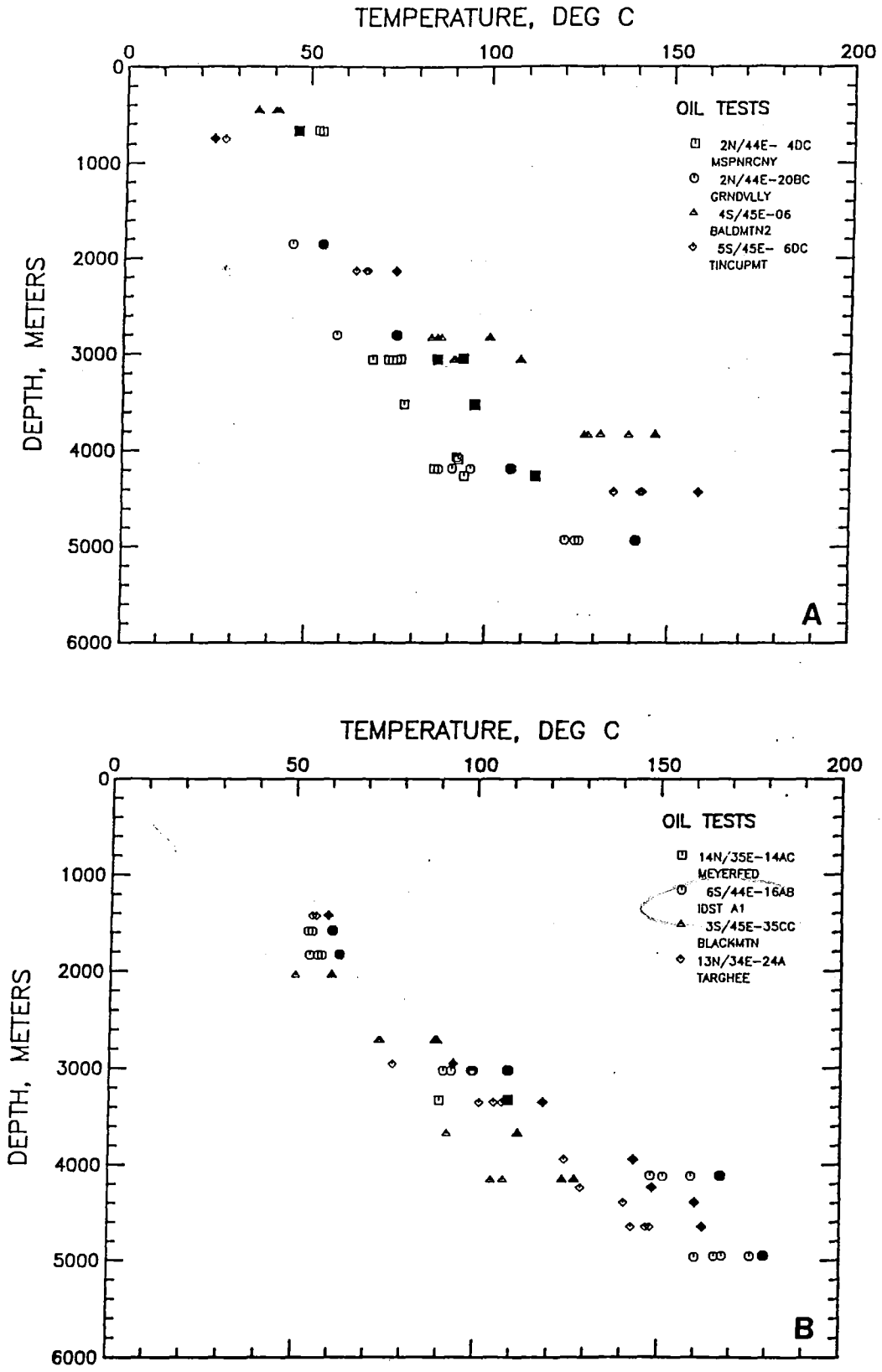

Figure 16. Figure 16a. and Figure 16b. Temperature-depth data (uncorrected and corrected BHT's) from deep hydrocarbon tests in the eastern Idaho Basin and Range. The open symbols are measured BHT values and the solid symbols are corrected BHT data.

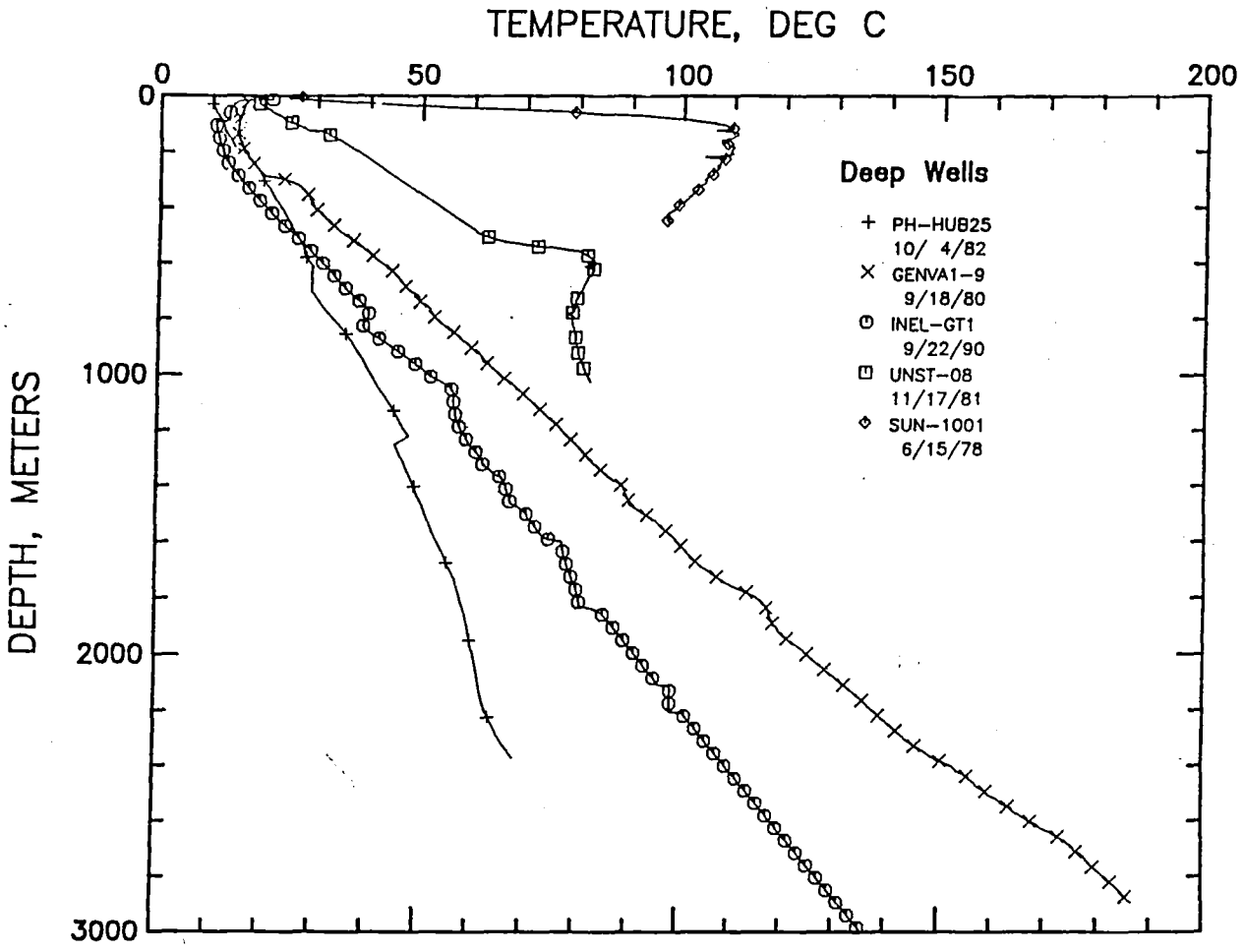

Figure 17. Temperature-depth curves for two deep and one intermediate depth geothermal test wells in the southeastern Idaho Basin and Range plus two holes for reference.

surprisingly low, but is consistent with the low gradients in shallow wells in the area.

A second deep test shows different results. The Gentile Valley #29-1 well (Table 3b) was drilled by CONOCO in 1979 and was later taken over by Phillips Geothermal. An equilibrium temperature log run with a Custer tool is shown in Figure 17. This well has an average gradient of 60 °C/km to a depth of 3 km with a bottom hole temperature of 190 °C. The lithology was evaluated for this well based on the geophysical well logs and stratigraphy. The temperatures that were calculated by assuming various heat flow values were compared to the observed temperatures to determine the heat flow that gave the best temperature fit. For the depth interval of 0 to 2000 m, the assumed heat flow that best fits the observed temperatures is 110 ± 5 mWm^{-2}. The gradients in the bottom third of the well, combined with the inferred lithologies, imply a heat flow of over 150 mWm^{-2} in this portion of the well. The BHT is best fit by a heat flow of 127 mWm^{-2} for the whole well. In any case the heat flow is significantly above the expected Basin and Range background in this area 50 km from the edge of the Snake River Plain.

Deming and Chapman (1989) determined heat flow for several sites in the thrust belt in northern Utah using BHT data. They found a heat flow of 65 mWm^{-2} and a gradient of 25°C/km at the Anschutz Ranch field in Utah just south of the area shown in Figure 13. This heat flow appears to be the minimum likely in any of the wells in Table 3b. Samples were collected from the Paleozoic and Mesozoic formations in the area of Teton Pass as part of this study and thermal conductivity values measured. Lithologic logs (but not wire-line logs) were available for the Grand Valley and Mike Spencer Canyon wells (2N/44E-20bc and 2N/44E- 4dc) and estimates of heat flow were made using the thermal conductivity results from Deming and Chapman (1989) and those measured as part of this study. These sites (orange circles on Figure 13) are about 40 km from the Snake River Plain, 10 km north of the South Fork of the Snake River, and 10 km west of the west edge of the Intermountain Seismic Belt. The heat flow value estimated for both wells of about 80 mWm^{-2} is close to the average background for the Northern Rocky Mountains/Basin and Range provinces, but is 15 mWm^{-2} higher than in the thrust belt to the south (although the Utah site is east of the Intermountain Seismic Belt). So, based on sketchy data, there may not be significantly elevated heat flow in this area north of the South fork of the Snake River.

Two wells south and east of the South Fork of the Snake River in addition to the Gentile Valley well have apparent average geothermal gradients of over 50°C/km to depths of 3-4 km . This value is higher than expected for the province and anomalous heat flow is suggested in these areas if the temperature measurements are valid and if the thermal conductivity values are not anomalously low. These wells may be in the geothermal anomaly associated with the Gentile Valley well. Based on the BHT data the gradients decrease to the south and east. Heat flow was estimated for two wells east of the area with the highest gradients, the Tincup Federal #1 and the Bald Mountain #2. Both wells have gradients in excess of 30 °C/km. The lithologic sections were determined on a detailed basis using

wire-line logs for the wells. The thermal conductivities for various lithologies were estimated from the literature and from measured values. Predicted temperature-depth curves were generated and fit to the BHT data, as described by Gallardo (1989). The heat flow values determined in this way are 80 ± 10 and 85 ± 10 mWm^{-2}; these values are similar to the regional heat flow values determined for the wells north of the Snake River. Although the gradients in these wells are higher than those in the wells north of the Snake River, the average thermal conductivity values are generally lower. Because different techniques were used to calculate the two sets of values, they may not be directly comparable. Since the thermal conductivity has not been determined for the remainder of the wells, the actual heat flow variations (if any) associated with the gradient variations are unknown.

The information available suggests highly variable heat flow in southeast Idaho. The data from the Hubbard and Gentile Valley wells are the best clues at this time to the characteristics of the Southeastern Idaho Basin and Range thermal pattern and the two values are sub- and super-regional. Thus identification any signal related to the hot spot will require detailed study of all the available wells.

THERMAL MODELING

Geological and Geophysical Constraints

Brott and others (1978 and 1981) presented the first thermal and structural models relating the subdivisions of the Snake River Plain/Yellowstone region to stages in the evolution of a continental region affected by a powerful hot spot. Subsequently, a number of geologic features outside the Snake River Plain have been related to the passage of the hot spot. And if, in fact, the region is underlain by a mantle plume, then there may well be thermal and/or mechanical effects on the lithosphere at distances of 500 km or more from the center of the plume (see Sleep, 1990 for example). Thinning of the lithosphere and presence of a thermal source outside of the Snake River Plain are not predicted by the thermal model of Brott and others (1981). Thus the model needs to be modified to take into account evidence that geologic features on the periphery may be related to its formation. Specific such features include the parabolic distribution of earthquakes around the eastern Snake River Plain, the patterns of topography in the Basin and Range valleys that intersect the Eastern Snake River Plain, the patterns of late Cenozoic Basin and Range faulting, and the locations of centers of basaltic volcanism.

Smith and others (1985), Blackwell (1989), Anders and others (1989), Westaway (1989a, 1989b), and Pierce and Morgan (1990) have speculated on the existence of, and the reasons for, the quasi-parabolic nature of the earthquake distribution around the Eastern Snake River Plain. This distribution is illustrated in Figure 18 where the earthquakes in eastern Idaho from the catalogue discussed by Smith and Arabasz (1991) are plotted. A plot of the earthquake locations from southern Utah to Montana is presented in Figure 1 of Smith and Arabasz (1991).

Anders and others (1989, 1990) discussed various models that have been proposed to explain the localization of the seismicity along the periphery of the Snake River Plain. They concluded that a model of the change of total lithospheric strength as a function of time related to the cooling of a crust modified by the addition of mafic material, and by the lateral deflection of mantle flow at the outer edge of the seismic zone could explain the observations of faulting and seismicity.

Uplift, faulting, and volcanism away from the Snake River Plain are also cited as possible effects of hot spot passage. For example the valleys in the central Idaho Basin and Range province show a systematic elevation versus distance pattern away from the Snake River Plain (Ruppel, 1967). The valley floors show a rise in elevation from 1500 to 1600 m to a drainage divide at 2200 to 2300 m at distance of 100 km (Medicine Lodge Creek) to 130 km (Big Lost River) from the axis of the Snake River Plain. In addition, all of the valleys north of the INEL site show a drainage divide at a distance of about 100 km from the axis.

Pierce and Morgan (1990) interpret a parabolic region of fault activity in terms of four belts: a belt of newly active faults with associated bedrock escarpments of 200 m or less at greatest distance from

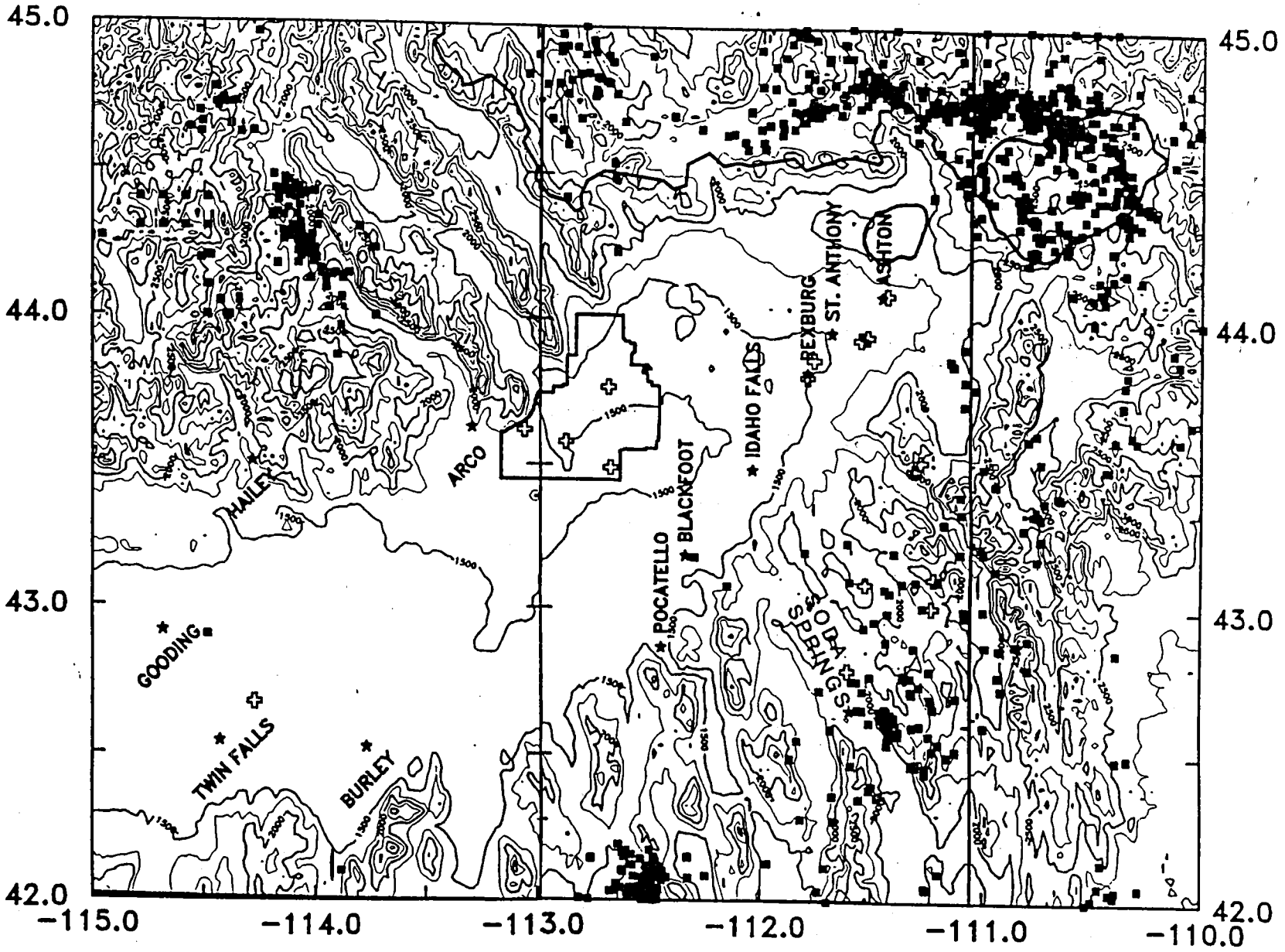

Figure 18. Topography, earthquakes and deep well locations for the Eastern Snake River Plain and vicinity. The earthquakes (squares) are from the catalogue of Smith and Arabaz (1991). The locations of the deep wells with heat flow data are shown as open crosses.

the axis of the Snake River Plain; a belt of faults active in the last 15 ka with bedrock scarps of 700 m or more; a belt of faults active between 15 and 200 ka and range-front scarps of 500 m; and a belt of inactive faults along the south side of the Snake River Plain. They relate this pattern, which also includes uplift of 500 m out to distances of 200 km from the axis of the eastern Snake River Plain, to the thermal effects of the hot spot acting over the last 10Ma.

The interpretation of the side effects as due to thermal effects is not universal, however. Westaway (1989a, 1989b) argues that the pattern of displacements on the active faults reflects the pattern of material flow in the upper mantle associated with the plume under the Snake River Plain/Yellowstone region. He postulates significant inward-directed flow in the plastic layer of the mantle in order to generate the observed pattern of historical faulting. Anders and others (1990) have taken sharp exception to this model, but it has been reiterated by Westaway (1990).

Direct evidence for the extent of the heat source might be inferred by the location of volcanic centers in and around the Snake River Plain. Scattered areas of basaltic volcanic rocks are widely dispersed in the western United States, but there are concentrations of volcanic centers in the Snake River Plain and vicinity, the Rio Grande rift, the Cascade Range, and the High Lava Plains. Basaltic volcanism active in the last 1 to 2 Ma outside of, but in the vicinity of, the Snake River Plain is found in a number of locations, as shown in Table 5. The centers are found as far as 65 km outside the edge of the Snake River Plain and at locations where the age of the silicic volcanism is as old as 10 to 15 Ma.

One major occurrence of basaltic volcanism north of the Snake River Plain is in the Smith Prairie area, including the Mores Creek and West Fall Creek flows (Howard and others, 1982). A series of flows ranging in age from 2 to less than 0.2 Ma are found there with centers that range from 20 to 25 km from the edge of the Snake River Plain. Some of the flows extend for over 70 km along the Boise River and tributaries. The hot spot passed this area over 10 Ma ago. Furthermore, the heat flow in this part of the Idaho batholith is typical for the region of central Idaho. The volcanism is a strong indication that the size of the heat source in the mantle is larger than the obvious topographic manifestation of the Snake River Plain, and that the thermal anomaly in the mantle may persist for at least 10 Ma after passage of the hot spot.

Quaternary basalts are also found in the Camas Prairie area (Leeman, 1982b; and Strusacker and others, 1982). The area is also the site of rhyolite volcanism of anomalously young age for its position in the Snake River Plain. The Magic Reservoir rhyolites have ages of 5.6 and 4.7 Ma and thus are about 5 Ma younger than the Mount Bennett rhyolites associated with the Snake River Plain hot spot. The Quaternary basalts are cut by east-west trending normal faults. The centers of basalt volcanism are as much as 30 km from the Snake River Plain. The major Magic Reservoir geothermal anomaly is located in this area also, and the heat flow may be higher than in central Idaho.

Further to the east there are no late Cenozoic volcanic rocks in the Central Idaho Basin and Range province, unlike the Southeastern Idaho Basin and Range province where they are extensive. The only

TABLE 5. Location of Late Quaternary/Holocene volcanic centers outside of the Snake River Plain.

Area	Distance from margin (km)	Age of hot spot activity (Ma)
Jordan Craters, Oregon	?	>15
Boise River (Mores Creek, Smith's Prairie, West Fall Creek)	25-35	10-12
Camas Prairie	25-35	8-12
Craters of the Moon	10	5
Blackfoot Reservoir Grey's Lake, etc.	50-65	<5

exceptions are near the young rift zones where basaltic centers occur up to 5 km outside the physiographic edge of the Snake River Plain.

On the south side of the Snake River Plain there are centers of volcanism in the Pocatello region and in the Greys' Lake/Blackfoot Reservoir/Gem lava fields area. The volcanics in the area are extensive and young (less than 0.1 Ma). Silicic volcanics also occur in the area and are similarly young (see Leeman and Getting, 1977 and the summary by Feisinger and others, 1982). A major question is the extent to which these volcanics (and indeed the seismicity in the Intermountain Seismic belt this far from the Snake River Plain) are related to the hot spot track. Pierce and Morgan (1990) argue that the portion of the Intermountain Seismic belt that is in Idaho is part of the larger Snake River Plain feature. If this interpretation is correct, then the volcanics in this area might be related to the hot spot rather than the Basin and Range setting. However, there are several major young volcanic centers along both the east and west borders of the Great Basin far from the effects of the hot spot (Coso, Long Valley, and Roosevelt/Cove Fort are examples). Thus the affinity question is unresolved.

While both geologic and seismic data were considered in constructing the thermal models presented in the following section, the most important data used in constraining the models are the thermal data. The thermal data from the INEL site provide the best evidence for high heat flow for the eastern Snake River Plain. The heat flow of 107 mWm^{-2} that is observed along the west side of the INEL is 20 to 30 mWm^{-2} above the expected heat flow in the Basin and Range province and the northern Rocky Mountains (in the broad sense, Blackwell, 1978, 1983, see also Table 1). The higher heat flow and the resulting higher temperatures in the crust imply that the rheology of the lithosphere must be evaluated separately from that in the surrounding Basin and Range province, as must any area outside the plain affected thermally by the hot spot. The criteria that a successful model needs to match are the heat flow values observed along the Snake River Plain, including the 107 mWm^{-2} value in the vicinity of the INEL, and the heat flow cross section shown in Figure 5 for the Western Snake River Plain.

Unfortunately, the crustal heat flow along the margins of the Eastern Snake River Plain was not well constrained by preexisting data (see the discussion above and Figures 18 and 22). Thus one of the foci of this study was the determination of the heat flow along the margins of the Eastern Snake River Plain. The results are illustrated as a cross section of heat flow in Figure 15 (Figure 5 is the equivalent Western Snake River Plain cross section). The figure emphasizes the conclusion of Brott and others (1981) and Blackwell (1989) that the thermal pattern at depths of 0 to 500 m is dominated by lateral flow of water toward the edges of the Eastern Snake River Plain, where it is forced toward the surface by topographic effects and by structural and stratigraphic changes along the margins. The new data collected from the Arco vicinity (Butte City and the Champagne Mine), from the Rexberg bench area, and from the Ft. Hall area reinforce this conclusion. These effects make the determination of the heat flow at the edge of the Eastern Snake River Plain problematical. From a statistical point of view, based on data from all holes, including those with depths less than 300 m, the mean heat flow for the northern

and southern margins is 100 $\pm$ 10 mWm^{-2}. The intermediate depth wells Sturm #1, UNST-#7 and UNST-#8 are consistent with the mean heat flow, but the Madison County and UGSS-3 wells have lower values which in this discussion are related to deep aquifer effects.

The thermal results from the deep hydrocarbon tests are useful in this conjunction. However, the tradeoff is a lack of precision in the heat flow determinations due to use of the poor quality temperature data to determine gradient and the lack of thermal conductivity samples. The preliminary results (Table 3b) are that the gradients along the margins of the Eastern Snake River Plain are 25 to 35 °C/km with no clear pattern of change as a function of distance from the margin. The two estimates of heat flow in two wells north of the South Fork of the Snake River are about the expected value for the background in the Basin and Range province (80 ± 5 mWm^{-2}). The estimated values for two wells south of the Snake River and near the Wyoming border also have near normal heat flow for the region. On the other hand, there is a very large area of high geothermal gradient in the vicinity of Grey's Lake and Blackfoot Reservoir. There gradients in hydrocarbon tests to 5.5 km depth range up to 61 °C/km, approximately twice those in the other areas. There are young silicic and basaltic rocks in the area and the area has been thought to have significant geothermal potential from the geologic setting alone (Leeman, 1985). These gradients are distinctly anomalous with respect to those elsewhere in the Southeastern Idaho Basin and Range province. Thus the thermal and strength characteristics of this area may have to be evaluated separately from the other areas along the margins of the Snake River Plain. This area has not been included in the criteria for fit for the various thermal models discussed below.

Thermal Cross Sections

Brott and others (1981) developed an analytical thermal model for a moving source plane in an infinite medium to approximate the thermal disturbance in the Snake River Plain/Yellowstone system. The model involved a number of simplifying assumptions including uniform thermal conductivity, no radioactive heat production, constant initial temperature in the anomaly region, and a source edge that corresponds to the edge of the Snake River Plain. Since that model was described, attention has been focused on other phenomena that may relate to the effects of the hot spot passage that are not addressed by that analytical model. Of particular interest are the apparent side effects of the hot spot. Thus in order to investigate the thermal implications of the various hypotheses about the side effects of the hot spot, we have calculated the thermal behavior of various models that may more realistically describe the conditions. A finite difference numerical program was used to make the calculations (Appendix B).

All of the various models were run with a starting condition that is more realistic than the simplified analytical model of Brott and others (1981). The initial conditions are illustrated in Figure 19. The starting temperature for all of the model runs described here was taken to be 800 °C between 5

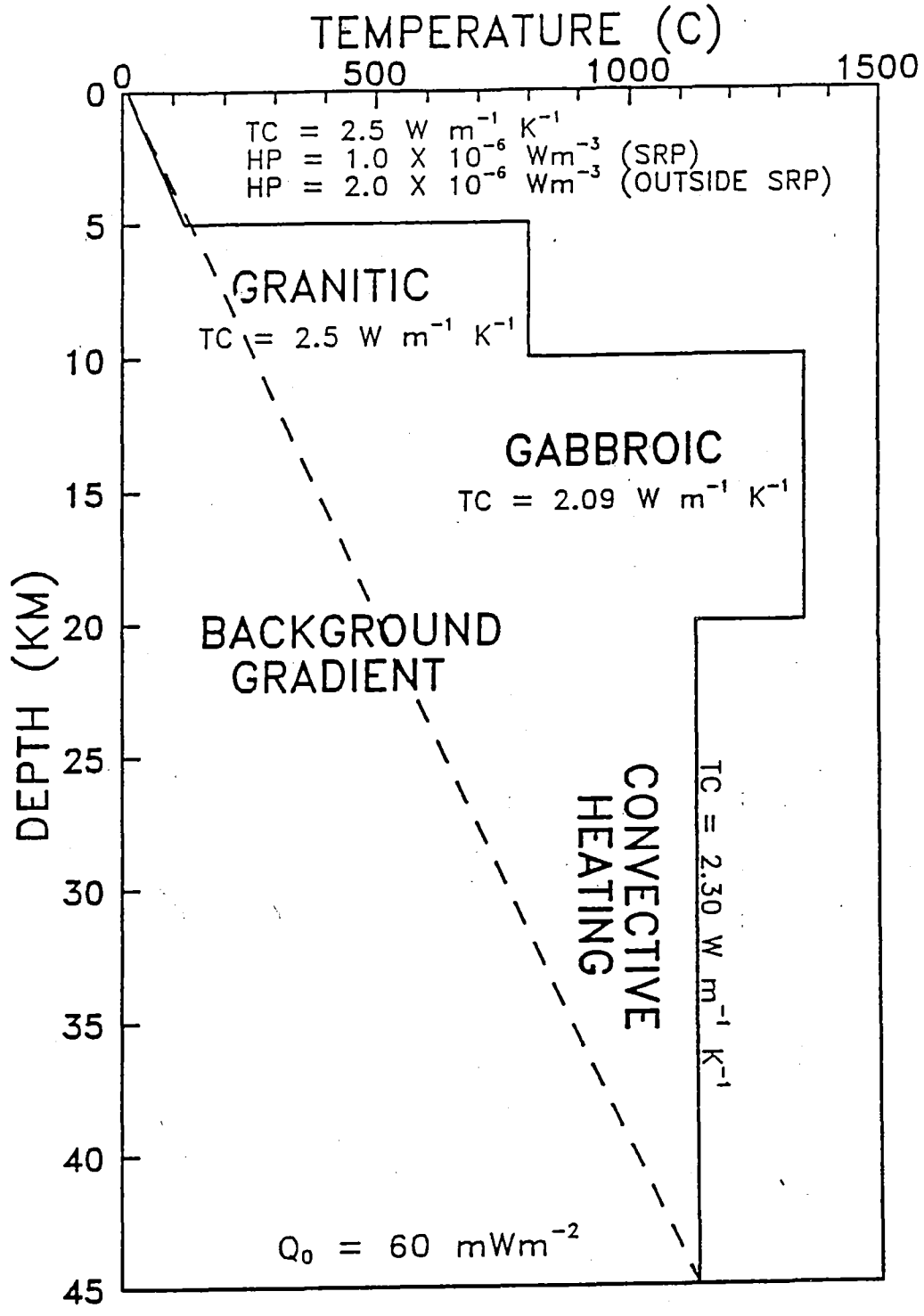

Figure 19. Initial conditions and background temperature-depth plot for thermal models. The thermal conductivity values and heat production values assumed for each layer are also shown.

and 10 km, 1350 °C between 10 and 20 km, and 1166 °C between 20 and 45 km. These initial conditions are imposed on a starting temperature assumed typical of the Basin and Range province, as described below. The base of the model is taken to be at 45 km, where the thermal conditions in the surrounding Basin and Range province are projected to reach the melting point curve of basalt and thus the base of the lithosphere is reached (Brott and others (1978, 1981) used 42 km for the base of their model).

The upper, high temperature zone approximates the high level granitic magma chamber associated with the hot spot and emplaced at a minimum melt temperature of 650 to 700 °C with an allowance of 100 to 150 °C to take into account the effects of latent heat. Lachenbruch and Sass (1978) used a value of 350 °C for the latent heat term in their models. The effect of a hotter chamber (950 °C, corresponding to a magma temperature of 800 to 850 °C) was also investigated. The middle, high temperature zone corresponds to the midcrustal gabbroic magma chamber in the Snake River Plain outlined by the seismic data (Braile and others, 1981). The melting point in this layer is also augmented by about 150 °C to allow for the effects of latent heat. The third layer at 1166 °C represents the convectively heated lower crust and upper mantle over the hot spot. The dashed curve shown in Figure 19 represents in a generalized way the background temperature in the surrounding Basin and Range province. In most of the models the whole section was allowed to cool after the passage of the hot spot, i.e. the high temperature zones were not replenished after the initial phase of heating. In other words, the models are instantaneous. In the real case the hot spot has some finite, but unknown, dimensions and so intrusion will continue for some period of time as the hot spot passes a given point. For example, the length of the Yellowstone caldera is 60 km and based on uplift observations, intrusion may be going on under it and also to the northeast (Pelton and Smith, 1982). If the hot spot velocity is 3.5 cm/yr, then the strike length that is associated with the active intrusion corresponds to about 1-2 Ma of motion for the hot spot. This finite length makes it difficult to pick the exact time for comparison of theoretical models to specific geographic positions. This assumption was investigated in some model runs by allowing heating for various periods of time before emplacement of the intrusions and by allowing continuing input of heat from the mantle after passage of the hot spot. The preheating effects are briefly summarized in the following section.

The essential feature of the model is the instantaneous pulse of heat within and in the immediate environs of the Snake River Plain/Yellowstone area as represented by the anomalous temperature regions. The heat loss associated with the hot spot apex is about 20 to 30 times the total background heat loss. Additional heat input outside of and along the track of the hot spot is less than or equal to 10 to 20 % of the regional heat flow or less than 0.1 % of the heat loss in Yellowstone. Thus the details of the model, excluding the initial conditions, are almost outside the resolution limits of observational data and the details are not well constrained. The thickened mafic crust is not observed seismically beneath the Yellowstone caldera (Smith and Braile, 1984). However, based on the heat transfer and the

volcanic patterns the bulk of the magmatic emplacement must be over by the time corresponding to the position of the Henry's Fork caldera so that the mafic batholith must be fully formed at that time. Thus the instantaneous model is the appropriate one to model the geologic situation.

Other conditions that differ from the model of Brott and others (1981) are the inclusion of regions of different thermal conductivity in the model to correspond to areas of different composition and temperature. The thermal conductivity values used in the models are shown on Figure 19. The highest thermal conductivity values are used for the upper crust of granitic composition, although the assumed value is lower than typical room temperature values to allow for the effect of temperature. The predominantly carbonate section in the upper several kilometers of the Idaho Basin and Range province will have a similar thermal conductivity value. The middle of the crust has a higher temperature and a more basic composition, so a lower thermal conductivity value was used. The high temperature basic and ultrabasic rocks of the lower crust and upper mantle in the third layer are assumed to have a slightly higher thermal conductivity based on compositional effects.

The effects of radioactivity in the upper crust were also not included in the Brott and others (1981) model. In the models in this discussion the radioactivity in the upper 10 km of the crust outside the Snake River Plain was assumed to be 2 μWm^{-3}, a typical value for the granitic crust and sufficient to imply a background heat flow of about 80 mWm^{-2} (assuming a typical mantle heat flow of 60 mWm^{-2} for the intermountain area, Blackwell, 1978). The temperatures calculated for this model were used as the starting conditions. Inside the Snake River Plain the radioactive heat production was assumed to be 1 μWm^{-3} to allow for the loss of radioactive sources due to possible extension, erosion, and ash dispersal (Brott and others, 1981). The only effect of the change in radioactive heat generation is to decrease the background heat flow in the Snake River Plain by about 10 mWm^{-2} so that the steady state value of heat flow is about 70 mWm^{-2}. The resulting decrease in temperature is offset by the effect of the low thermal conductivity in the sedimentary basin, so the temperatures are higher, even at steady state, in the Western Snake River Plain than in the Basin and Range province (Brott and others, 1978)..

To fit the thermal pattern in the Western Snake River Plain a model was run that simulated the development of a sedimentary basin subsequent to the passage of the hot spot. The results shown in Figure 22 are compared to the data (solid circles) from the cross section in Figure 5. Given the uncertainty from a variety of sources the fit is satisfactory. The heat flow data do not conclusively require the presence of low heat generation crust in the Snake River Plain, but predicted heat flow values match the measured values best when low heat generation is included in the model (Figure 22). As was demonstrated by Brott and others (1978), this type of model gives a good fit to the regional conductive characteristics of the heat flow distribution, but does not match the heat flow in shallow geothermal systems along the edges. The data plotted on the figure are not contaminated by such effects as described in the discussion of Figure 5.

The equilibrium heat flow for the models inside the Snake River Plain will approach 70 mWm^{-2}

away from the thermal refraction at the edges of the Western Snake River Basin as the thermal effect of the hot spot disappears. In comparison, the heat flow of the Columbia Plateau region, a possible point of the initiation of the hot spot according to Morgan (1981), is 60 to 65 mWm^{-2} (Blackwell and others, 1990). The crust is dominantly mafic in the Columbia Basin (Catchings and Mooney, 1988), and so the crustal heat production there is very small. Thus any residual thermal effect of the proposed hot spot in the Columbia Basin is now negligible.

The geometries of the different regions used in the modeling are illustrated in Figure 20. Since insulated side boundary conditions are used in the finite difference model (Appendix B), the half-width of each of the high temperature regions is shown, with zero on the x-axis corresponding to the center of the Snake River Plain/Yellowstone zone. There are four basic configurations used in the modeling (models PL3, PL5, PL8, and PL9). The PL3 model is an approximation to the analytical model of Brott and others (1981). The other models have some combination of wider thermal anomalies so that the thermal effects in the crust extend well beyond the edge of the Snake River Plain. The half-width assumed for the models with heat sources extending outside the Snake River Plain is somewhat arbitrary and is discussed below. The 50 km half-width assumed in the modeling for the shallow-silicic chamber is reasonable based on the extent of silicic source areas; however, this half-width could range from 25 to 75 km. In any reasonable case the results shown are not dependant on the details of the local half-widths.

Heat flow cross sections and temperature maps were output at approximately 2.5 Ma intervals for each model. The heat flow results for model PL9 (an intermediate-width heat source in the lower crust and a wide, gabbroic, heat source in the middle crust) are shown in Figure 21a as an example. Heat flow over the center is about 130, 100, 90, and 74 mWm^{-2} at ages of 2.6, 5, 7.5 and 10 Ma. At 10 km inside the edge of the Snake River Plain the heat flow values are within 10% of the peak value. At a distance of 60 km from the margin the heat flow anomaly drops to zero. After 2.6 Ma the model is cooling almost everywhere, even over the regions where the depth to the anomalous heat source is 20 km.

Thermal subsidence was also calculated as a function of time and the results for model PL9 are shown on Figure 21b. To determine the subsidence of the models the integrated background temperature (the steady state profile in the Basin and Range province) was subtracted from the integrated temperature for each column in the finite difference model at a particular time. The temperature difference was related to length using a thermal expansion coefficient of $7.4*10^{-5}$ /°C (Brott and others, 1981). The subsidence at each distance was determined by subtracting the elevation difference calculated at a given time from a base level of zero elevation at time equal to zero. Thus simple point isostasy is assumed and no initial uplift is taken into account. Brott and others (1981) argued that the hot spot is not preceded by significant heating and uplift because of its high relative velocity and the shape of the streamlines associated with the flow (see Sleep, 1990). Thus the primary

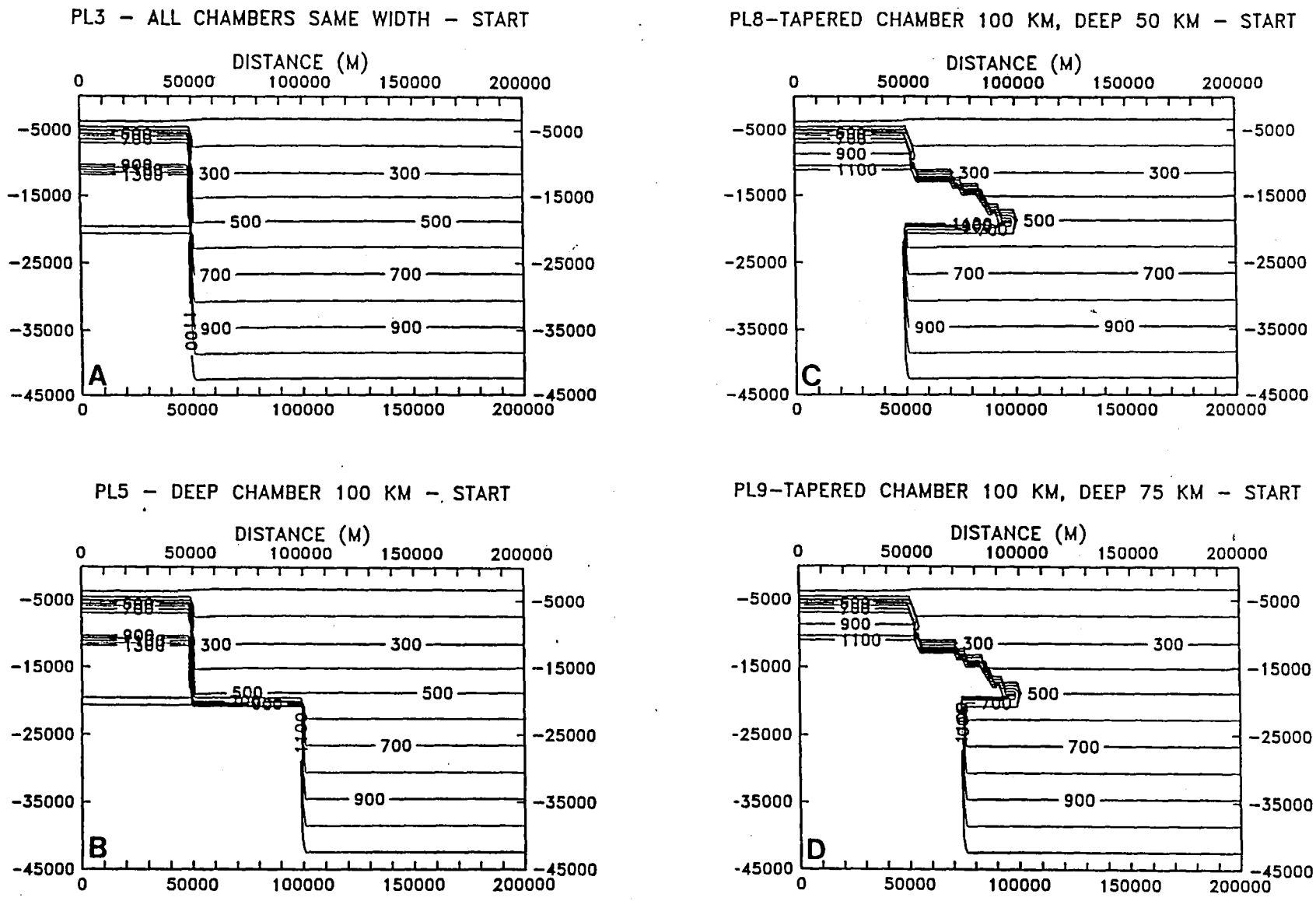

Figure 20a-d. Initial conditions for instantaneous models PL3, PL5, PL8, and PL9.

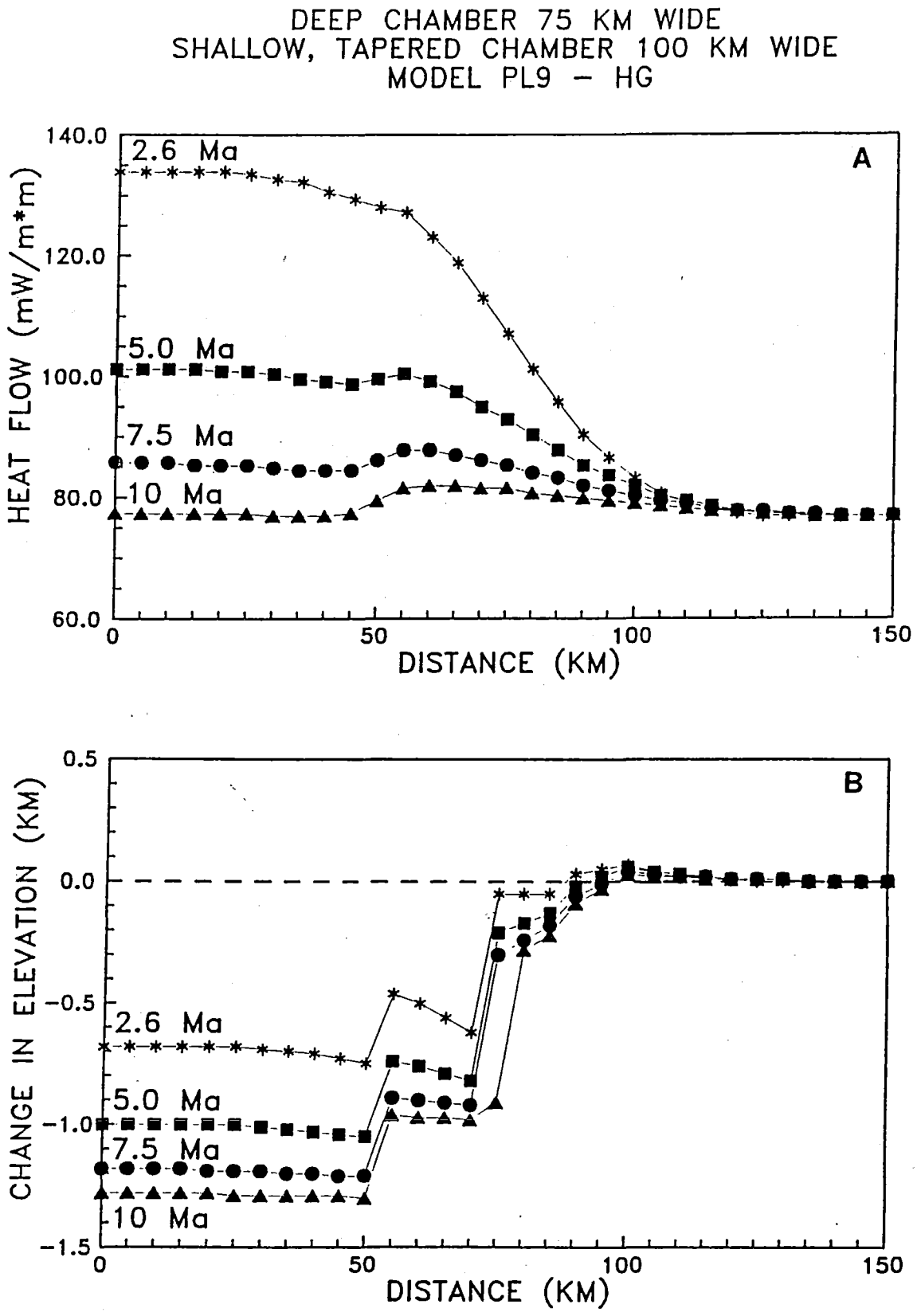

Figure 21. Figure 21a. Heat flow as a function of time for model PL9. Figure 21b. Subsidence as a function of time for model PL9.

effect is subsidence. Most of the subsidence predicted by the models has occurred by 5 Ma with only about 200 m predicted for the remainder of the cooling. A maximum subsidence of about 700 and 1000 m is predicted for 2.6 and 5 Ma, respectively.

Heat flow curves for the four models of Figure 20 are shown in Figure 23. The calculated heat flow values are compared for times of 2.6 and 5.0 M.y. since intrusion emplacement. The heat flow curve for PL9 at 10 Ma, which is similar to the 10 Ma curve for the other three models, is also shown for reference. The lower heat flow in the Snake River Plain (0 to 50 km) that is evident on the 5 and 10 Ma curves is due to the assumed difference in crustal heat generation between the Snake River Plain and the Basin and Range.

If neither the gabbroic nor lower crustal heat sources extend beyond the edge (PL3), the heat flow 10 to 20 km into the Snake River Plain is substantially below the axial value. If the edge of either one, or both, of the deep heat sources extends more than 10 km past the edge of the Snake River Plain, then the heat flow inside the plain at the INEL-GT1 site, for example, would be similar to the axial value (Figures 21 and 23). The predicted axial heat flow values at 5 Ma are 102 mWm^{-2} for all models. This value is in reasonable agreement with the observed value at INEL-GT1, particularly if the age of the hot spot is taken to be slightly less than 5 Ma due to the finite time for the passage of the peak of the hot spot.

In contrast, the heat flow value predicted by model PL3 at 5 Ma for the location of INEL-GT1 (10 km inside the plain) is about 90 mWm^{-2}. This value is significantly lower than the observed value of 107 mWm^{-2}. Thus if the heat source is narrow the heat flow at INEL-GT1 should be much lower than that further toward the axis of the Snake River Plain and the heat flow there might be on the order of 120 mWm^{-2}. Because there are no heat flow data closer to the center the various possible source widths cannot be tested in this manner at this time.

Because the models that have the crustal heat source extending outside the Snake River Plain have a heat flow along the margins that is similar to the axial heat flow, a portion of the high heat flow that is characteristic of the margins might be related to the regional heat flow configuration, particularly if there is some local thermal conductivity refraction associated with the edge of the Snake River Plain (as shown on a larger scale in Figure 22) so that some high heat flow values (locally as high as 150 mWm^{-2} or so) could be explained without the need for groundwater flow, as discussed in a previous section. The relatively high permeability indicated by the productive capabilities of the wells and the artesian nature of many of the systems are evidence that there is active groundwater flow in many areas, but not enough is known about the extent of the systems to characterize the proportion of conductive versus convective heat transport along the margins.

The heat flow on the margins for the first 5 Ma is very sensitive to the lateral dimensions of the heat sources. However, by 10 Ma the heat flow values for the models with wide thermal anomalies are only about 5 mWm^{-2} above the Basin and Range background, and the presence of a wide heat source

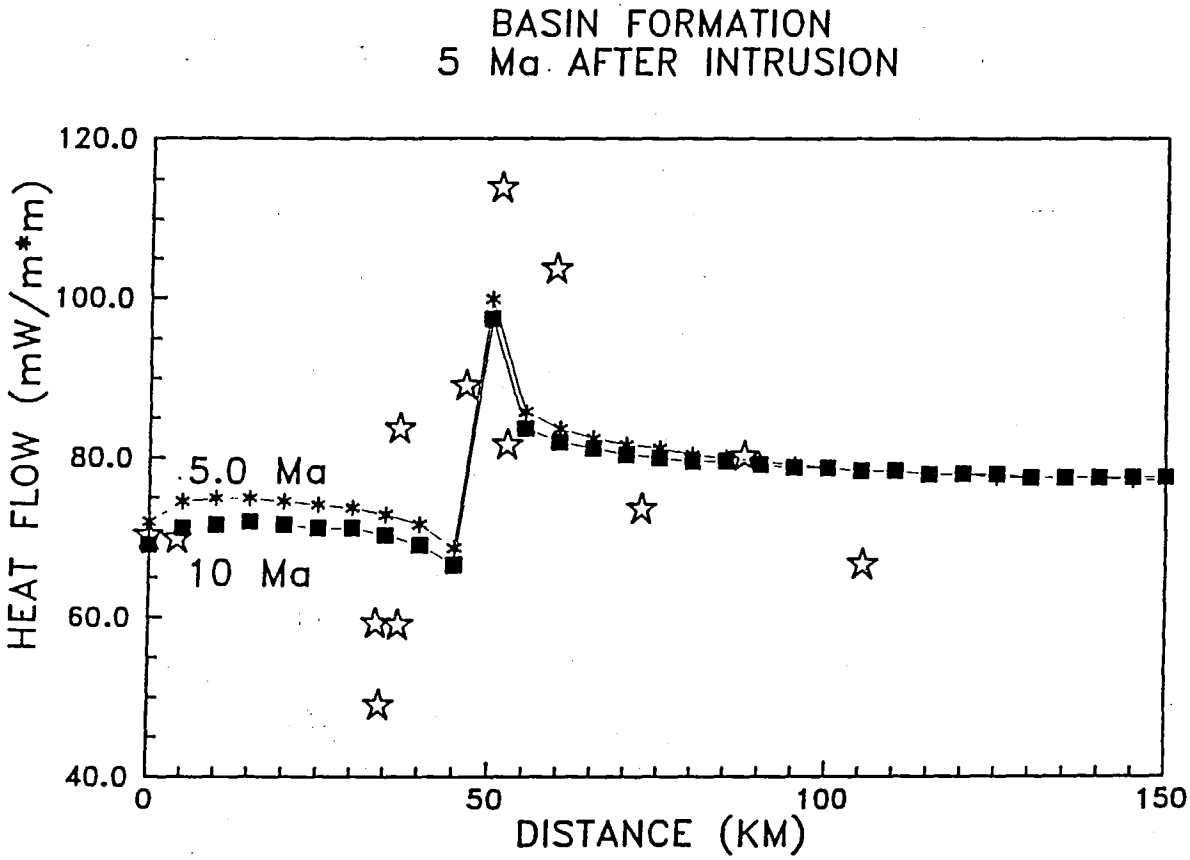

Figure 22. Heat flow as a function of time following formation of a sedimentary basin at 5 Ma after hot spot passage. The times of 5 and 10 Ma on the curves refer to the time since basin formation, and represent the heat flow 10 and 15 Ma after the passage of the hot spot, respectively. Heat flow sites shown as dots in Figure 5 are plotted as stars.

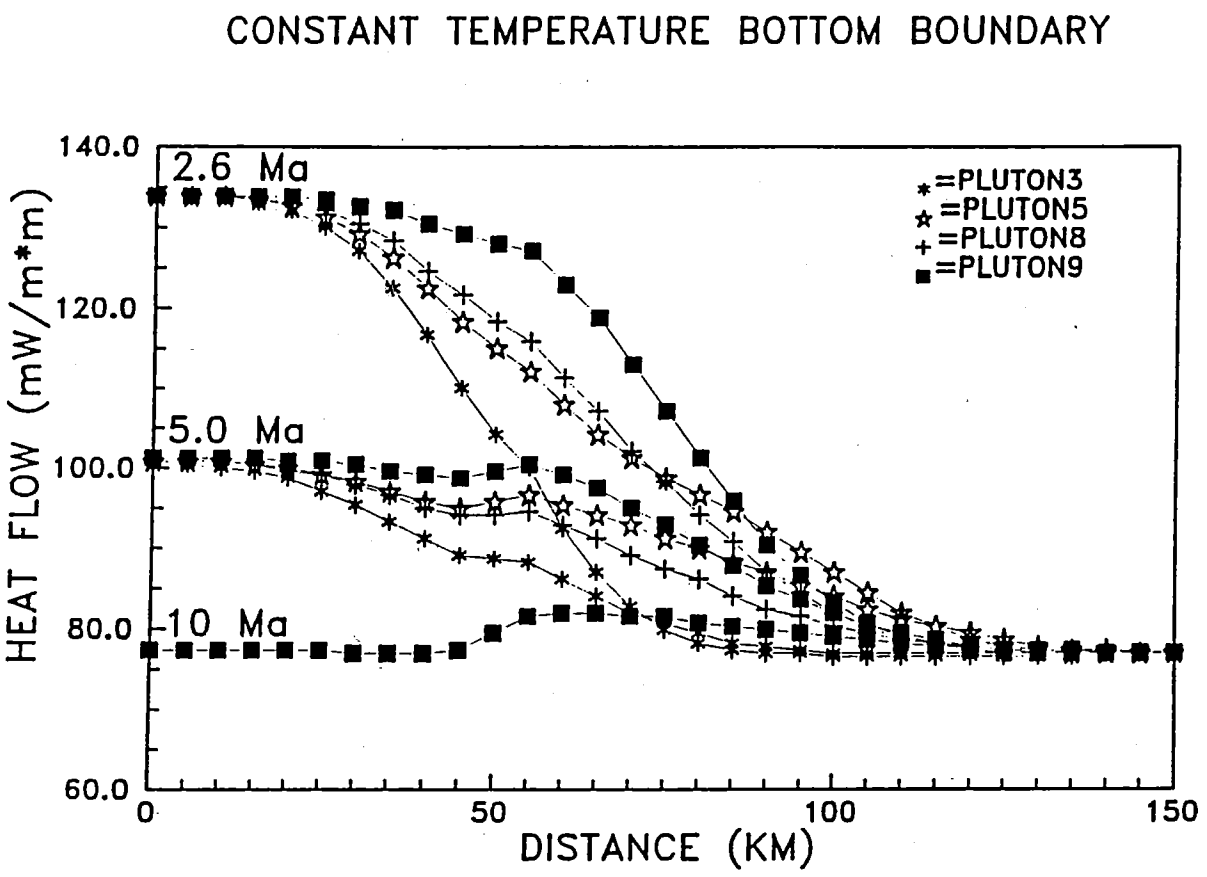

Figure 23. Comparison of heat flow at 2.6 and 5.0 Ma for the PL3, 5, 8, and 9 models.

probably could not be resolved based on heat flow data alone. Model PL9, with both gabbroic and lower crustal sources extending beyond the margins, has a heat flow at 5 Ma equivalent to the axial heat flow at a distance that is 10 to 15 km beyond the edge of the Snake River Plain. The two models with one of the two sources extending beyond the edge (PL5 and PL8) are similar at 2.6 Ma, and all three models (including PL9) have heat flow values that are about 90 mWm^{-2}, or about 10 mWm^{-2} above Basin and Range background, 20 to 40 km into the Basin and Range for at least 5 Ma. The thermal results from the deep hydrocarbon wells should be able to resolve heat flow variations from the edge outward of this order of magnitude to constrain the range of possible crustal heat sources.

All three models with broad heat sources have heat flow-versus-time curves that show cooling after 2.6 m.y. at almost all positions. The areas of heating are limited to the outside edges of the models and the amounts of heating are minimal. As an illustration of the temporal variations, the changes in temperature as a function of time are presented as a temperature difference map, where the temperatures resulting from the model with the heat source confined to the Snake River Plain (PL3) were subtracted from those resulting from the model with a wide, mid-crustal heat source and intermediate width, deep heat source (PL9-Figure 24). Similarly a temperature difference map was calculated for the wide, deep chamber (PL-5) subtracted from the Basin and Range background (Figure 25). These plots illustrate the increase in temperature along the margins if the source extends outside the edge of the Snake River Plain. The models with heat sources outside the Snake River Plain (Figure 24) show much higher temperatures in the inside edge of the earthquake zones although the differences be 5 Ma are small. Compared to the background in the Basin and Range all models with wide thermal anomalies (e.g. Figure 25) are significantly hotter starting within 10 to 20 km of the edge of the earthquake zones. Thus thermal models that have wide heat sources might influence the crustal properties in the vicinity of the edge of the seismic parabola.

The extent of the heat source should be testable if information was available on the details of the crustal structure along the margins. However, such data are not available. The interpretation of Braile and others (1982) and Sparlin and others (1982) is that the midcrustal high velocity body that is thought to be the gabbroic heat source layer is essentially confined to the Snake River Plain. The cross sections shown by Sparlin and others (1982) have the top of the basic chamber dipping to a background depth in the Basin and Range province of the midcrustal layer at 15 km over a lateral distance of about 10 km away from the margin. However, the seismic data from southwestern Idaho (Hill and Pakiser, 1961) indicate that the thin silicic/thick mafic layer combination underlies both the Owyhee Plateau as well as the western Snake River Plain (see Blackwell, 1989 for comparative cross sections). Additional detailed seismic data in the Basin and Range adjacent to the Eastern Snake River Plain are necessary to address the problem.

As discussed above, the heat flow data from the Western Snake River Plain are best fit by a model where the crust in the Snake River Plain has a lower heat generation than the crust in the Basin and

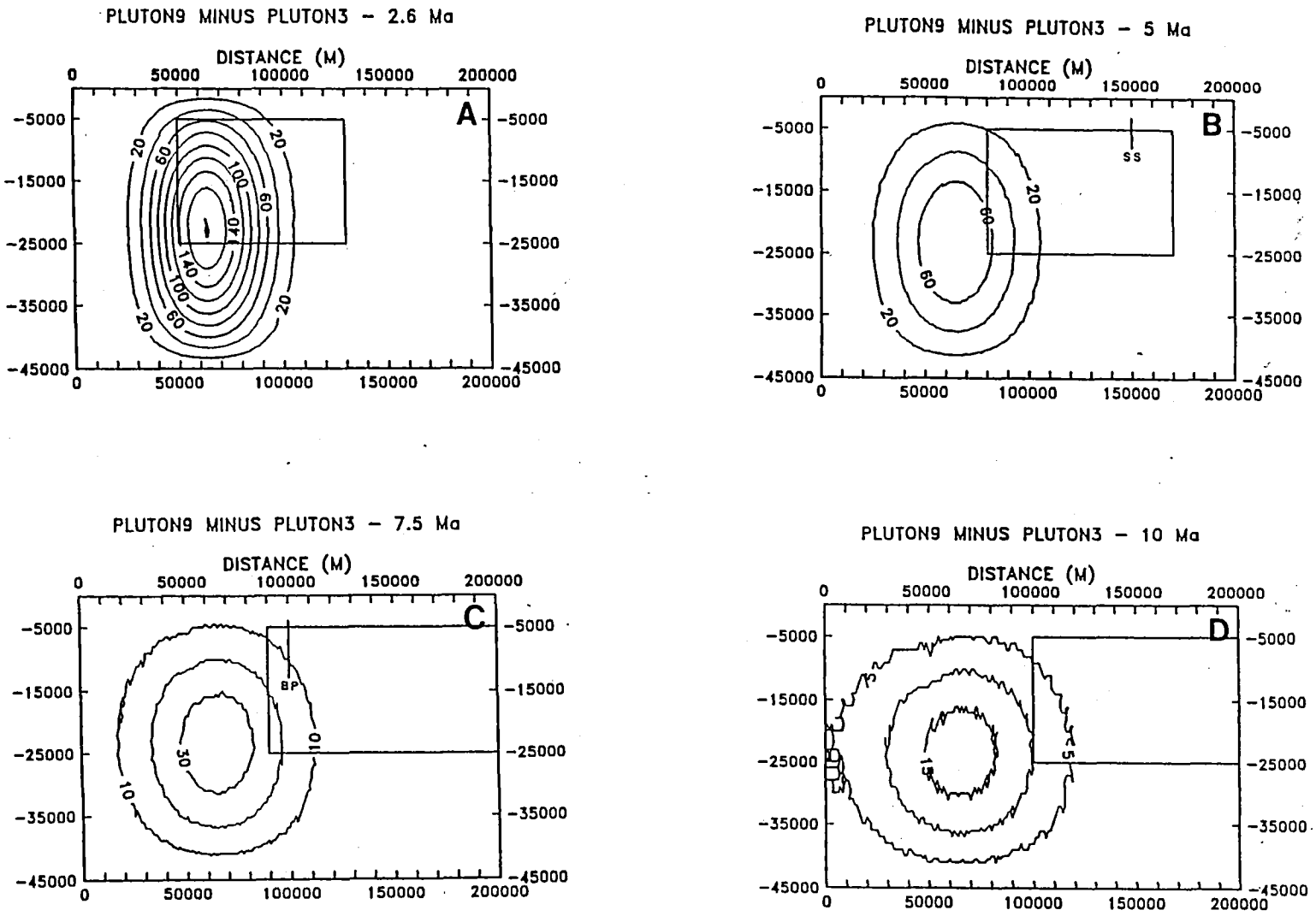

Figure 24a-d. Temperature difference models for models PL3 and PL9 at 2.6, 5, 7.5, and 10 Ma. Boxes represent the general dimensions and depths of the earthquake parabola as a function of time from Anders and others (1989) and Smith and Arabatz (1991). Locations of Borah Peak (BP) and Soda Springs (SS) earthquake swarms from Smith and Arabatz (1991).

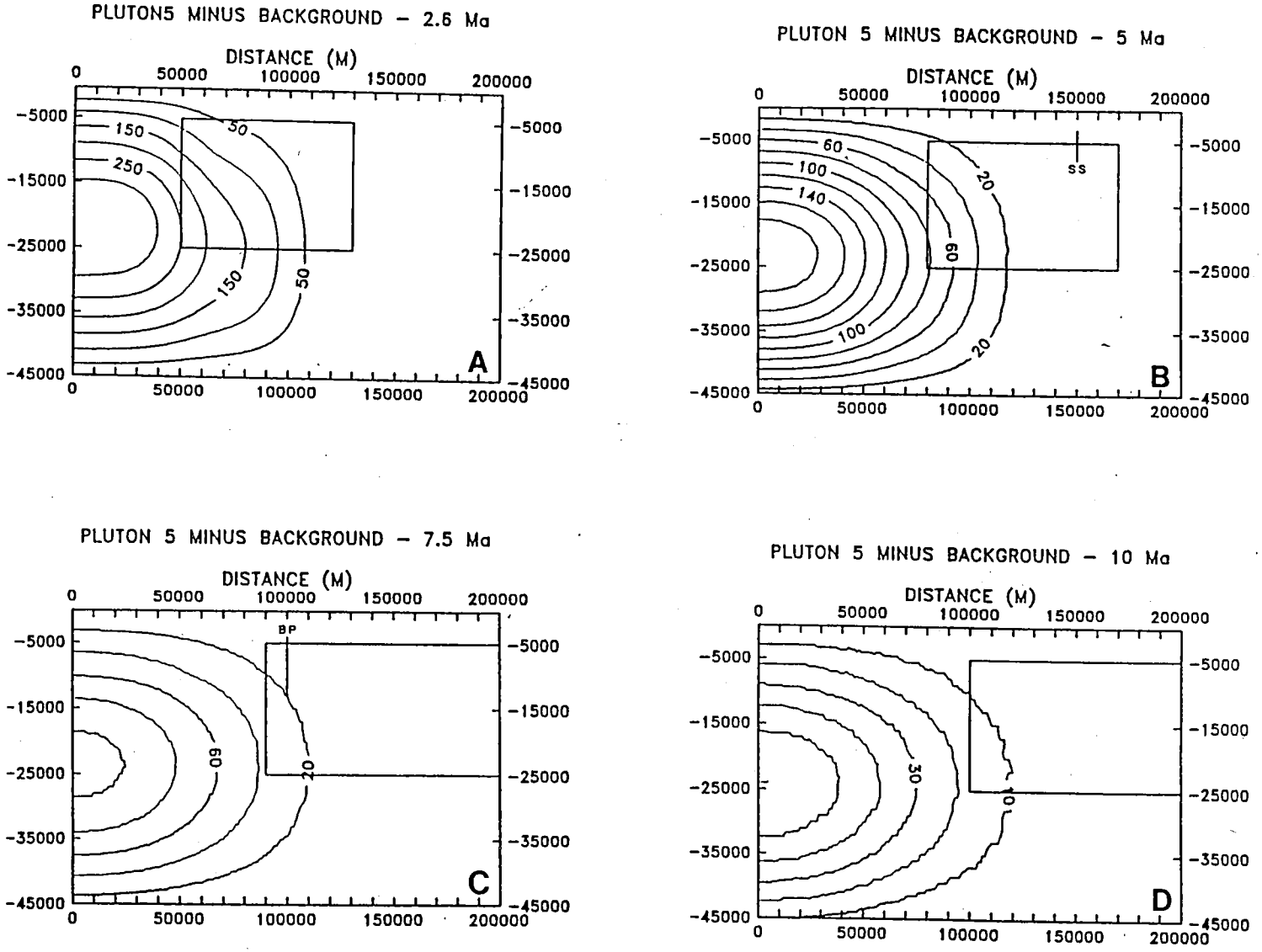

Figure 25a-d. Temperature difference models for models PL5 and the assumed Basin and Range regional background at 2.6, 5, 7.5, and 10 Ma.

Range province. In order to test the consequences of this assumed model configurations on the calculated heat flow and crustal temperatures in the Snake River Plain, a model with a 10 km thick layer with a constant heat generation of 2 μWm^{-3} throughout the layer was run and compared to the model described previously. At distances greater than 55 km from the axis of the plain, the heat flow values and crustal temperatures calculated by the two models are identical. The maximum divergence of the Figure 24 model results occurs in the center of the plain; the heat flow at each time step is $7mWm^{-2}$ higher for the model with higher heat generation in the Snake River Plain. The maximum temperature difference between the models is 15°C in the depth range of 6 to 10 km at 10 Ma, and for the 5 Ma model the temperature difference is generally less than 10°C for any given depth. This small difference in temperature between the models has no significant effect on the predicted rheological properties of the crust, to be discussed in a later section.

A model with a 950°C shallow, granitic magma chamber was run to compare the heat flow and crustal temperatures predicted from this model with the results from a similar model with an 800°C shallow chamber. The maximum difference between the models occurs at 2.6 Ma in the center of the plain, where the heat flow for the 950°C chamber is $2mWm^{-2}$ higher than the heat flow for the 800°C chamber. However, by 5 Ma, the heat flow and temperatures predicted by the two models are virtually identical.

Other Models

None of the models discussed in the previous section show heating in the margins at any time 2 Ma after passage of the hot spot. Thus to investigate the hypotheses that heating of the margins is related to the unusual set of tectonic effects observed there, other types of models must be considered. We investigated models in which the mantle heat flow of the margins increases after passage of the center of the hot spot. The basis for such models is that the radius of the hot spot in the mantle, particularly downstream, is probably more than the 100 km width of the Snake River Plain/Yellowstone feature and the shape must be strongly influenced by the North American plate motion over it. Thus there might be a component of heat flow from the mantle superimposed on the crustal types of sources investigated in the preceding discussion. The magnitude of such a source is constrained by the fact that the heat flow in the areas along the track, including in the possible spot of initiation of the plume, where the passage was over 10 Ma are the same as in the rest of the back-arc region of the Western United States (Blackwell and others, 1991).

Several models with a superimposed heat flow component above the background assumed for the previous models were also investigated. These models simulated a mantle heat source that is bigger than the width of the volcanic track alone. The heat flow increases have to be kept below about 10 mWm^{-2} so that the observational constraints are not violated. The effect of an increase in the heat flow

at the base of the model of 4 mWm^{-2} at the center dying off to 2 mWm^{-2} at 100 km, and 0.8 mWm^{-2} at 200 km was calculated for the model with a crustal heat source distribution like PL8. There is a increase in the surface heat flow outside the Snake River Plain with time in this model. The heat flow along the axis is higher than in the models previously described at long times as the effect of the initial conditions ceases to dominate the heat flow. This type of model is more consistent with the interpretation that the locations of the earthquakes are related to heating over the time scale of the passage of the hot spot through southern Idaho. However, the actual temperature effects are modest except beneath the Snake River Plain, where the temperatures are significantly higher for the models with imposed heat flow (up to 300 °C) compared to the models with the constant temperature bottom boundary condition. A constant heat flow bottom condition implies a reflective bottom boundary, so that the heat diffusing from the magma builds up at the bottom of the model. In contrast, the bottom boundary for the constant temperature condition allows heat to escape from the model more quickly. As a result the temperatures of the constant heat flow versus the constant temperature models cannot be directly compared and comparisons of rheological profiles calculated using the two types of models may not be relevant to the questions of interest in this report. Thus these models are not discussed in detail. For examples in the one-dimensional case the differences in the temperature implications of constant heat flow, constant temperature, and semi-infinite bottom boundary conditions have been discussed by Vitrello and Pollack (1980).

A model that does address the possibility of a large time dependent heat flow outside the Snake River Plain and is comparable to the thermal models discussed above is PL11; the initial conditions are the same as for model PL8. This model is instantaneous, so the temperatures are directly comparable to those from the models discussed above. In model PL11 the thermal anomaly was assumed to extend for up to 100 km outside of the Snake River Plain in the lower crust as shown in Figure 26a. Temperatures in the lower crust in the region indicated were raised to 1150 °C at 1.0 Ma after cooling started. The heat flow from PL11 is shown in Figure 26b. The surface heat flow effects are modest, but the crustal temperature effects are more significant as shown in Figure 27. In this case the temperature increases in the area of the earthquakes (boxes on the figures) are significant. At 2.6 Ma, just 1.6 Ma after the lower crustal heat source in emplaced, the temperature effect is centered at a model distance of 100 km and is over 100 °C. At 5 Ma the temperature effect is at the inside edge of the earthquake zone and is over 70 °C. Clearly this type of model could be tweaked to produce a zone of maximum temperature anomaly at the edge of the earthquake box. So the argument could be made that the localizing factor is the edge of heating (and thus the crustal strength transition zone) associated with lower crustal intrusion along the outer sections of the hot spot.

This type of temperature field could be produced with many combinations of time-dependent intrusions along the margins. The difficulty is that there is no obvious way to independently test the geological possibility of the different models.

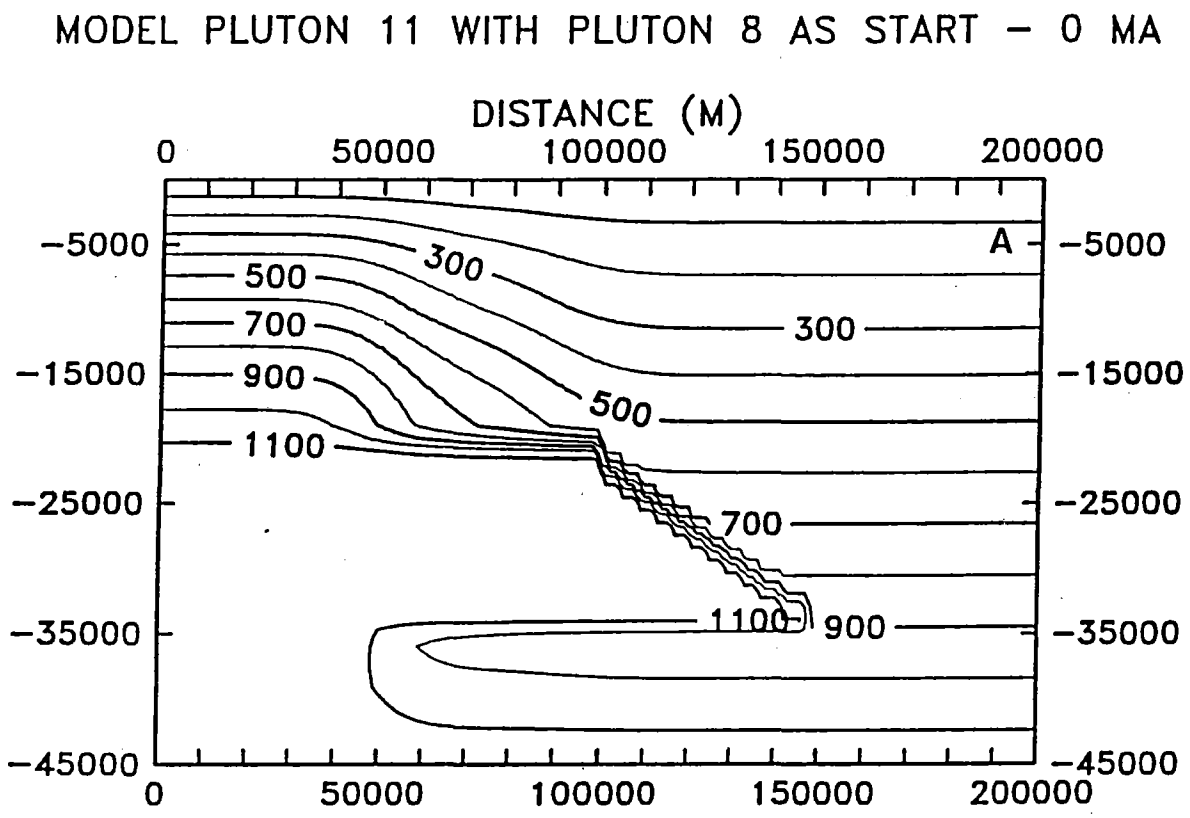

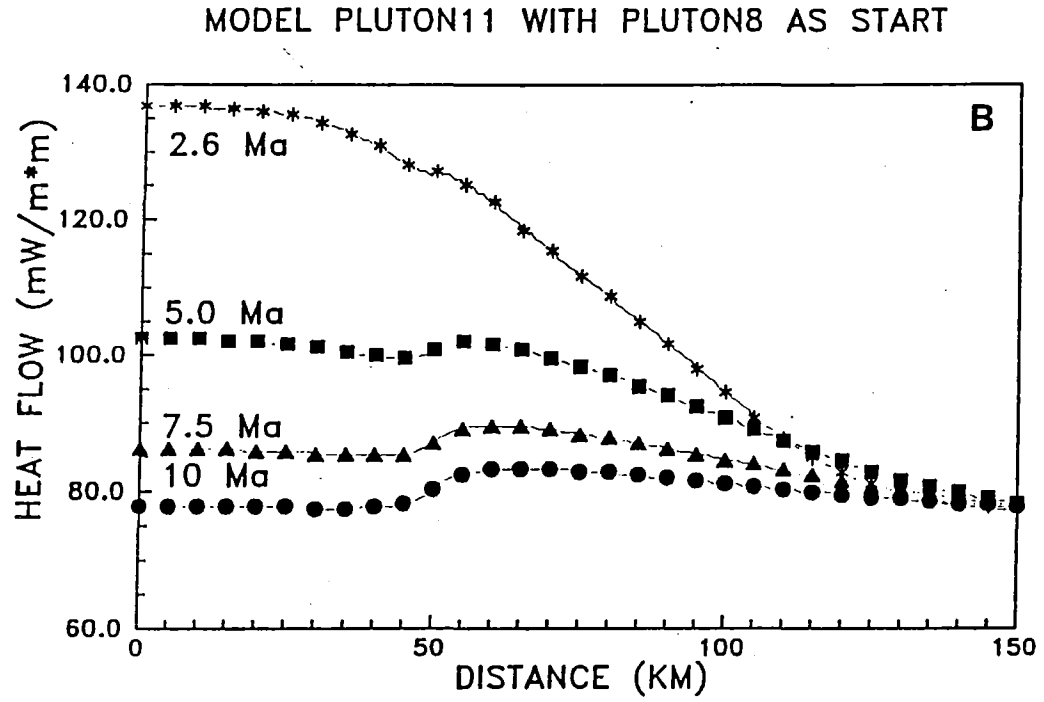

Figure 26. Figure 26a. Initial isotherms for PL11. Figure 26b. Heat flow as a function of time and position for model PL 11.

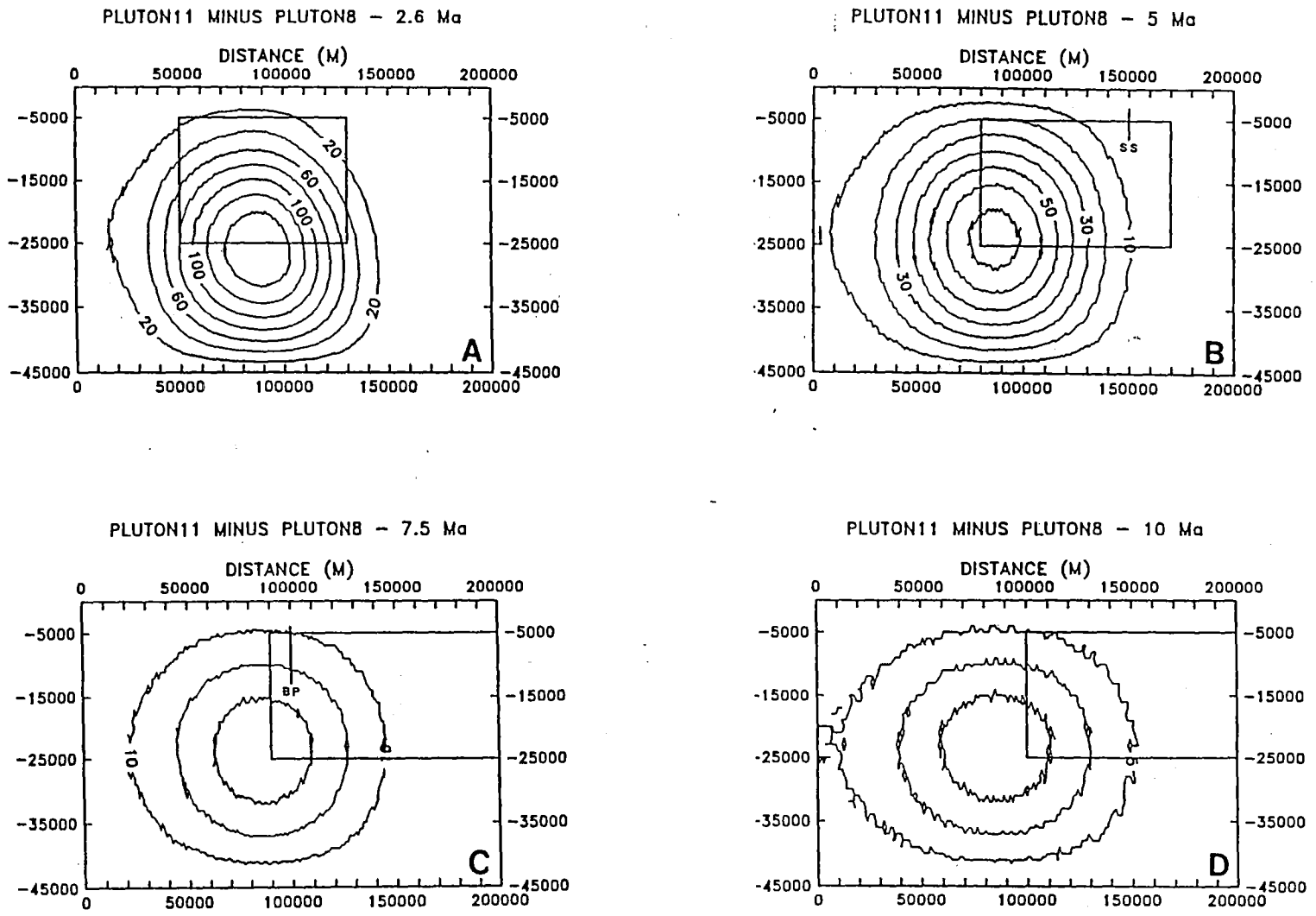

Figure 27a-d. Temperature difference as a function of time and space between the models with the crustal conditions of PL8 and model PL11.

DISCUSSION

Topographic Evidence for Dimensions

Profiles of topography in four valleys intersecting the north side of the Eastern Snake River Plain are shown in Figure 28. The valleys rise about 700 to 800 m from the level of the Eastern Snake River Plain to drainage divides 100 to 140 km away. Typical decreases in elevation of 500 m then occur over the next 25 km. The shapes of the valley profiles are compatible with subsidence and deposition on the south sides and uplift and/or erosion on the north sides of the topographic divides. The systematic topography may be due to the elastic response of the lithosphere to the load in the Snake River Plain, to thermally related subsidence, to thermally related uplift away from the edges due to the side effects of the hot spot, or some combination of these and other effects. We believe that these topographic effects plus the presence of basaltic volcanism outside the boundaries of the Snake River Plain are the strongest evidence that the heat source must be wider than the physiographic feature alone.

The amounts of subsidence predicted (Figure 29) are qualitatively and quantitatively similar to those predicted from the thermal models PL5, PL8, and PL9, particularly when allowance is made for the effect of the ranges and the probable topography at the end of the heating. On the other hand, the predictions from model PL3 with no lateral heating do not match the actual topography at all. While the effects of an elastic layer will smooth out and distribute the load somewhat, the models with a significant lateral thermal component fit the observations much better. Thus the topographic effects (Figure 28) are taken as evidence for significant crustal cooling (presumably following heating) outside the Snake River Plain as a function of time following passage of the hot spot.

We investigated the expected amount of relief due to an elastic effect of the deformation associated with the Snake River Plain. The calculations were based on the Westerly Granite rheology, a thin sheet approximation of the deformation, a strain rate of 10^{-14}, and two different thermal gradients of 25 and 40 °C/km. The predicted elastic bulge had an amplitude of 45 to 90 m and occurred at a distance of 90 km from the load. While the distance is more or less correct, the amplitude of the bulge is much smaller than that actually observed.

Crustal Rheology

The model of Anders and others (1989) specifically depends on the modification of the crust by the thermal effects of the hot spot and by the change in mechanical profile accompanying the modification of the crust by emplacement of the mafic batholith. The effects of the models discussed above on the rheology of the crust were investigated. Possible yield envelopes for the crust and mantle for temperature-depth curves calculated for various regions were calculated as a qualitative comparison of

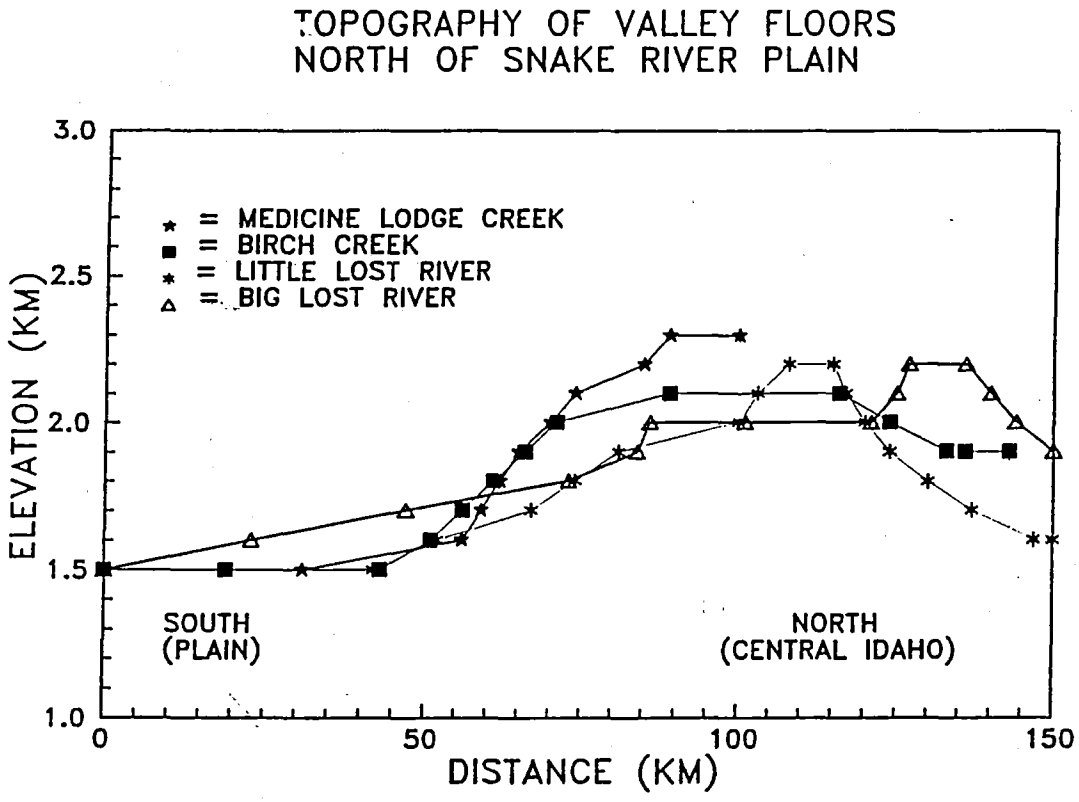

Figure 28. Elevation as a function of distance from the axis of the Eastern Snake River Plain northward along the major Basin and Range valleys intersecting it.

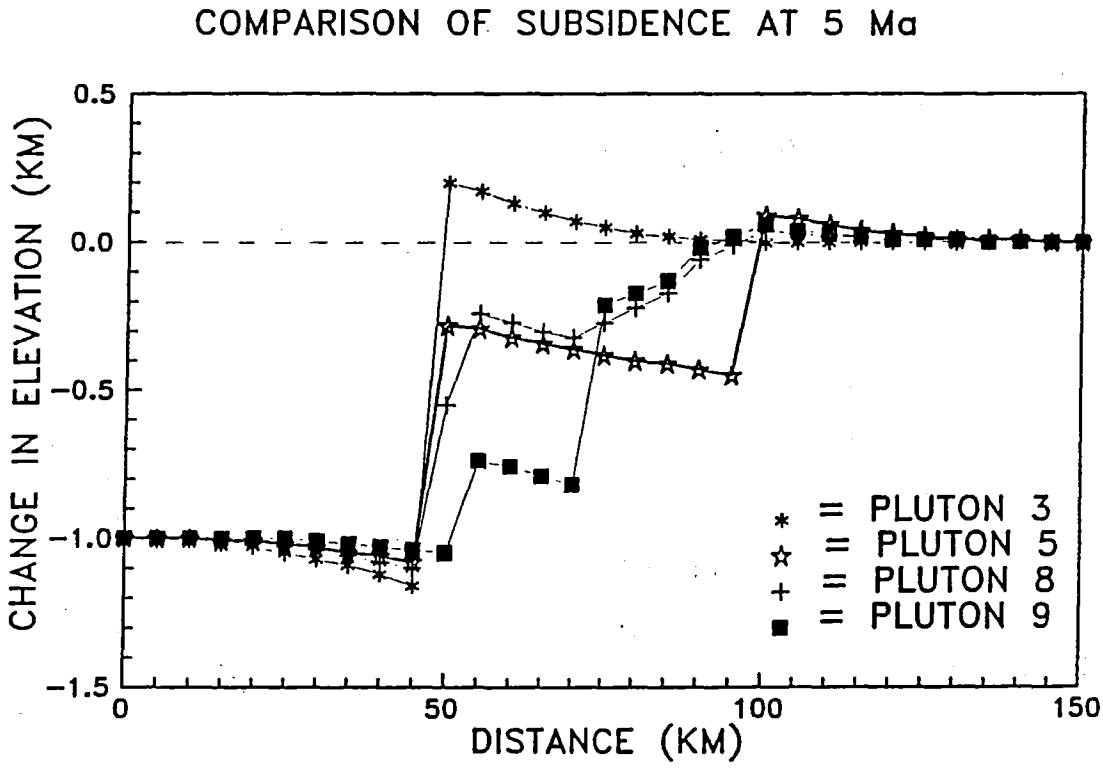

Figure 29. Predicted subsidence as a function of distance from the axis of the Snake River Plain for the PL3,5,8,and 9 models.

these effects. These curves are shown in Figure 30. In no case was a significant strength calculated for the mantle portion of the sections.

The brittle portion of the yield envelope was calculated using the Byerlee's Law relation (Byerlee, 1968) as formulated by Brace and Kohlstedt (1980). The ductile part of the yield envelope was determined from the power law equation published by Goetze and Evans (1979) using a strain rate of 1 x 10^{-14} s^{-1}. The power law constants used in this study for Westerly Granite and Maryland Diabase are from Table 4 of Carter and Tsenn (1987). The temperature profiles for the middle of the Snake River Plain, the edge of the Snake River Plain (50 km from the center), and background temperatures at 200 km away from the center are based on the thermal models discussed above. The crust is assumed to be composed of granitic material to a depth of 10 km in the Snake River Plain and of diabase at depths below 10 km. The Basin and Range crustal composition is similar, except that the granitic layer extends to a depth of 15 km.

The background strength envelopes calculated assuming an extensional regime for the Basin and Range and the Snake River Plain are shown in Figure 30a. The integrated strength for the Snake River Plain at thermal steady state should be larger because of the mafic material (with a plagioclase dominated rheology) occurs at shallower depth. This situation was postulated by Anders and others (1989) as the reason for the localization of the earthquake zones as the strain is localized along the contact between the weak Basin and Range crust and the strong Snake River Plain crust. The evolution of the strength envelope as a function of time for the models discussed in detail (PL5, PL8, PL9)again assuming an extensional regime is shown in Figure 30b. Due to the higher temperatures the integrated strength will be less, but in addition at ages of less than 8 to 9 Ma there will be a distinct mechanical layering of the Snake River Plain crust due to the high temperature gradients and the different compositions of the upper and lower crust.

However, in the Basin and Range province the only part of the crust to have significant strength is the upper layer. Thus for example at 2.6 Ma the elastic layer of the crust could be a thin as 8 km along the edge. The strength of the crust of the surrounding Basin and Range will be weakest at the edge and will become larger as the crust becomes cooler away from the edge of the Snake River Plain. Thus the strength pattern will be complicated in space and time. The strongest area at any time-constant cross section will be the coolest part of the Snake River Plain type crust and the weakest will be the warmest part of the Basin and Range type of crust. Thus the boundary of the two provinces may be a zone of maximum strength mismatch and represent a potential zone of decoupling. Thus the model of Anders and others (1989) for the parabola of seismic activity has a major difficulty. There is no evidence that crustal modification by the addition of a significant fraction of mafic material far away from the edges of the Snake River Plain/Yellowstone area has occurred. Seismic data do not at this time appear to support any such crustal modifications (Sparlin and others, 1981).

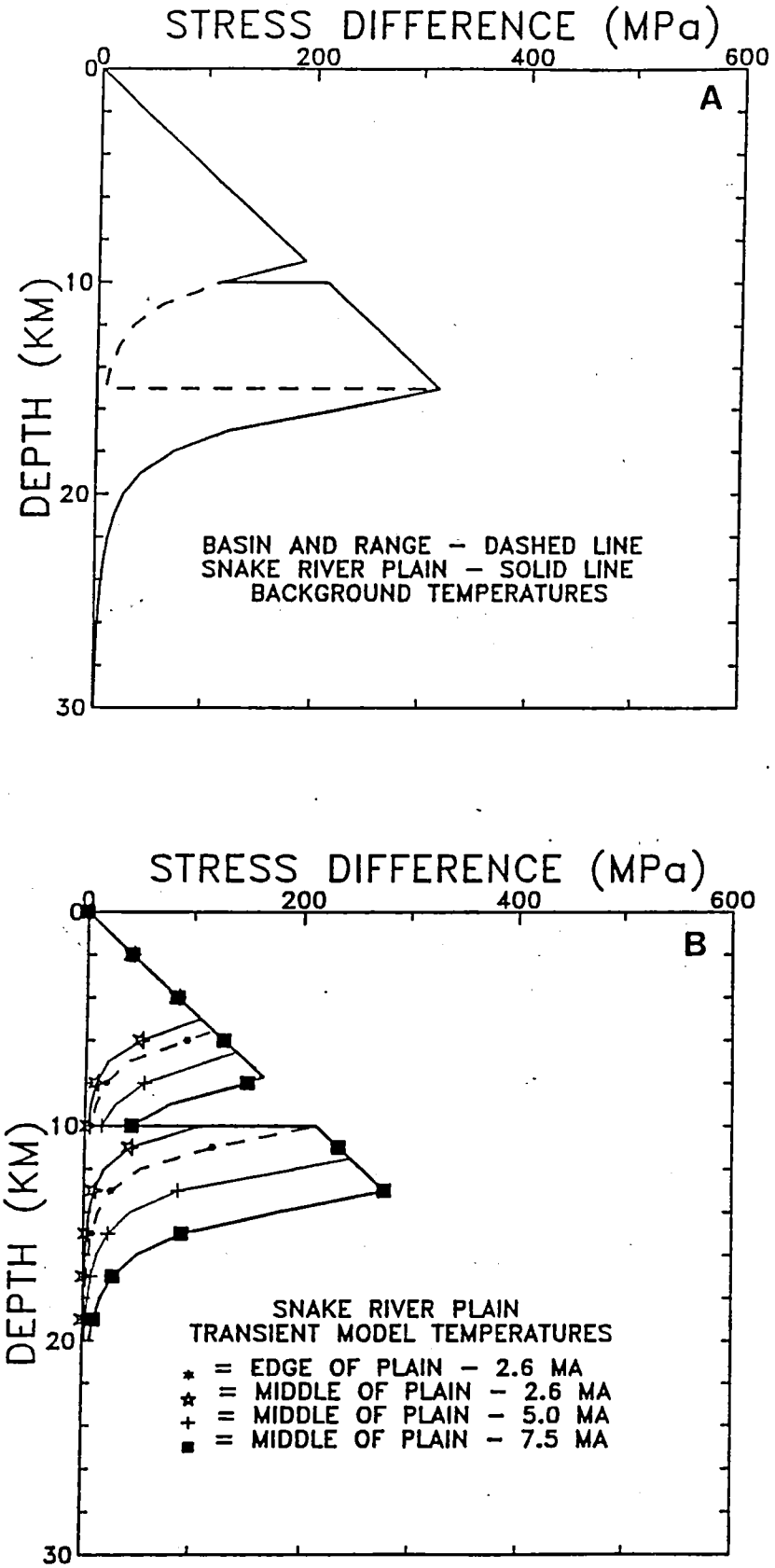

Figure 30. Strength envelopes in extension for crustal sections in the Snake River Plain and Basin and Range.

Thus if the parabola of seismic activity is to be related to the thermal effects there must be heating subsequent to the hot spot passage as suggested by model PL11. Furthermore the thermal models show that significant heating of the crust as far away as the outside edge of the earthquake parabola is not consistent with the thermal data unless the surface heat flow effects are minor. The tentative results indicate that the heat flow associated with the seismic belt in southeastern Idaho is quite variable. How is this observation to be resolved with the model that requires such systematic changes in strength with time? The strength profiles shown do illustrate the fact that the crust in this region must have extremely heterogeneous rheology. The Basin and Range crust should be the weakest along the margins with the Snake River Plain where it must be effected by heating. In this area the only strength in the lithosphere is in a thin zone in the granitic layer.

Contemporary Strain Field

Reilinger and others (1977) showed that the present vertical behavior of the Yellowstone/Snake River Plain region is as predicted by the hot spot concept. The Yellowstone region is rising and the Snake River Plain is subsiding. Within the Snake River Plain the stress differences appear to be small as indicated by borehole breakout analysis and the aseismicity of the region (Smith and Arabaz, 1991). In contrast significant horizontal strain is occurring in the surrounding region as indicated by seismicity and evidence of active faulting. Westaway (1989a, 1989b, 1990) explained the activity in terms of the strain imposed on the crust by the motions of mantle material flow driven by the hot spot flow. The correlation with actual motions remains debatable (Anders and others, 1990) and needs to be investigated by detailed determination of the actual directions of motion on the faults in question.

Within the Snake River Plain there is significant strain due to the subsidence. Strain rates due to the thermal contraction as shown in Figures 21b and 29 are between 10^{14} and 10^{-15} /sec or on the order of .1 to 1%/Ma. Thus the contractional strain rate due to cooling is of the same order of magnitude as the horizontal strain rate in the Basin and Range province. Hence the lack of horizontal strain in the Snake River Plain compared to the surrounding areas is only apparent. Rogers and others (1990) suggest that the strain is accommodated by dike intrusion in the Snake River Plain. Such dike intrusion could contribute to the heat flow in the Eastern Snake River Plain. The magnitude of the thermal contribution can be estimated by the relations between a steady rate of strain as accommodated by intrusion and the resulting heat flow developed by Lachenbruch and Sass (1978). The estimated shallow intrusion rate corresponds to a dike of basalt with a width of about 0.4 km every 1 Ma intruded between the depths of 0 and 10 km (W. R. Hackett, personal communication, 1992). The average contribution to the surface heat flow might be on the order of 5 mWm^{-2} (using equation 25, Lachenbruch and Sass, 1978, with an ambient temperature of 400 °C). Because in the case of very shallow intrusions the heat is lost even faster than predicted from the assumption of conductive cooling, the actual contribution to the regional

conductive heat flow will be even less and would probably not be dectable given the small amount of information on the heat flow regime.

Precursory Uplift

Weakening preceding the Yellowstone hot spot would require heating of the midcrustal region. Such heating would require significant uplift as no deformation (extension) has reached the areas more than 20 km ahead of the Yellowstone caldera. Anders and others (1989), Rogers and others (1990), and Pierce and Morgan (1990) argue that the uplift in the Beartooth Mountains is related to the precursory effects. However, evidence from fission track (FT) studies on apatite (sensitive to temperatures of about 60-140°C) from surface samples and from an Amoco well drilled through the Beartooth Mountains thrust indicates that there has been little differential, late Cenozoic, uplift of this block with respect to other mountain ranges in the Middle Rocky Mountains. Apatite FT ages for surface samples in the vicinity of Red Lodge record relatively rapid Laramide uplift (Cerveny, 1990). Apatite FT ages in the Amoco drill hole range from 282 to 57 Ma between the surface and 1.5 km and are in the 40 to 57 Ma range between a depth of 1.5 km and 5 km (Omar and others, 1991); the apatites in the deeper part of the well reflect about 6 km of Laramide uplift and perhaps as much as 4 km of uplift between 5 and 15 Ma. The late Cenozoic uplift inferred from the fission track data probably affected other mountain blocks in the Middle Rocky Mountains (Cervany and Steidtmann, 1992). Furthermore, the physiography of the Beartooth Mountains does not differ from that in the remainder of the Middle Rocky Mountain uplifts that are far removed from the hot spot effects of the hot spot and that have similar surface fission-track age patterns (Cerveny, 1990; Cervany and Steidtmann, 1992).

Yellowstone is in the center of a broad topographic dome, but it is not the highest region in the dome. Regional elevations in the Beartooth and Gallatin Mountains, in the Absaroka Range, etc. are much higher. Brott and others (1981) argued that there is little precursory uplift because of the motion of the plate over the hot spot. In the case of the Hawaiian hot spot there also is little precursory uplift. Brott and others (1981) argued that the primary effect is subsidence following the passage of the hot spot and that the crustal elevation is lower afterwards because of densification of the crust that occurs as a consequence of the volcanic and intrusive effects.

CONCLUSIONS

The thermal characteristics of the Snake River Plain/Yellowstone region have been examined based on new data and new model results. The implications of the thermal results on the rheology of the crust have also been discussed. The thermal model of the Snake River Plain discussed by Brott and others (1978 and 1981) has been modified to be more realistic in the way several aspects of the model are

thermally described. Averages of geothermal gradient and heat flow data discussed in this report are summarized in Table 1. The best thermal constraints are presented in the cross sections in Figures 5 and 15 and in the data in Table 4. The class of models that treat the effects of the hot spot as an instantaneous heat source with the majority of the thermal effect confined to the Snake River Plain fit the various observations the best. The heat flow in the Eastern Snake River Plain (about 107 ± 5 mWm^{-2} near INEL) is significantly above that in the surrounding provinces with "Basin and Range" heat flow of 80 ± 5 mWm^{-2} and the heat flow along the edge may be similar the axial heat flow. Regional temperatures are about 175 ± 25°C at a depth of 3 km all over the Snake River Plain. The background temperature in the adjacent Basin and Range province is about 100 ± 25°C at the same depth. In the east the high temperature is due to higher heat flow while in the west the high temperature is due to the low thermal conductivity of the Cenozoic sediments and a slightly elevated heat flow.

The modified thermal models presented match the observed heat flow data within the uncertainty of the data, but several important uncertainties remain, especially the lateral thermal effects of the hot spot. Significant lateral effects are not present beyond about 50 km from the edges and measurable enhancement of the surface heat flow may not extend that far. However, the volcanic centers and subsidence outside the Snake River Plain are evidence that the thermal effect of the Snake River Plain hot spot extends at least some distance beyond the physiographic margins. A number of deep wells in the Southeastern Idaho Basin and Range province have heat flow values of 80 ± 5 mWm^{-2} which is approximately the expected heat flow for the Basin and Range in general. However, the heat flow along the margins is variable because in the case of the Gray's Lake/Soda Lake area heat flow in deep wells ranges from 50 to 120 mWm^{-2}.

Based on the models investigated and the thermal observations the parabolic zone of earthquakes and active late Cenozoic deformation around the Eastern Snake River Plain may be related to direct or indirect effects of the heating, crustal flow, and/or uplift driven by heating from the hot spot. The crustal rheology profile in and around the Snake River Plain must have a complex geographic variation with a complex pattern of stronger and weaker regions related to variations in strain rate due to cooling and regional strain, variations in midcrustal temperature, and variations in crustal composition. Strain rate discontinuities and/or stress level mismatches related to differences in the crustal strength profiles and late Cenozoic tectonic regimes must also be involved in the location of the earthquakes. However, neither thermal nor seismic data are available in enough detail to independently constrain the geographic position of these discontinuities nor the exact mechanism of the relationship.

REFERENCES

Anders, M.H., Geismann, J.W., Piety, L.A., and Sullivan J.T., 1989, Parabolic Distribution of Circumeastern Snake River Plain seismicity and latest quaternaty faulting: migratory pattern and association with the Yellowstone hotspot: Jour. Geophys. Res., v. 94,p. 1589-1621.

Anders, M.H., Geissman, J.W., and Sleep, N.H., 1990, Comment and reply on "Northeastern Basin and Range province active tectonics: An alternative view": Geology, v. 18, p. 914-915.

Arabasz, W.J., Smith, R.B., and Richins, W.D., 1980, Earthquake studies along the Wasatch Front Utah: Network monitoring, seismicity, and seismic hazards: Seismol. Soc. Amer. Bull., v. 70, p. 1479-1499.

Armstrong, R.L, Leeman, W.P, and Malde, H.E., 1975, Quaternary and Neogene volcanic rocks of the Snake River Plain, Idaho: Amer. Jour. Sci., v. 275, p. 225-251.

Arney, B.H., Goff, F., and Harding Lawson Associates, 1982, Evaluation of the hot dry rock geothermal potential of an area near Mountain Home, Idaho: Los Alamos Natl. Lab Report LA-9365-HDR, 65p.

Arney, B.H., 1982, Evidence of former higher temperatures from alteration minerals, Bostic 1-A well, Mountain Home, Idaho: Geothermal Resources Council Trans, v. 6, p. 3-6.

Bennett, E.H., II, 1974, The general geology of that part of the Northern Rocky Mountain province containing the Idaho batholith: U.S. Forest Service Contract 1032-R4-74, 228p.

Birch, F., 1950, Flow of heat in the Front Range, Colorado: Geol. Soc. Amer. Bull., v. 61, p.567-630.

Blackwell, D.D., 1978, Heat flow and energy loss in the western United States, p. 175-208, in Cenozoic Tectonics and Regional Geophysics of the western Cordillera: Smith, R.B., and Eaton, G.P., eds., Geol. Soc. Amer. Memior 152, 385 pp.

Blackwell, D.D., 1983, Heat flow in the northern Basin and Range province, p. 81-92, in The Role of Heat in the Development of Energy and Mineral Resources in the Northern Basin and Province: Geothermal Resources Council Special Report 13, 384 pp.

Blackwell, D.D. 1988, Heat flow and geothermal resources of Idaho: unpublished manuscript, 91pp.

Blackwell, ,D.D., 1989, Regional implications of heat flow of the Snake River Plain, Northwestern United States: Tectonophysics, v. 164, p. 323-343.

Blackwell, D.D., 1990, Temperatures and heat flow in INEL-GT1, Snake River Plain, Idaho: unpublished report to EG&G Idaho, 18pp.

Blackwell, D.D., Steele, J.L., and Carter, L.S., 1991, Heat-flow patterns of the North American continent; A discussion of the Geothermal Map of North America, p. 423-436, in Slemmons, D.B., Engdahl, E.R., Zoback, M.D., Zoback, M.L., and Blackwell, D.D., eds., Neotectonics of North America: Boulder, Colorado, The Geological Society of America, DMV V-1, 498 pp.

Blackwell, D.D., Steele, J.L., and Brott, C.A., 1980, The terrain effect on terrestrial heat flow: Jour. Geophys. Res., v. 85, 4757-4772.

Blackwell, D.D., Hull, D.A., Bowen, R.G., and Steele, J.L., 1978, Heat flow of Oregon: Oregon Dept. Geol. and Min. Industries Special Paper 4, 42 pp.

Bonini, W.E., 1963, Gravity anomalies in Idaho: Idaho Bur. of Mines and Geol., Boise, Pamphlet 133, 10 pp.

Brace, W.F., and Kohlstedt, D.L., 1980, Limits on lithospheric stress imposed by laboratory experiments: Jour. Geophys. Res., v. 85, 6248-6252.

Braile, L.W., Smith, R.B., Ansorge, J., Baker, M.R., Sparlin, M.A., Prodehl, C., Schilly, M.M., Healy, J.H., Mueller, S. and Olsen, K.H., 1982, The Yellowstone Snake River Plain seismic profiling experiment: Crustal structure of the Eastern Snake River Plain: Jour. Geophys. Res., v. 87, 2597-2610.

Brott, C.A., Blackwell, D.D., and Mitchell, J.C., 1976, Heat flow study of the Snake River Plain region, Idaho: Idaho Dept. Water Resource Water Info. Bull. 30, Part 8, 195 p.62.

Brott, C.A., Blackwell, D.D., and Mitchell, J.C., 1978, Tectonic implications of the heat flow of the Western Snake River Plain, Idaho: Geol. Soc. Amer. Bull., v. 89, p. 1697-1707.

Brott, C.A., Blackwell, D.D., and Ziagos, J.P., 1981, Thermal and tectonic implications of heat flow in the Eastern Snake River Plain, Idaho: Jour. Geophys. Res., v. 86, p. 11709-11734.

Byerlee, J.D., 1968, Brittle-ductile transition in rocks: Jour. Geophys. Res., v. 73, p. 4741-4750.

Carter, N.L., and Tsenn, M.C., 1987, Flow properties of continental lithosphere: Tectonophysics, v. 136, 27-63.

Catchings, R.D., and Mooney, W.D., 1988, Crustal structure of the Columbia Plateau: Evidence of continental rifting: Jour. Geophys. Res., v. 93, p. 459-474.

Cerveny, P.F., 1990, Fission-track thermochronology of the Wind River Range and other basement cored uplifts in the Rocky Mountain Foreland, Ph.D. Dissertation, Univ. of Wyoming, 189 pp.

Cerveny, P.F., and Steidtmann, J.R., 1992, Fission-track thermochronology of the Wind River Range, Wyoming; Evidence for timing and magnitude of Laramide Exhumation: Tectonics, (in press).

Christiansen, R.L., and Lipman, P.W., 1972, Cenozoic volcanism and plate tectonic evolution of the western United States, II, Late Cenozoic: Philos. Trans. R. Soc. London, Ser. A., v. 271, p. 249-234.

Christiansen, R.L., 1982, Late Cenozoic volcanism of the Island Park area, p. 345-368, in Bonnichsen, B., and Breckenridge, R.M., eds., Cenozoic Geology of Idaho: Idaho Bur. of Mines and Geol. Bull. 26, 725 pp.

Corbett, M.K., Anderson, J.E., and Mitchell, J.C., 1980, An evaluation of thermal water occurrences in the Tyhee area, Bannock County, Idaho: Idaho Dept. Water Resources, Water Info. Bull. No. 30, Part 10, 67 pp.

Criss, R.E., and Taylor, H.P., 1983, An $^{18}O/^{16}O$ and D/H study of Tertiary hydrothermal systems in the southern half of the Idaho batholith: Geol. Soc. Amer. Bull., v. 94, p. 640-663.

Criss, R.E., Lanphere, M.A., and Taylor, H.P., 1984, Effects of regional uplift, deformation, and meteoric-hydrothermal metamorphism on K-Ar ages of biotites in the southern half of the Idaho batholith: Jour. Geophys. Res., v. 87, p. 7029-7046.

Crone, A.J., and Haller, K.M., 1991, Segmentation and the coseismic behavior of Basin and Range normal faults: Examples from east-central Idaho and southwestern Montana: Jour. Struct. Geol., v. 13, p. 151-164.

Davis, E.E., and Lewis, T.J., 1984, Heat flow in a back-arc environment: Intermountain and Ominica crystalline belts, southern Canadian Cordillera: Can. Jour. Earth Sci., v. 21, p. 715-726.

Deming, D.and Chapman, D.S., 1989, Heat flow in the Utah-Wyoming thrust belt from analysis of bottom-hole temperature data measured in oil and gas wells: Jour. Geophys. Res., v. 93, p. 13,654-13,672.

Doherty, D.J., McBroome, L.A., and Kuntz, M.A., 1979, Preliminary geological interpretation and lithologic log of the exploratory geothermal test well (INEL-1), Idaho National Engineering Laboratory, Eastern Snake River Plain, Idaho: U.S. Geol. Surv. Open-File Rept. 79-1248, 9p.

Domenico, P.A., and Palciauskus, V.V., 1973, Theoretical analysis of forced convective heat transfer in regional ground-water flow: Geol. Soc. Amer. Bull., v. 84, p. 3803-3814.

Doser, D.I., and Smith, R.B., 1985, Source parameters of the 28 October 1983 Borah Peak, Idaho earthquake from body wave analysis: Seismol. Soc. Amer. Bull., v. 75, p. 1041-1051.

Embree, G.F., McBroome, L.A., and Doherty, D.J., 1982, Preliminary stratigraphic framework of the Pliocene and Miocene rhyolite, eastern Snake River Plain, Idaho: p. 333-344, in Cenozoic Geology of Idaho: Bonnichsen, B., and Brechenridge, R.M., eds., Bur. Mines and Geol. Bull. 26, 725 pp.

Feisinger, D.W., Perkins, W.D., and Puchy, B.J., 1982, Mineralogy and petrology of Tertiary-Quaternary volcanic rocks in Caribou County, Idaho, p. 465-488, in Cenozoic Geology of Idaho: Bonnichsen, B. and Breckenridge, R.M., eds., Idaho Bur. Mines and Geol. Bull., v. 26, 725 pp.

Furlong, K.P., 1979, An analytical stress model applied to the Snake River Plain (Northern Basin and RaAnge province, U.S.A.): Tectonophysics, v. 58, p. T11-T15.

Gallardo, J.D., 1989, Emperical model of temperature structure, Anadarko Basin, Oklahoma: Unpublished M.S. Thesis, Southern Methodist University, 186 pp.

Garabedian, S.P., 1989, Hydrology and digital simulation of the regional aquifer system, Eastern Snake River Plain, Idaho: U.S. Geological Survey, Open-file Rept 87-237, 151 pp.

Goetze, C. and Evans, B., 1979, Stress and temperature in the bending lithosphere as constrained by experimental rock mechanics: Geophys. Jour. Royal Astro. Soc., v. 59, p. 463-478.

Hamilton, W., 1965, Geology and petrogenesis of the Island Park caldera of rhyolite and basalt, eastern Idaho: U.S. Geol. Surv. Prof. Paper 504-C, 37 pp.

Hasket, G.I., and Hampton, L.D., 1979, Geothermal investigations for Salmon Falls Division, Idaho and aspects of pumping from the Snake Plain Aquifer: draft, 49 pp., U.S. Bur. of Reclam., Boise, Idaho.

Hildreth, W., Christiansen, R.L., and O'Neil, J.R., 1984, Catastrophic isotopic modification of rhyolitic magma at times of caldera subsidence, Yellowstone Plateau volcanic field: Jour. Geophys. Res., v. 89, p. 8339-8369.

Hill, D.P., 1963, Gravity and crustal structure in the western Snake River Plain, Idaho: Jour. Geophys. Res., v. 68, p. 5807-5818.

Hill, D.P., and Pakiser, L.C., 1966, Crustal structure between the Nevada Test Site and Boise, Idaho, from seismic-refraction measurements, p. 391-419, in The Earth Beneath the Continents, Geophys. Monogr. Ser., v1 10, Steinhart, J.S., and Smith, T.J., eds., Amer. Geophys. Union, Washington, D.C., 663 pp.

Hoover, D.B., Pierce, H.A., and Long, C.L., 1985, Is Island Park a hot dry rock system?: Trans. Geothermal Resources Council, v. 9, p. 25-29.

Hoover, D.B., and Long, C.L., 1975, Audiomagnetotelluric methods in reconniassance geothermal exploration: Proc. 2nd United Nations Symp. on the Development and use of geothermal resources, v. 2, p. 1039-1064.

Howard, K.A., Shervais, J.W., and McKee, E.H., 1982, Canyon-Filling Lavas and Lava Dams on the Boise River, Idaho, and Their Signifigance for Evaluationg Downcutting During the Last Two Million Years, p. 629-642, in Cenozoic Geology of Idaho, Bonnicksen, B. and Breckenridge, R.M., eds., Idaho Bur. Mines and Geol. Bull., v. 26, 725pp.

Kahle, R.O., Schoppel, R.J., and Deford, R.K., 1970, The AAPG geothermal survey of North America: U.N. Symposium on the Development and Utilization of Geothermal Resources, Pisa, Geothermics Special Issue 2(1), p. 358-378.

Kunze, J.F., and Marlor, J.K., 1982, Industrial food processing and space heating with geothermal heat: U.S. DOE Rept. DOE/ET/27028-6, 117p.

Lachenbruch, A.H., and Sass, J.H., 1978, Models of an extending lithosphere and heat flow in the Basin and Range province: p. 209-250, in Cenozoic Tectonics and Regional Geophysics of the western Cordillera, Smith, R.B., and Eaton, G.P., eds., Geol. Soc. Amer. Memoir 152, 385 pp.

Leeman, W.P., 1982a, Development of the Snake River Plain-Yellowstone Plateau Province, Idaho and Wyoming: An Overview and Petrologic Model, p 155-178, in Cenozoic Geology of Idaho: Bonnichsen, B., and Breckenridge, R.M., eds., Idaho Bur. Mines and Geol. Bull. 26, 725 pp.

Leeman, W.P., 1982b, Geology of the Magic Reservoir area, Snake River Plain, Idaho, p. 369-376, in Cenozoic Geology of Idaho: Bonnichsen, B., and Breckenridge, R.M., eds., Idaho Bur. Mines and Geol. Bull. 26, 725 pp.

Leeman, W.P., and Getting, M.E., 1977, Holocene rhyolite in SE Idaho and geothermal potential, EOS (Trans. Amer. Geophys. Union), v. 58, p. 1249.

Lewis, R.E., and Young, H.W., 1980a, Thermal springs in the Payette River basin, west-central Idaho: U.S. Geol. Surv. Water Resources Investigations Open-File Rept. 80-1020, 23 pp.

Lewis, R.E., and Young, H.W., 1980b, Geothermal resources in the Banbury Hot Springs area, Twin Falls County, Idaho: U.S. Geol. Surv. Water-Resources Investigations Open-File Rept. 80-563, 35 pp.

Lewis, R.E., and Young, H.W., 1982, Thermal Springs in the Boise River Basin, south-central Idaho: U.S. Geol. Surv. Water-Resources Investigations 82-4006, 22 pp.

Lindholm, G.F., 1985, Snake River Plain regional aquifer system, Idaho and eastern Oregon, U.S. Geol. Surv. Circular 1002, p. 88-106.

Mabey, D.R., 1976, Interpretation of a gravity profile across the western Snake River Plain, Idaho: Geology, v. 4, p. 53-55.

Mabey, D.R., 1978, Regional gravity and magnetic anomalies in the eastern Snake River Plain, Idaho: Jour. Res. U.S. Geol. Surv., v. 6, p. 553-562.

Malde, H. E., 1991, Quaternary geology and structural history of the Snake River Plain, Idaho and Oregon, p. 251-281, in Quaternary nonglacial history of the conterminous U.S.: Morrison, R.B., ed., Geol. Soc. Amer., The Geology of North America, v. K-2, 672 pp.

Malde, H.E., and Powers, H.A., 1962, Upper Cenozoic stratigraphy of western Snake River Plain, Idaho: Geol. Soc. Amer. Bull., v. 73, p. 1197-1220.

Malde, H.E., Powers, H.A., and Marshall, C.H., 1963, Reconnaissance geologic map of west-central Snake River Plain, Idaho: Misc. Geol. Invest. Map I-373, U.S. Geol. Surv., Reston, Va.

Mantei, C.L., 1974, Snake Plain Aquifer, Idaho, electric analog studies, third progress report: U.S. Bur. of Reclam., Boise, Idaho, 29 pp.

Mitchell, J.C., 1976a, Geochemistry and geologic setting of the thermal waters of the Camas Prairie area, Blaine and Camas Counties, Idaho: Idaho Dept. Water Res., Water Info. Bull. No. 30, Part 7, 44 pp.

Mitchell, J.C., 1976b, Geochemistry and geologic setting of the thermal and mineral waters of the Blackfoot Reservoir Area, Caribou County, Idaho: Idaho Dept. of Water Resources, Water Info. Bull. No. 30, Part 6, 47 pp.

Mitchell, J.C., Johnson, L.L., and Anderson, J.E., 1980, Potential for direct heat application of geothermal resources: Idaho Dept. Water Resource, Water Info. Bull. 30, Part 9, 396 pp.

Moreland, J.A., 1976, Digital-model analysis of the effects of water-use alternatives of spring discharges, Gooding and Jerome counties, Idaho: Water Info. Bull. Idaho Dept. Water Resource, v. 42, 46 pp.

Morgan, L.A., Doherty, D.J., and Leeman, W.P., 1984, Ignimbrites of the eastern Snake River Plain: Evidence for major caldera- forming eruptions: Jour. Geophys. Res., v. 89, p. 8665-8678.

Morgan, W.J., 1981, Hot spot Tracks and the opening of the Atlantic and Indian Oceans, p. 443-487, in The Sea: Emiliana, C., ed., vol.7, New York, Wiley-Interscience, pp.

Mundorff, M.J., Crosthwaite, E.G., and Kilburn, C., 1964, Ground water for irrigation in the Snake River Plain, Idaho: U.S. Geol. Surv. Water Supply Paper, 1654, 244 pp.

Nathenson, M., Urban, T.C., Diment, W.H., and Nehring, N.L., 1980, Temperatures, heat flow, and water chemistry from drill holes in The Raft River geothermal system, Cassia County, Idaho: U.S. Geol. Surv. Open-File Rept. 80-2001, 29 pp.

Newton, V.C., and Corcoran, R.E., 1963, Petroleum geology of the western Snake River Basin: Oreg. Dept. Geol. and Mineral Ind., Oil Gas Invest. #1, 67 pp.

Norvitch, R.F., Thomas, C.A., and Madison, R.J., 1969, Artificial recharge to the Snake River Plain aquifer, and evaluation of potential and effect: Idaho Dept. Water Resource Water Info. Bull., No. 12, 59 pp.

Omar, G.I., Giegengak, R., and Lutz, T.M., 1991, Uplift history of the Red Lodge Corner of the Beartooth block, Montana-Wyoming from apatite FT analysis: new evidence for post-Laramide uplift: Geol. Soc. Amer. Abstracts with Progams, v. 24, p. A 482.

Pelton, J.R., and Smith, R.B., 1982, Contemporary vertical surface displacements in Yellowstone National park: Jour. Geophys. Res., v.. 87, p. 2745-2761.

Perry, W.J., Wardlaw, B.R., Bostick, N.H., and E.K. Maughan, 1983, Structure, burial history, and petroleum potential of frontal thrust belt and adjacent foreland, southwest Montana: Amer. Assoc. Petrol. Geol. Bull., v. 67, p. 725-743.

Pierce, K.L., and Morgan, L.A., 1990, The track of the Yellowstone hotspot: volcanism, faulting, and uplift: U.S. Geological Survey, Open-File Report 90-415, 67 pp.

Ralston, D.R., and Mayo, A.L., 1983, Thermal groundwater flow systems in the thrust zone in southeastern Idaho: U.S. Dept. Energy Report DOE/ET/ 28407-4, 336 pp.

Reilinger, R.E., Citron, G.P., and Brown, L.D., 1977, Recent vertical crustal movements from precise leveling data in southwestern Montana, western Yellowstone National Park, and the Snake River Plain: Jour. Geophys. Res., v. 82, p. 5349-5359.

Rogers, D.W., Hackett, W.R., and Ore, H.T., 1990, Extension of the Yellowstone plateau, eastern Snake River Plain, and Owyhee plateau: Geology, v. 18, p. 1138-1141.

Ross, S.H., 1971, Geothermal potential of Idaho: Idaho Bur. of Mines and Geol. Pamph. 150, 72 pp.

Roy, R.F., Decker, E.R., and Blackwell, D.D., 1972, Continental heat flow, p. 506-543, in The Nature of the Solid Earth: Robertson, E.C., ed., McGraw-Hill Book Company, New York, 677 pp.

Ruppel, E.T., 1967, Late Cenozoic drainage reversal, east central Idaho, and its possible economic implications: Econ. Geol., v. 62, p. 648-663.

Sass, J.H., Lachenbruch, A.H., Munroe, R.J., Greene, G.W.,and Moses, T.H.,Jr., 1971, Heat flow in the western United States: Jour. Geophys. Res., v. 76, p. 6376-6413.

Scott, W.E., Pierce, K.L., and Hait, M.J., Jr., 1985, Quaternary tectonic setting of the 1983 Borah Peak earthquake, central Idaho: Seismol. Soc. Amer. Bull., v. 75, p. 1053-1066.

Sleep, N.H., 1990, Hotspots and mantle plumes: Some phenomenology: Jour. Geophys. Res., v. 95, p. 6715-6736.

Smith, R. B., and Arabaz, W.J., 1991, Seismicity of the Intermountain Seismic Belt, p. 185-229, in Neotectonics of North America: Slemmons, D.B., Engdahl, E.R., Zoback, M.D., Zoback, M.L., and Blackwell, D.D., eds., Boulder, Colorado, The Geological Society of America, DMV-1, 498 pp.

Smith, R.B., and Braile, L.W., 1984, Crustal structure and evolution of an explosive silicic volcanic system at Yellowstone National Park, p. 96-111, in Explosive volcanism: Inception, evolution, and hazards: Studies in Geophysics: Washington, D.C., National Academy Press, 176 pp.

Smith, R.B., and Sbar, M., 1974, Contemporary tectonics and seismicity of the western United States with emphasis on the Intermountain seismic belt: Geol. Soc. Amer. Bull., v. 85, p. 1205-1218.

Smith, R.B., Richins, W.D., Doser, D.I., Eddington, P.K., Leu, L.L., and Chen, G., 1985, The Borah Peak earthquake: Seismicity, faulting kinematics and tectonic mechanism, in Proceedings of Workshop XXVII on the Borah Peak, Idaho Earthquake: Stein, R.S., and Buckham, R.C., eds., U.S. Geol. Surv. Open-file Rept. 85-290, 686 pp.

Smith, R.L., and Shaw, H.R., 1979, Igneous related geothermal systems, p. 12-18, in Assessment of Geothermal Resources of the United States - 1978: Muffler, L.J.P., ed., U.S. Geol. Surv. Circular 790, 163 pp.

Smith, R.N., 1980, Heat flow of the Western Snake River Plain: M.S. Thesis, Washington State Univ., 150 pp.

Smith, R.N., 1981, Heat flow in the Western Snake River Plain: p. 79-114, in Part 11, Geological, Hydrological, Geochemical and Geophysical Investigation of the Nampa-Caldwell and adjacent areas, southwestern Idaho: Mitchell, J.C., ed., Idaho Department Water Resources, Water Info. Bull.No. 30, 143 pp.

Sparlin, R.B., Braile, L.W., and Smith, R.B., 1982, Crustal structure of the Eastern Snake River Plain determined from ray trace modeling of seismic refraction data: Jour. Geophys. Res., v. 87, p. 2619-2633.

Stanley, W.D., Boehl, J.E., Bostick, F.X., and Smith, H.W., 1977, Geothermal significance of magnetotelluric sounding in the eastern Snake River Plain-Yellowstone region: Jour. Geophys. Res., v. 82, p. 2501-2514.

Struhsacker, D.H., Jewell, P.W., Zeisloff, J., and Evans, S.H., Jr., 1982, The geology and geothermal setting of the Magic Reservoir area, Blaine and Camas Counties, Idaho, p. 337-393, in Cenozoic Geology of Idaho: Bonnichsen, B., and Breckenridge, R.M., eds., Idaho Bur. Mines and Geol. Bull. 26, 725 pp.

Struhsacker, E.M., Smith, C., and Capuano, R.M., 1983, An evaluation of exploration methods for low-temperature geothermal systems in the Artesian City area, Idaho: Geol. Soc. Amer. Bull., v. 94, p. 58-79.

Swanberg, C.A., and Blackwell, D.D., 1973, The areal distribution and geophysical significance of heat generation in the Idaho batholith and adjacent intrusives in eastern Oregon and western Montana: Geol. Soc. Amer. Bull., v. 84, p. 1261-1282.

Turko, J.M., and Knuepfer, P.L.K., 1991, Late Quaternary fault segmentation from analysis of scarp morphology: Geology, v. 19, p. 718-721.

Urban, T.C., and Diment, W.H., 1975, Heat flow on the south flank of the Snake River Rift: Geol. Soc. Amer. Abstr. Programs, v. 1, p. 647.

Urban, T.C., Diment, W.H., Nathenson, M., Smith, E.P., Ziagos, J.P., and Shaeffer, M.H., 1986, Temperature, thermal-conductivity, and heat-flux data: Raft River area, Cassia County, Idaho (1974-1976): U.S. Geol. Surv. Open-File Report 86-123, 200 pp.

Walton, W.C., 1962, Groundwater resources of Camas Prairie, Camas and Elmore Counties, Idaho, U.S. Geol. Surv. Water Supply Paper 1609, 57 pp.

Westaway, R. 1989a,. Northeastern Basin and Range province active tectonics: An alternative view: Geology, v. 17, p. 779-783.

Westaway, R., 1989b, Deformation of the NE Basin and Range province: The response of the lithosphere to the Yellowstone Plume?: Geophys. Jour. Inter., v. 99, p. 33-62.

Westaway, R., 1990, Reply: Geology, v. 18, p. 915-917.

Whitehead, R.L., 1978, Water resources of the Upper Henrys Fork Basin in eastern Idaho: Idaho Dept. Water Resources Water Info. Bull., v. 46, 91 pp.

Whitehead, R.L., and Lindholm, G.F., 1985, Results of geohydrologic test drilling in the Eastern Snake River Plain, Gooding County, Idaho: U.S. Geol. Surv. Water-Resources Investigations Rept., 84-4294, 30 pp.

Whitehead, R.L., 1986, Geohydrologic framework of the Snake River Plain, Idaho and eastern Oregon: U.S. Geol. Surv. Hydrologic Inv. Atlas HA-681.

Young, H.W., Harenberg, W.A., and Seitz, H.R., 1977, Water Resources of the Weiser River basin, west-central Idaho: Idaho Dept. Water Resources, Water Info. Bull No 44, 104 pp.

Young, H.W., and Lewis, R.L., 1982, Hydrology and geochemistry of thermal water in southwestern Idaho and north-central Nevada: U.S. Geol. Surv. Prof. Paper 1044-J, 20 pp.

APPENDIX A: DATA SOURCES AND TEMPERATURE-DEPTH CURVES

A. New temperature logs from 12 sites in 1991

Temperature-depth curves from all of these wells are included in section E.

B. Idaho Department of Water Resources Geothermal Files: Geothermal test wells with temperature logs now in the public domain.

Intermediate depth wells

UNOCAL State 07;
UNOCAL State 08;

Temperature-depth curves shown with text.

Deep well

Phillips Gentile Valley #1-9

Temperature-depth curve shown with text.

C. Southern Methodist University files, geothermal test wells released to the SMU Geothermal Laboratory.

Shallow geothermal gradient tests

Hunt, Carey area, 5 wells, maximum depth 150 m, temperature-depth curves shown in section E.
Hunt. Magic Reservoir area, 14 wells, maximum depth 150 m, temperature-depth curves shown in section E.
OXY Geothermal, Inc., ESRP, 18 wells, maximum depth 300 m, selected temperature-depth curves shown in text.

Intermediate depth well

SUN # 1001, 450 m deep

Temperature-depth curve shown with text.

Deep well

SUN Hubbard #1, 2500 m deep

Temperature-depth curve shown with text.

D. Hydrocarbon tests (BHT data only). Data from 31 wells with BHT data.

E. Temperature-depth curves for wells not previously published.

Following pages.

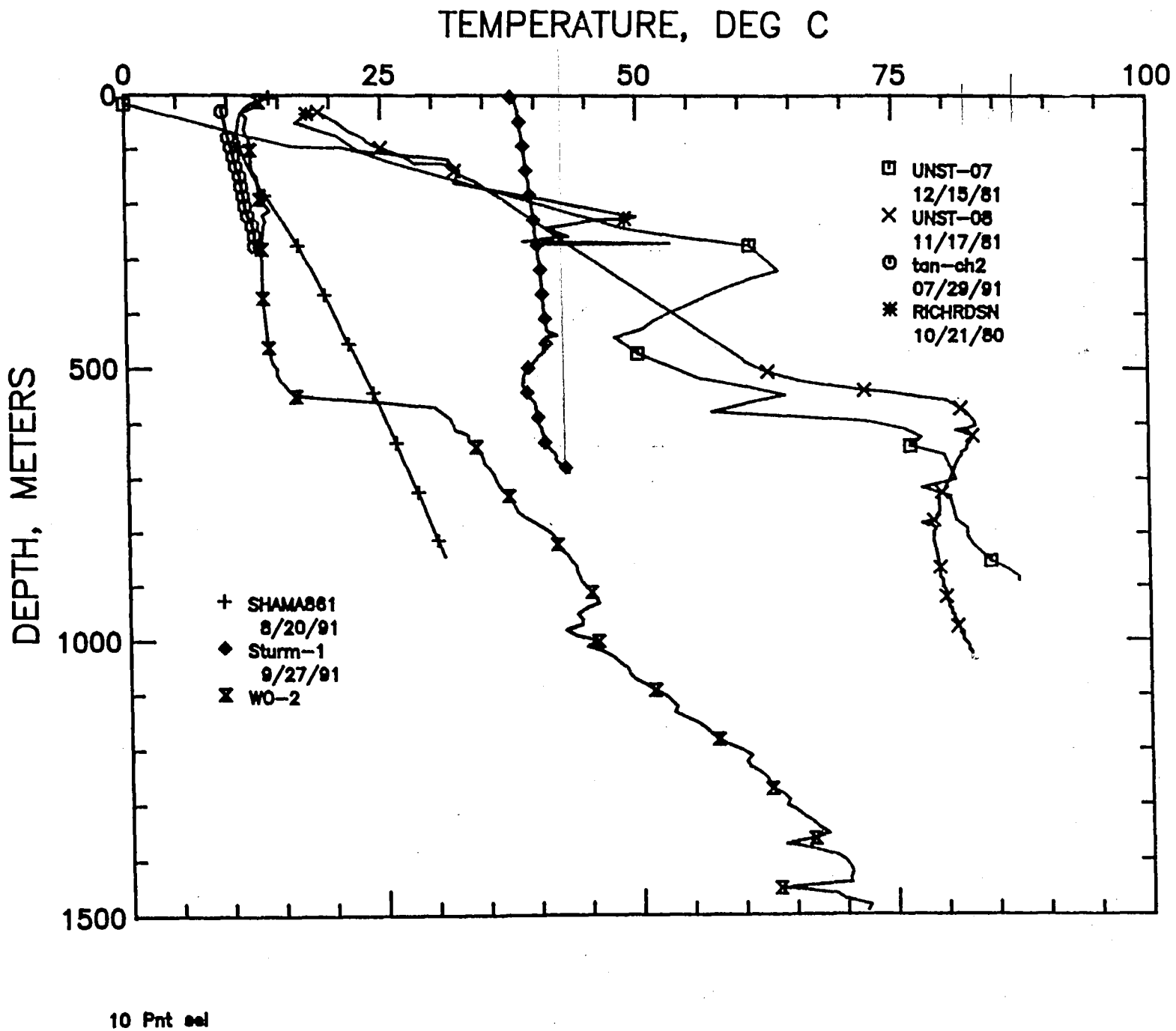
TEMPERATURE, DEG C
0
25
50
75
100
DEPTH, METERS
0
500
1000
1500
UNST-07
12/15/81
UNST-08
11/17/81
tan-ch2
07/29/91
RICHRDSN
10/21/80
SHAMA861
8/20/91
Sturm-1
9/27/91
WO-2
10 Pnt sel

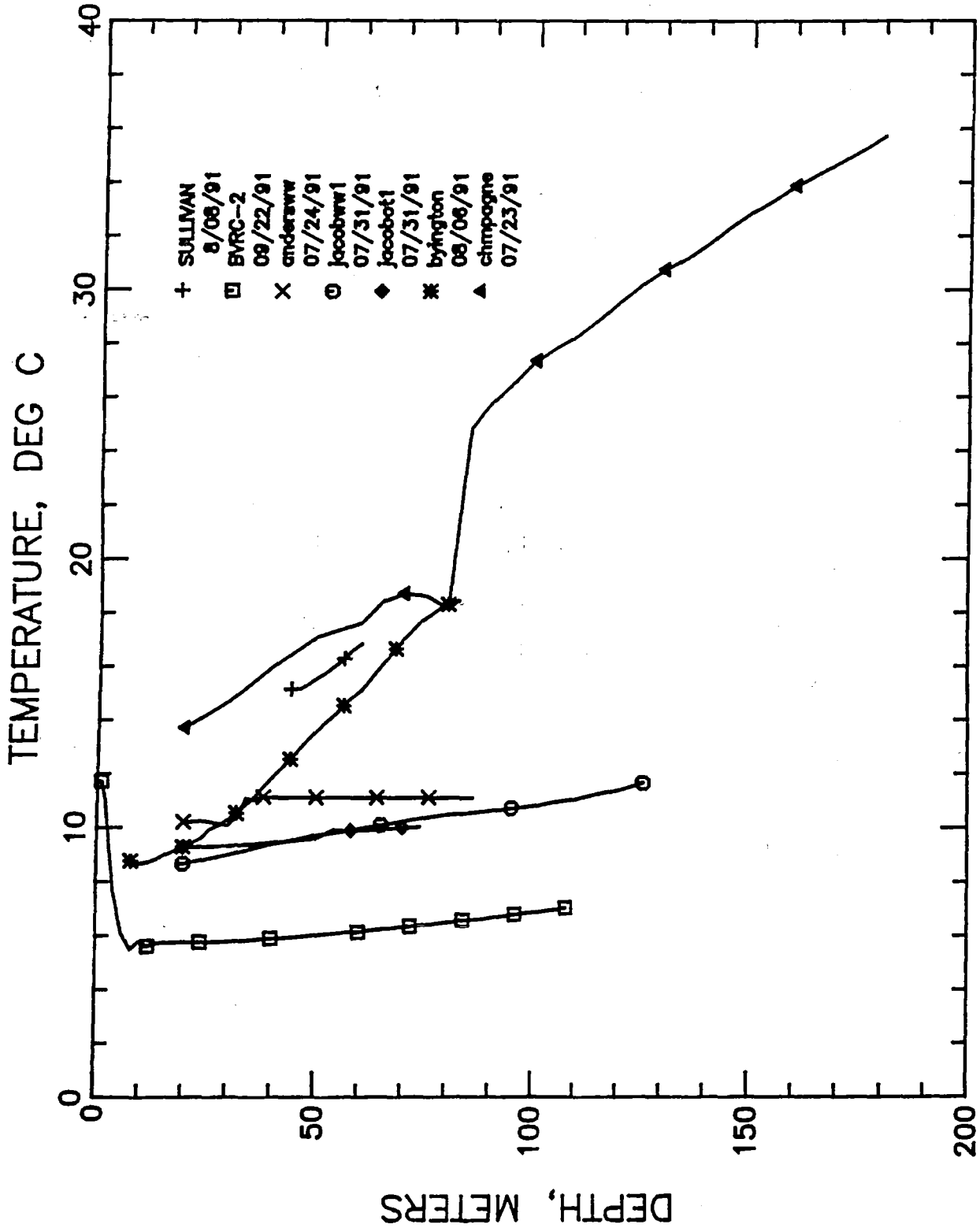
TEMPERATURE, DEG C
DEPTH, METERS
0
10
20
30
40
0
50
100
150
200
+ SULLIVAN 8/06/91
BVRC-2 09/22/91
cmderswv 07/24/91
jacobwwr1 07/31/91
jacobot1 07/31/91
byington 08/06/91
chmpagne 07/23/91

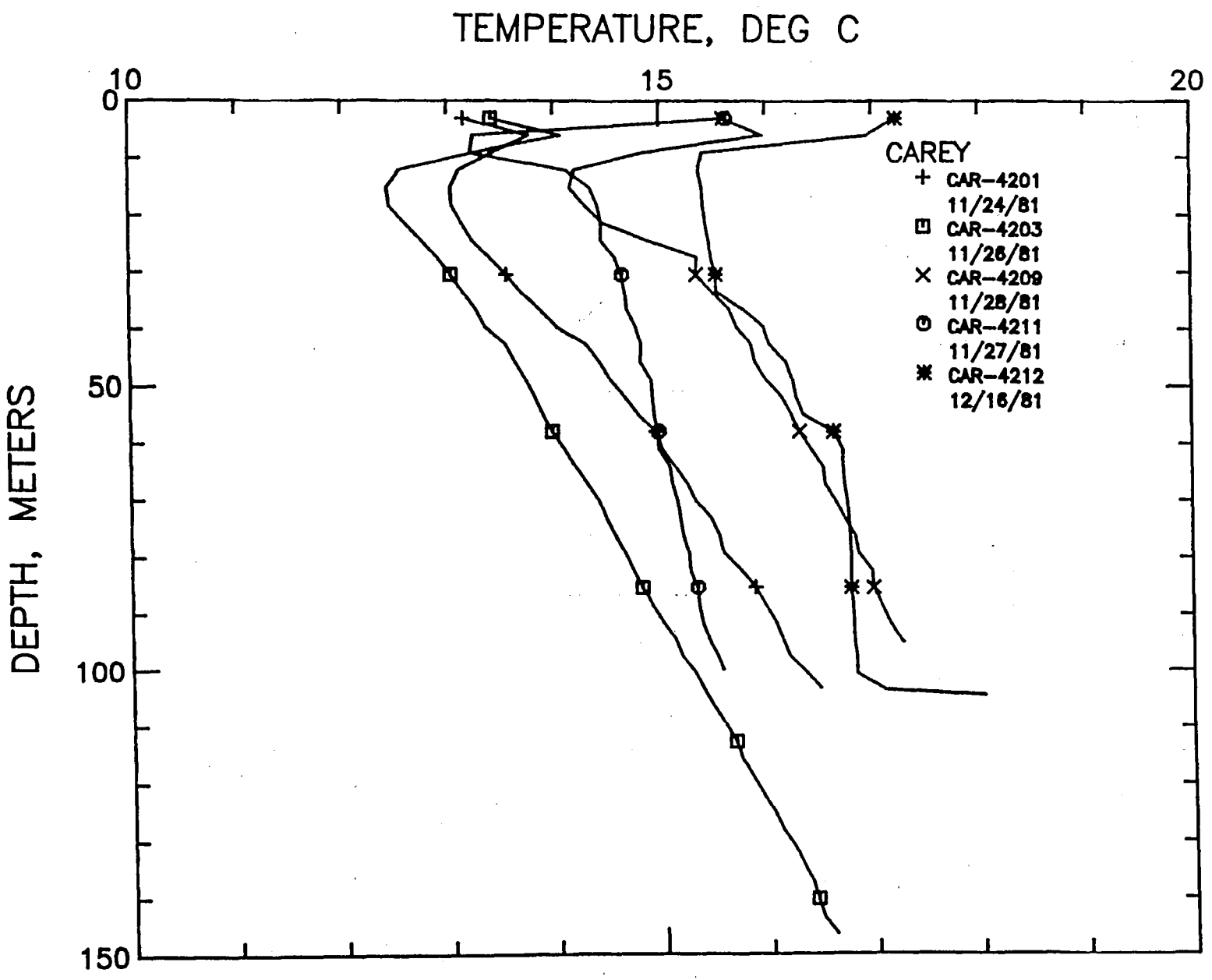
TEMPERATURE, DEG C
10
15
20
0
50
100
150
DEPTH, METERS
CAREY
CAR-4201
11/24/81
CAR-4203
11/26/81
CAR-4209
11/28/81
CAR-4211
11/27/81
CAR-4212
12/16/81

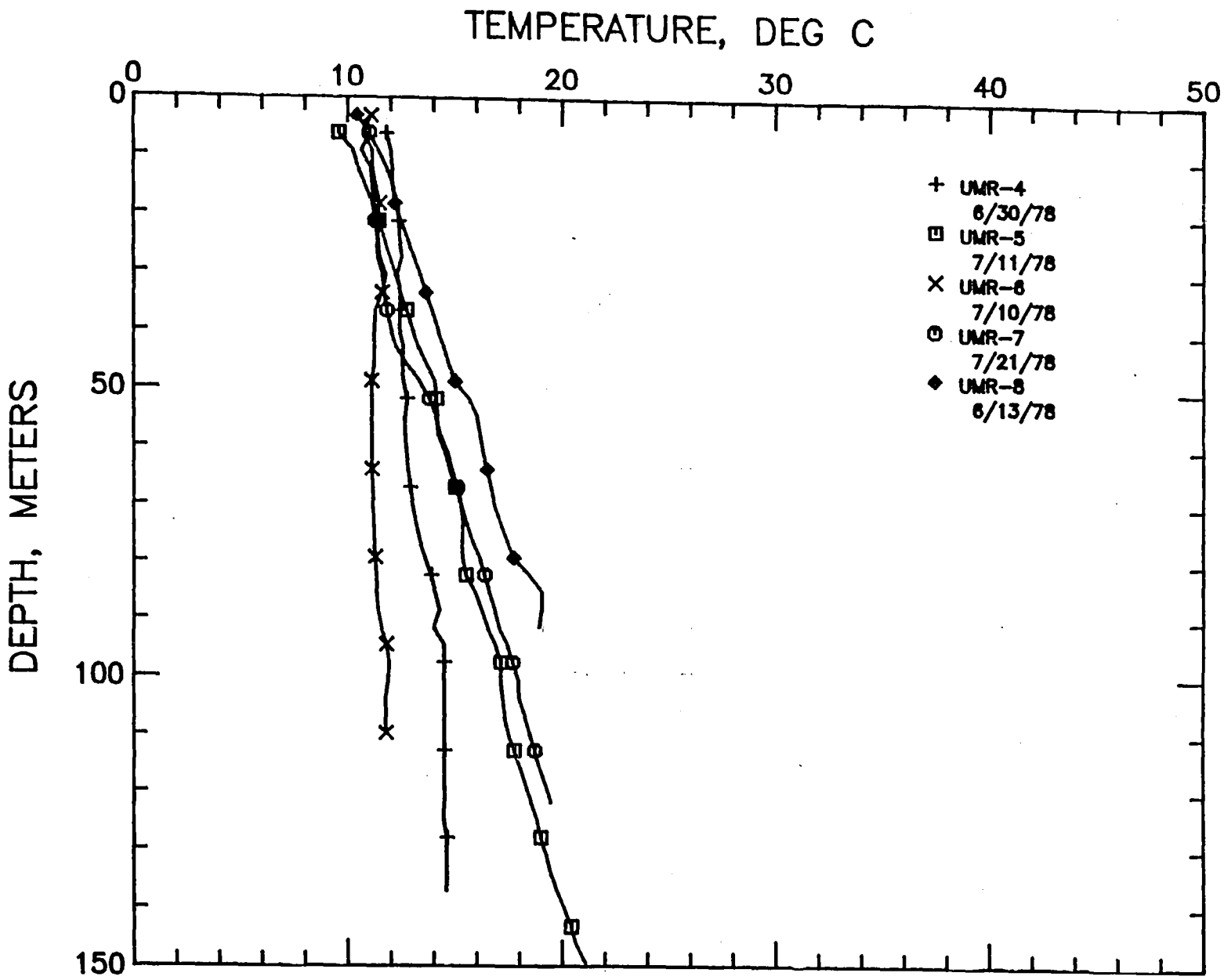
TEMPERATURE, DEG C
0
10
20
30
40
50
DEPTH, METERS
0
50
100
150
UMR-4
6/30/78
UMR-5
7/11/78
UMR-6
7/10/78
UMR-7
7/21/78
UMR-8
6/13/78

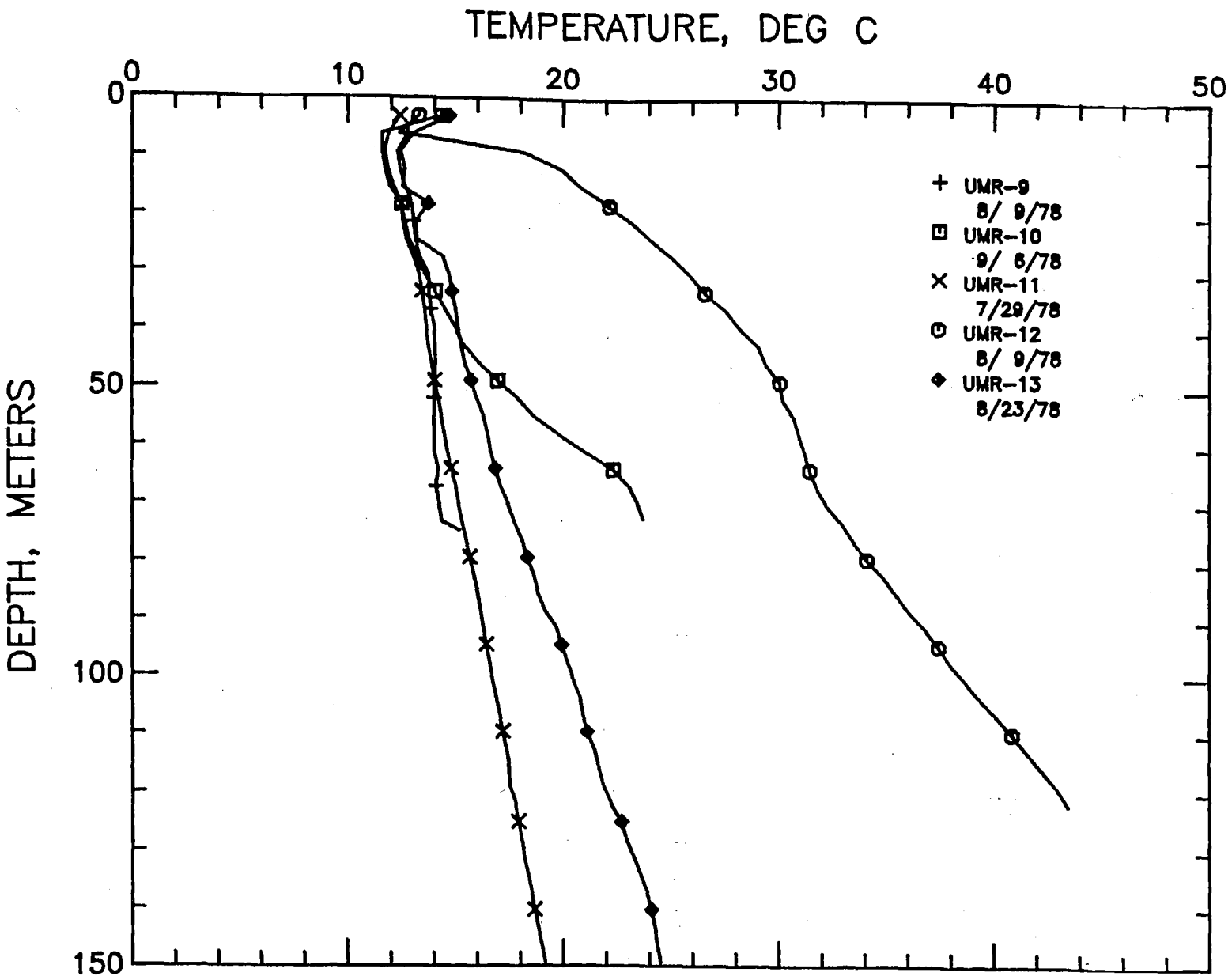
TEMPERATURE, DEG C
0
10
20
30
40
50
DEPTH, METERS
0
50
100
150
+ UMR-9
8/ 9/78
UMR-10
9/ 6/78
× UMR-11
7/29/78
UMR-12
8/ 9/78
◆ UMR-13
8/23/78

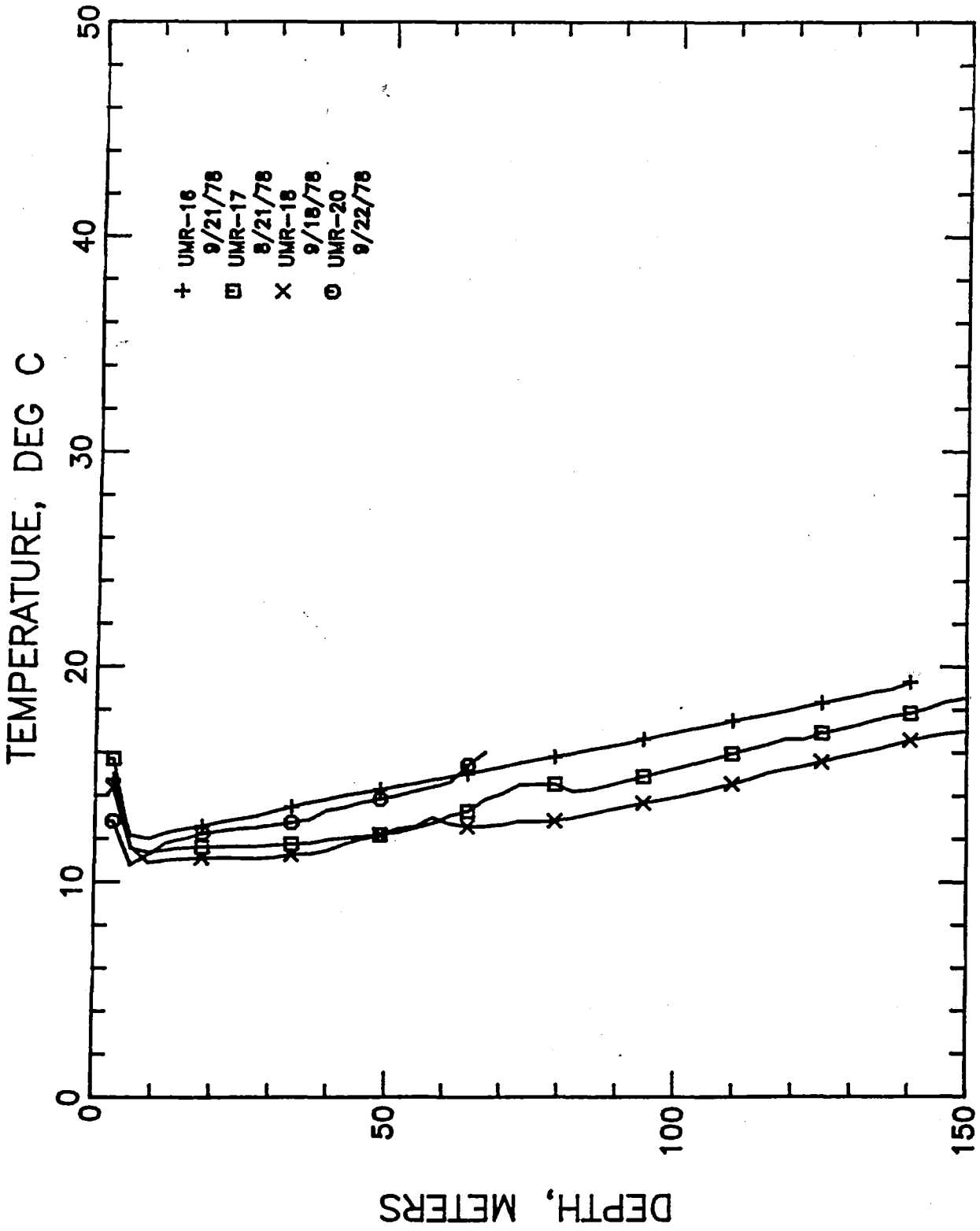
TEMPERATURE, DEG C
DEPTH, METERS
0
10
20
30
40
50
0
50
100
150
+ UMR-16 9/21/78
⊡ UMR-17 8/21/78
× UMR-18 9/18/78
⊙ UMR-20 9/22/78

APPENDIX B. DISCUSSION OF TEST CASES FOR RECTAN.FOR

The numerical thermal models presented in this report were generated using a program called RECTAN.FOR. RECTAN.FOR can be used to solve two-dimensional heat flow problems in a rectangular coordinate system where x is not equal to y. The program is based on explicit, central difference equations. A total of nine regions of contrasting thermal conductivity, heat generation, and/or temperature can be examined with this model. In addition, a constant heat flux, a constant temperature, or a variable heat flux can be applied to the base of the model. The top boundary of the model represents a topographic surface (flat or irregular) with a constant temperature through time. The surface heat flow produced by the thermal conditions within the model as a function of time is determined from the gradient and the thermal conductivity values for the top two nodes of the model.

The side boundaries and bottom heat flux boundary are insulated and are, in effect, mirror image boundaries (i.e., points on opposite sides of the boundary are the same). This type of boundary allows the user to model half of a symmetric system, which allows for smaller grid spacing and more detailed analysis of the system.

The thermal model for the Snake River Plain contains several components, including the presence of magma chambers in the crust, crustal heat generation, and to a lesser extent, near surface thermal conductivity refraction. The thermal effects of each of the components of the model were tested separately against analytical or other numerical solutions before the complete Snake River Plain thermal model was assessed.

Magma Chamber in Crust

The test case for a single magma chamber in the crust is illustrated in Figure B1. The basaltic magma chamber in this model has dimensions that correspond to the size of the 6.5 km/sec layer that has been observed on seismic lines across the eastern Snake River Plain (Iyer, 1984). The top of the magma chamber is at 10 km, the base is at 20 km, and the half-width of the chamber is 49 km. The thermal conductivity and thermal diffusivity values are constant throughout the grid and no crustal heat generation is considered. The initial temperature of 1350°C is assigned to the magma to take into account the effects of the latent heat of crystallization. A constant temperature of 10°C at the surface and a constant temperature of 1410°C at a depth of 50 km were maintained through the model runs.

The results from the numerical model were compared to the two-dimensional, analytical solution of Lachenbruch and others (1976). The comparisons between the two solutions a various times are summarized in Figures B1-B3. Times of 1 Ma or less are examined because at times beyond 1 Ma, the calculated temperatures interact with the bottom boundary. The analytical solution assumes diffusion into an infinite half space; consequently, the analytical solution is not directly comparable to the numerical model with a constant temperature bottom boundary condition.

Examination of Figures B1 to B3 clearly illustrates that the numerical and analytical solutions diverge from one another in detail as time increases. The numerical model is consistently low above the magma chamber and high below the magma chamber compared to the analytical solution. One reason for the discrepancy is related to the fact that the top boundary condition in the numerical solution is a non-reflective constant temperature condition, while the analytical solution is based on the method of images, which give rise to a reflective top boundary. A secondary source of the discrepancy is due to the large grid size (1 km by 1 km) imposed on the model by the large scale of the problem that we are trying to examine, which introduces truncation error into the Taylor series approximations of the finite difference equations.

Although the two solutions differ from each other in detail, two similarities between the models show that the numerical model is capable of accurately predicting regional elevation trends in the vicinity of the Snake River Plain. First, the integrated temperatures for each column, which are useful in determining the elevation related to thermal expansion, differ by no more than 2%. Second the lateral conduction of heat is nearly identical for the two models. The lateral conduction effects from both models clearly indicate that the topographic features about 100 - 150 km from the middle of the Snake River Plain are not related to crustal magma chambers immediately under the plain.

Heat Generation in Crust

The temperatures for a 10 km thick layer that contains heat-producing elements capable of generating $20mWm^{-2}$ (.48 HFU) with a basal heat flow of $58.6mWm^{-2}$ (1.4 HFU) and a thermal conductivity of 7 TCU were calculated using RECTAN. The results after 3000 iterations, which approximate steady state conditions, are compared to the one-dimensional results for a layer of crustal heat generation (Blackwell, 1971). At a depth of 5 km the calculated temperature is 137°C, which is comparable to the predicted value of 135°C. Similarly, at a depth of 10 km the calculated temperature is 246°C, which is nearly identical to the predicted temperature of 244°C. Corresponding results are obtained throughout the grid. The predicted surface heat flow is 1.88 HFU and the calculated heat flow is 1.87 HFU. The numerical model after 3000 time iterations is not quite at steady state.

Thermal Conductivity Refraction

In the western Snake River Plain, the rhyolites and basalts are overlain by low thermal conductivity sediments, and the thermal conductivity refraction effect is clearly seen in the heat flow pattern (Brott and others, 1978; Blackwell, 1989). However, in the eastern Snake River Plain, the thermal conductivity refraction effect is not important because the sedimentary cover is negligible. Although, thermal conductivity refraction modeling is not applicable to this particular project, the test

results for a refraction problem are presented here to verify the previously published results for the western Snake River Plain.

Two-dimensional analytical solutions for heat flow refraction in the vicinity of media with contrasting thermal conductivities have been derived for cylindrical coordinates (Lee and Henyey, 1974), but similar expressions for rectangular coordinates have not been published. Consequently, the thermal conductivity refraction model was tested against the finite element model of Lee and others (1980).

The heat flow and subsurface temperatures calculated by the two models for a basin with a half-width of about 30 km and a depth of 5 km are very similar (Figures B4 and B5). The finite element results are steady-state and the difference model was run for 2500 time iterations. The slight difference between the two models is related to the fact that the difference model is not quite at steady state; this model should be run to approximately 4000 iterations to achieve steady state. The surface heat flow values for the two models at the boundary of the basin are disparate because the nodal conductivities are calculated differently by the two algorithms. RECTAN averages the conductivity of the surrounding nodes, while FINITE assigns either the higher or the lower conductivity to the element, depending on the weighted average of the area of the element.

Figure B1.
Rectan with constant temperature bottom boundary
Time=0.2 Ma compared to analytical solution

Depth	Distance (km)								
	0	8	16	24	32	40	48	56	64
5km	**302**	**302**	**302**	**302**	**302**	**300**	**248**	**160**	**150**
	302	302	302	302	302	299	239	158	150
	0	*0*	*0*	*0*	*0*	*+0.3*	*+4*	*+1*	*0*
10km	**809**	**809**	**809**	**809**	**809**	**801**	**617**	**325**	**290**
	808	808	809	809	809	798	596	319	290
	+0.1	*+0.1*	*0*	*0*	*0*	*+0.2*	*+3*	*+2*	*0*
	Magma								
15km	**1123**	**1123**	**1123**	**1123**	**1123**	**1113**	**869**	**477**	**430**
	1116	1116	1116	1116	1116	1103	835	468	430
	+0.6	*+0.6*	*+0.6*	*+0.6*	*+0.6*	*+1*	*+4*	*+2*	*0*
	Chamber								
20km	**964**	**964**	**964**	**964**	**964**	**956**	**822**	**597**	**570**
	951	951	951	951	951	944	795	591	570
	+1	*+1*	*+1*	*+1*	*+1*	*+1*	*+4*	*+1*	*0*
25km	**798**	**798**	**798**	**798**	**798**	**797**	**765**	**715**	**710**
	791	791	791	791	791	789	758	714	710
	+1	*+1*	*+1*	*+1*	*+1*	*+1*	*+1*	*+0.1*	*0*
30km	**856**	**856**	**856**	**856**	**856**	**856**	**854**	**850**	**850**
	856	856	856	856	856	856	853	850	850
	0	*0*	*0*	*0*	*0*	*0*	*+0.1*	*0*	*0*
35km	**990**	**990**	**990**	**990**	**990**	**990**	**990**	**990**	**990**
	990	990	990	990	990	990	990	990	990
	0	*0*	*0*	*0*	*0*	*0*	*0*	*0*	*0*

Normal: Analytical
Bold: **Rectan**
Italic: *Percentage difference between numerical and analytical solution*

Inte-	**5842**	**5165**
grated	5814	5814
Temp.	*+0.5%*	*+1.9%*

Heat	**2.30**	**2.30**	**2.30**	**2.30**	**2.30**	**2.29**	**2.04**	**1.46**	**1.40**
Flow	2.30	2.30	2.30	2.30	2.30	2.30	1.90	1.50	1.40

Figure B2.
Comparison of results from Rectan with constant temp. at bottom boundary. Time=0.5 Ma vs.analytical solution results

Depth	Distance (km)								
	0	8	16	24	32	40	48	56	64
5km	**366**	**366**	**366**	**366**	**365**	**348**	**276**	**187**	**154**
	396	396	396	396	394	372	287	188	154
	-8	*-8*	*-8*	*-8*	*-8*	*-7*	*-4*	*-0.5*	*0*
10km	**712**	**712**	**712**	**712**	**710**	**677**	**538**	**364**	**298**
	739	739	739	739	736	695	540	360	297
	-4	*-4*	*-4*	*-4*	*-4*	*-3*	*-0.4*	*+1*	*+0.5*
	Magma								
15km	**924**	**924**	**924**	**924**	**921**	**882**	**719**	**516**	**439**
	917	917	917	917	914	870	701	506	437
	+1	*+1*	*+1*	*+1*	*+1*	*+1.4*	*+2*	*+2*	*+0.04*
	Chamber								
20km	**941**	**941**	**941**	**941**	**938**	**909**	**787**	**634**	**576**
	902	902	902	902	900	870	755	622	575
	+4	*+4*	*+4*	*+4*	*+4*	*+4*	*+4*	*+2*	*+0.02*
25km	**888**	**888**	**888**	**888**	**887**	**873**	**815**	**741**	**713**
	851	851	851	851	850	837	788	732	712
	+4	*+4*	*+4*	*+4*	*+4*	*+4*	*+3*	*+1*	*+0.5*
30km	**904**	**904**	**904**	**904**	**904**	**900**	**882**	**859**	**851**
	886	886	886	886	886	883	870	856	851
	+2	*+2*	*+2*	*+2*	*+2*	*+2*	*+1*	*+0.03*	*0*
35km	**1000**	**1000**	**1000**	**1000**	**1000**	**1000**	**996**	**992**	**990**
	995	995	995	995	995	995	993	991	990
	+.05	*+.05*	*+.05*	*+.05*	*+.05*	*+.05*	*+.03*	*+.01*	*0*

Normal: Analytical
Bold: **Rectan**
Italic: *Percentage difference between numerical and analytical solution*

Inte-	**5735**	**5013**
grated	5686	4934
Temp.	*+0.8%*	*+1.5*

Heat	**3.50**	**3.50**	**3.50**	**3.50**	**3.48**	**3.32**	**2.62**	**1.76**	**1.44**
Flow	3.95	3.95	3.95	3.95	3.95	3.70	2.80	1.80	1.45

Figure B3.
Comparison of results from Rectan with constant bottom temperature at 1.0 Ma versus results from analytical model.

Depth	Distance (km)								
	0	8	16	24	32	40	48	56	64
5km	**332**	**332**	**332**	**331**	**326**	**302**	**252**	**196**	**162**
	371	371	371	370	362	332	270	203	164
	-12	*-12*	*-12*	*-12*	*-11*	*-10*	*-7*	*-3*	*-1*
10km	**606**	**606**	**606**	**604**	**594**	**554**	**467**	**370**	**312**
	636	636	636	635	622	574	477	372	312
	-5	*-5*	*-5*	*-5*	*-5*	*-4*	*-2*	*-0.5*	*0*
	Magma								
15km	**790**	**790**	**790**	**789**	**777**	**731**	**632**	**521**	**455**
	784	784	784	782	770	721	621	514	452
	+2	*+2*	*+2*	*+1*	*+1*	*+1*	*+2*	*+1*	*+0.6*
	Chamber								
20km	**882**	**882**	**881**	**880**	**870**	**830**	**745**	**648**	**591**
	839	839	839	838	828	791	716	634	587
	+5	*+5*	*+5*	*+5*	*+5*	*+5*	*+4*	*+2*	*+0.7*
25km	**919**	**919**	**919**	**919**	**912**	**885**	**828**	**763**	**724**
	865	865	865	864	858	837	794	747	720
	+6	*+6*	*+6*	*+6*	*+6*	*+5*	*+4*	*+2*	*+0.5*
30km	**960**	**960**	**960**	**960**	**956**	**942**	**912**	**878**	**857**
	917	917	917	916	914	905	886	866	854
	+4	*+4*	*+4*	*+4*	*+4*	*+4*	*+3*	*+1*	*+0.3*
35km	**1035**	**1035**	**1035**	**1035**	**1034**	**1028**	**1016**	**1001**	**993**
	1011	1011	1011	1011	1010	1007	1001	995	991
	+2	*+2*	*+2*	*+2*	*+2*	*+2*	*+1*	*+0.6*	*+0.3*

Normal: Analytical
Bold: **Rectan**
Italic: *Percentage difference between numerical and analytical solution*

Inte-	**5524**	**4852**
grated	5423	4765
Temp.	*+1.8%*	*+1.8*

Heat	**3.30**	**3.30**	**3.30**	**3.29**	**3.23**	**2.99**	**2.46**	**1.88**	**1.53**
Flow	3.90	3.90	3.90	3.90	3.80	3.45	2.75	2.00	1.55

Comparison of results from Rectan for thermal conductivity refraction vs. Lee's numerical solution

Depth	Edge of Basin ↓ Distance (km)												
	0	8	16	24	32	40	48	56	64	72	80	88	96
5km	**145**	**144**	**143**	**138**	**120**	**114**	**112**	**112**	**111**	**111**	**111**	**110**	**110**
	144	144	142	136	120	114	112	112	111	111	111	111	111
	0.7	*0*	*0.7*	*1.5*	*0*	0	0	0	0	0	0	-0.9	-0.9
10km	**242**	**241**	**239**	**233**	**223**	**217**	**215**	**213**	**212**	**212**	**211**	**211**	**211**
	240	240	237	232	222	217	214	213	212	212	212	211	211
	0.8	*0.4*	*0.8*	*0.4*	*0.4*	*0*	0.4	0	0	0	-0.5	0	0
20km	**436**	**436**	**433**	**430**	**425**	**421**	**418**	**415**	**414**	**413**	**412**	**412**	**412**
	435	434	432	428	424	420	417	415	414	413	413	412	412
	0.2	*0.5*	*0.2*	*0.5*	*0.2*	*0.2*	*0.2*	0	0	0	-0.2	0	0
30km	**633**	**632**	**631**	**628**	**625**	**622**	**619**	**617**	**615**	**614**	**613**	**612**	**612**
	631	631	629	627	624	621	618	616	615	614	615	613	613
	0.3	*0.2*	*0.3*	*0.2*	*0.2*	*0.2*	*0.2*	*0.2*	0	0	-0.3	-0.2	-0.2
40km	**831**	**831**	**829**	**827**	**825**	**822**	**820**	**818**	**816**	**814**	**813**	**813**	**812**
	829	829	828	826	824	822	819	817	816	815	815	814	814
	0.2	*0.2*	*0.1*	*0.1*	*0.1*	*0*	0.1	0.1	0	-0.1	-0.2	-0.1	-0.2
50km	**1031**	**1030**	**1029**	**1027**	**1025**	**1022**	**1020**	**1018**	**1016**	**1015**	**1014**	**1013**	**1013**
	1029	1028	1027	1026	1024	1022	1019	1017	1016	1015	1015	1014	1014
	0.2	*0.2*	*0.2*	*0.1*	*0.1*	*0*	0.1	0.1	0	0	-0.1	-0.1	-0.1
Heat Flow at Surface	**1.35**	**1.34**	**1.33**	**1.28**	**1.61**	**1.46**	**1.44**	**1.42**	**1.42**	**1.41**	**1.41**	**1.41**	**1.41**
	1.34	1.34	1.32	1.29	1.60	1.46	1.43	1.42	1.42	1.41	1.41	1.41	1.41

Normal: **Finite (Lee et al., 1980)**
Bold: Rectan
Italic: Percentage difference between numerical and analytical solution

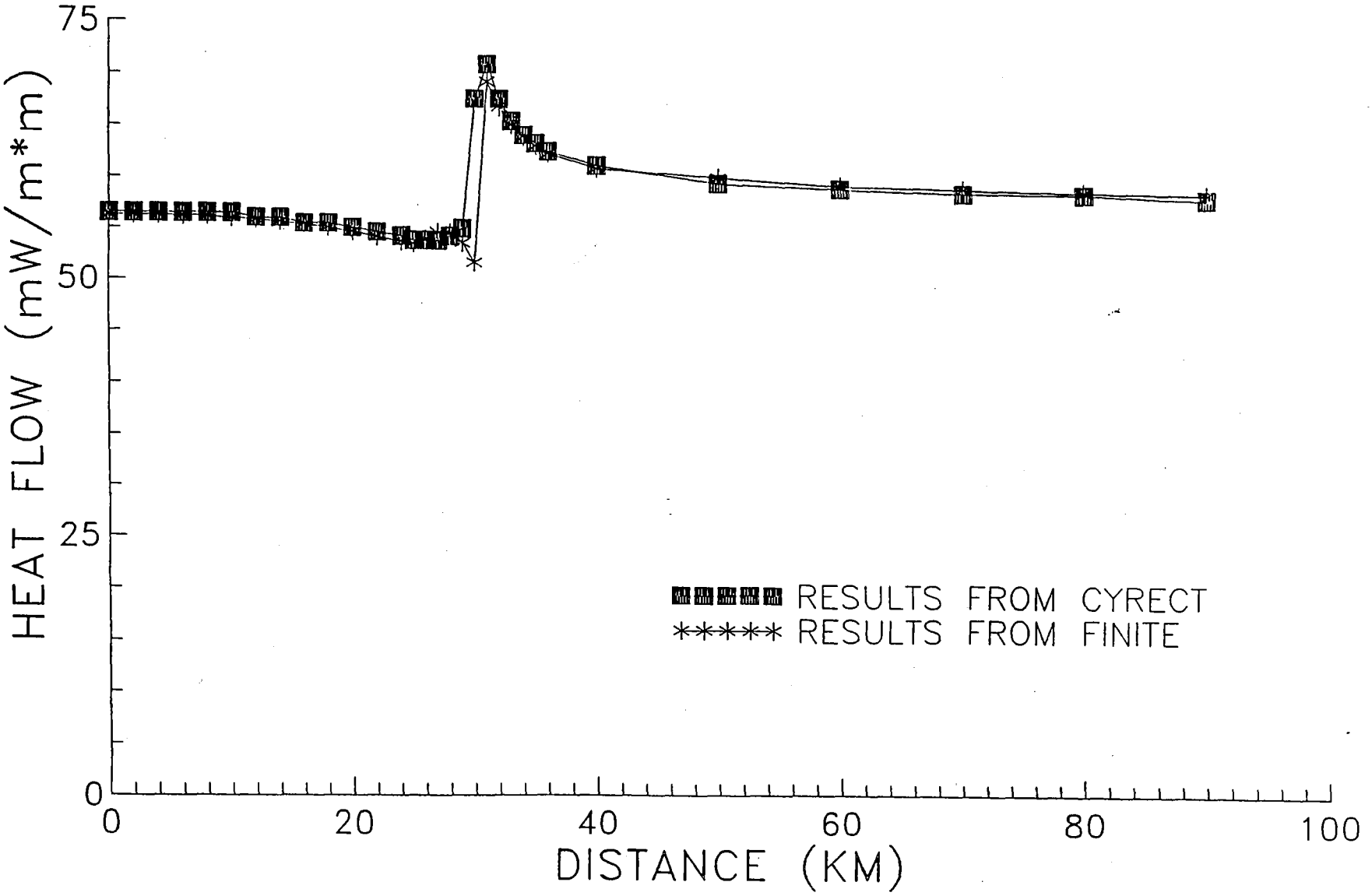

Figure B5. Comparision of numerical models, lateral thermal conductivity contrasts.